7
Initiation of Protein Synthesis

7.1
Initiation of Protein Synthesis in Eubacteria

Daniel N. Wilson

7.1.1
Overview of Initiation in Eubacteria

The initiation phase of protein synthesis is one of the rate-limiting steps of translation and as such is also the principal target of translation regulation (see Chap. 11). There are significant differences between translation-initiation events in eukaryotes (see Chap. 7.2), archea and eubacteria; however, the final state of the ribosome following initiation is principally the same, namely, a ribosome programed with an initiator tRNA and mRNA, such that the start codon and tRNA are both positioned at the P-site. Indeed, the production of functionally active proteins necessitates that translation initiates at the start codon within the mRNA. As well as the use of the correct codon as the start codon, the placement at the P-site of the ribosome must also be precise; since codons are composed of three bases, incorrect placement by one or two bases will result in a complete loss of the correct reading frame. There are two major contributors to ensure the fidelity of this process: (i) the mRNA itself and (ii) a subset of translation factors termed the initiation factors (IFs).

In eubacteria, the majority of mRNAs contain, upstream of the initiation codon in an untranslated region (UTR), a purine-rich sequence called the Shine–Dalgarno (SD) sequence [1, 2], which has sequence complementary to the 3′-end of the 16S rRNA (termed the anti-SD sequence). Base-pairing between these complementary sequences has been conclusively demonstrated using the specialized ribosome system, where expression of mRNAs was shown to be abolished by mutations within the SD sequence and then restored by compensatory mutations (that restore the complementarity with the SD sequence of the mRNA) within an exogenously expressed copy of the 16S rRNA gene ([3]; reviewed in Ref. [4]). This complementarity is thought to enhance the translation of the downstream mRNA, by helping to position the AUG start codon in P-site. Recently, the SD–anti-SD complex was visualized directly in the 5.5 Å structure of *Thermus thermophilus* 70S bound with three tRNAs and SD containing mRNA [5]. This study showed that the SD–anti-SD complex formed a helical structure located above the platform and behind the head of

Protein Synthesis and Ribosome Structure. Edited by K. H. Nierhaus and D. N. Wilson

ISBN 3-527-30638-2

the 30S structure, whereas the AUG codon of the mRNA was in a single-stranded conformation, positioned at the P-site and exposed for interaction with the anti-codon of the P-site tRNA, i.e., if the spacing is too long then the AUG codon will not be positionable in the P-site. Certainly, when the spacing between the SD and the coding becomes to small, the strong interaction between the SD and anti-SD sequence can lead to destabilization of tRNA binding. The RF2 recoding site seems to have taken advantage of this effect since this recoding site contains a SD-like sequence that requires a spacing of two nucleotides and increasing or decreasing the spacing by even a single nucleotide dramatically reduced the frameshifting efficiency [6, 7]. The short spacing and sequence complementarity of the SD–anti-SD interaction encroaches directly on the E-site and causes loss of the tRNA from this site, which in turn destabilizes the translating ribosome and induces +1 frameshifting [8]; see also Chap. 8.2.5). However, it should be noted that there are a special subset of mRNAs, particularly predominant in Gram-positive bacteria and archaea, termed leaderless mRNAs, because the start codon is preceded by only a few nucleotides or simply starts with the 5′-terminal AUG codon (reviewed in Ref. [9]). Translation initation of leaderless mRNAs can follow a different pathway (Fig. 7.1-1B), than that described for canonical mRNAs (Fig. 7.1-1A; Sect. 7.1.2 for more details).

Unlike the multitude of initiation factors present in archea and eukaryotes, only three initiation factors, IF1, IF2 and IF3, are present in eubacteria. IF3 has been proposed as the first initiation factor to associate with the ribosome since this factor has been shown to be involved with dissociation of bacterial 70S ribosomes into their component 30S and 50S subunits (Fig. 7.1-1a). The presence of IF3 may have a role in positioning of the mRNA in conjunction with the SD sequence to move the 30S–mRNA complex from a standby state to one where the mRNA is positioned such that the start AUG codon is at the P-site (as seen in Fig. 7.1-1b). The binding of the initiator fMet-tRNA^{fmet} can occur non-enzymatically by direct binding to the programed 30S subunit or enzymatically in the form of a ternary complex with IF2 and GTP (Fig. 7.1-1c). This second pathway is stimulated by the presence of IF1, although the exact order of binding of IF1 and IF2 is unclear (Fig. 7.1-1c). The presence of all three IFs, the initiator tRNA and mRNA positioned with AUG at the P-site of the 30S subunit is termed the 30S (or pre)-initiation complex. The association of this complex with the 50S subunit results in the release of the initiation factors (Fig. 7.1-1d), presumably release of IF3 is immediate, since the anti-association action of IF3 would prohibit 70S formation. IF1 has also been proposed to be released concomitantly with subunit association (Fig. 7.1-1d). The 50S subunit acts as the GTPase-activator protein (GAP) for IF2, thus stimulating the GTPase activity of IF2, ultimately leading to the release of IF2 from the ribosome (Fig. 7.1-1e). Only after release of IF2 can full accommodation of the initiator-tRNA into the P-site on the 50S subunit occur, resulting in the P_i state. Furthermore, since IF2 binds within the A-site region, overlapping the binding sites of both EF-Tu and the A-site tRNA, release of IF2 is a prerequisite for the binding of the next aminoacyl-tRNA to the A-site, i.e., the first step into the elongation pathway (see Chap. 8).

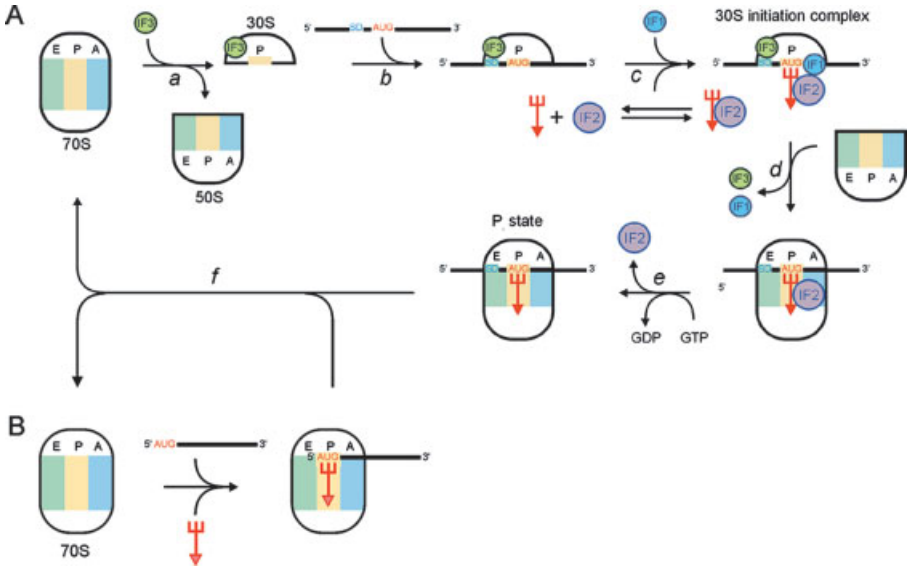

Figure 7.1-1 A schematic representation of the initiation of protein synthesis. A. Canonical mRNAs; (a) Binding of IF3 to the 30S subunit dissociates empty 70S ribosomes into the component 30S and 50S subunits. (b) IF3 aids in positioning of the mRNA such that the AUG start codon is located at the P-site of the 30S subunit. The Shine–Dalgarno (SD) sequence of the mRNA is located in the vicinity of the binding position of IF3, where it makes interaction with the anti-SD sequence of the 16S rRNA in the 30S subunit. (c) Binding of the initiator fMet-tRNA (red) can occur directly or in the form of a ternary complex with IF2 (purple) and GTP and is stimulated by the presence of IF1 (blue) and results in the formation of the 30S initiation complex. (d) Association of the 50S subunit with 30S initiation complex causes the release of IF3 and IF1, but IF2 remains bound at the A-site. (e) The GTPase activity of IF2 is stimulated by the presence of the 50S subunit and ultimately leads to the release of IF2.GDP from the ribosomes, allowing full accommodation of the initiator tRNA at the P-site on the 50S subunit. This complex is termed the Pi state, i.e., P-site is occupied and the A- and E-sites are free. (f) Following translation elongation, termination and ribosome recycling, the empty 70S ribosomes are ready to re-enter the translation-initiation phase. B. Leaderless mRNAs. Binding of leaderless mRNAs may utilize an alternative pathway without requiring initiation factors and using 70S monosomes directly.

7.1.2 Specialized initiation events: translational coupling, 70S initiation and leaderless mRNAs

In the bacteria, most mRNAs are transcribed from transcriptional units that usually contain several, often functionally related, genes. The product is a polycistronic mRNA, where each cistron carries the information of a single protein. In *E. coli*, polycistronic mRNAs usually contain four cistrons. Such mRNAs contain multiple translation initiation sites, one for each cistron, with a Shine-Dalgarno (SD) sequence and an AUG initiation codon. Recognition of the translation start sites within the mRNAs is performed by an initiation complex comprising the small ribosomal subunit (30S), the initiator transfer RNA carrying the amino acid formylmethionine (fMet-tRNA$_f^{Met}$) and three proteins called initiation factors (IF1, IF2, and IF3; Fig. 7.1-1). In principle, the various initiation codons of a bacterial polycistronic mRNA can be recognized independent of one another. Aided by the SD sequences, the 30S initiation complexes can land on any of the available translation initiation sites (30S *de novo* initiation). It has been observed that to be accessible for the 30S subunit, an initiation region (including the start codon and the SD motif) must be in a single-stranded, non-hydrogen-bonded state, i.e. not buried within a secondary structure. This is the rule, but an important exception is seen for the polycistronic mRNAs encoding ribosomal proteins. Here the first cistron is usually accessible for the 30S *de novo* initiation, whereas the second and following initiation sites are sequestered within secondary structure. However, once the first initiation site has been recognized, translation commences and the translating ribosome can unfold the secondary structure to reveal the second initiation site. In this way, the second and all downstream cistrons are translationally coupled, i.e. if one cistron is translated, all the downstream ones are translated. On the other hand, if the first cistron is not translated, then the whole polycistronic mRNA cannot be translated. This phenomenon is termed *translational coupling*.

Translational coupling is exploited for what is called *autogenous translational regulation* (see Chap. 11 for details). Briefly, a repressor protein (usually a translation product of the second or third cistron of the same polycistronic mRNA) will bind to the first initiation site on the mRNA, thereby inhibiting the translation of the first cistron, as well as translation of the downstream cistrons. Repression is relieved and, therefore, translation resumes, only when the regulatory ribosomal protein dissociates from the low-affinity binding site on the mRNA and is recruited by the high-affinity binding site on the rRNA during assembly of ribosomes.

Often, the downstream cistron is translated by re-initiation, meaning that the ribosome that terminates translation of the upstream cistron does not dissociate from the mRNA but proceeds directly to the next cistron, occasionally shifting the reading frame if this is required (70S-type initiation; [104, 105]). This is seen not only for ribosomal proteins but also for translation factors, for example, the *prfB* gene, encoding the translation termination factor RF2, where the final *UGA* stop codon overlaps with the start AUG codon (A*UGA*) of the *hemK* gene, which encodes a methylase

that modifies the termination factor (see Chap. 9 for more details). Therefore, it is easy to envisage that a 70S ribosome, after undergoing termination and peptide release at the UGA stop codon of the first cistron (for example, of the RF2-mRNA), does not dissociate from the polycistronic mRNA, but instead translates the downstream cistron (in this case the hemK mRNA). An empty 70S (following termination and peptide release) is capable of scanning up- and downstream along the mRNA, until it is "caught" by a nearby SD sequence (which occurs through base-pairing with the 3′-end of 16S rRNA). This promotes the correct position of any following AUG-start codons at the P-site. Whether or not the "scanning" 70S ribosomes actually carry an fMet-tRNA is not clear. The 70S type of initiation is the only reason for the formylation of the initiator Met-tRNA, since a 30S subunit can easily form an initiation complex with both Met-tRNA$_f^{Met}$ and fMet-tRNA$_f^{Met}$, whereas the presence of fMet-tRNA$_f^{Met}$ facilitates the formation of the 70S initiation complex [105].

Translation of leaderless mRNAs has been proposed to occur on 70S ribosomes [106], as well as being able to proceed through the 30S pre-initiation pathway (cf. Fig. 1A and B), and there is growing evidence to support this view (reviewed in Ref. [9]). Recently, Ueda and coworkers demonstrated, using an *in vitro* translation system comprising only purified components, that translation of leaderless mRNAs could occur in the absence of initiation factors [107]. Furthermore, the stability of leaderless mRNAs with 70S ribosomes in the presence of initiator-tRNA has been shown to be up to 10-fold higher than with 30S subunits [107, 108]. Since the increased stability of binding of canonical mRNAs with the 30S subunit probably derives from elements within the 5′ untranslated region (UTR), such as the SD sequence, which interact with the 16S rRNA, these sorts of interactions are unavailable to leaderless mRNAs (the 5′ UTR being absent). By forming initiation complexes directly with 70S ribosomes (Fig. 7-1B), rather than through the 30S pre-initiation complex pathway (Fig. 7-1A), the stability of the mRNA–tRNA complex is increased because 85% of the contacts of a P-tRNA are with the 50S subunit in the 70S ribosome [109, 110].

Although downstream stabilization elements have been proposed to exist in leaderless mRNAs, these could not be confirmed. Thus, it seems that the 5′ AUG codon is the major, if not the only, element within the leaderless mRNA required for their efficient translation. Indeed, mutations at this position have been shown to reduce significantly the efficiency of translation, even when the AUG is replaced by other canonical initiation codons, such as CUG, GUG or UUG (see Ref. [9]). In addition, for 30S initiation of leaderless mRNAs, the concentration of the initiation factors is an important factor, such that high concentrations of IF2 stimulate translation, whereas IF3 has an inhibitory effect. Thus, the ratio of IF2 and IF3 seems to influence significantly the expression level of leaderless mRNAs [111].

The additional stability of 70S initiation complexes may explain why translation of leaderless mRNAs, but not canonical mRNAs, continues in the presence of the antibiotic kasugamycin (see Ref. [112]). Kasugamycin has also been shown to affect assembly of the 30S subunit, producing a particle that is deficient in a number of small ribosomal proteins. While this particle cannot translate canonical mRNAs, translation of leaderless mRNAs remains unaffected (U. Blaesi, pers. Comm). Of the

proteins missing, S1 has been shown to be dispensable for translation of leaderless mRNAs [113]. The S1 protein has two N-terminal RNA-binding motifs necessary and sufficient for ribosome binding and four C-terminal RNA-binding motifs associated with mRNA binding. Although S1 is absent in the crystal structures of the 30S subunits [32, 92], the binding position has been located, using cryo-EM, to the platform side of the subunit, in close proximity to the anti-SD sequence [114]. It is therefore easy to envisage that the absence of a 5′ UTR in leaderless mRNAs circumvents the necessity of S1.

As yet, the role of leaderless mRNAs is not clear; certainly there is little correlation (or homology) between the genes encoding leaderless mRNAs in different organisms, let alone across the kingdoms [9]. Despite this, under certain physiological conditions, for example, low temperature or in the presence of antibiotics, the 70S initiation pathway open to leaderless mRNAs might be competitively favorable over that of canonical mRNAs [9, 106]. In this respect, it is interesting to note that in many *Streptomyces* species, a number of antibiotic resistance genes are leaderless mRNAs [9]. Blasi and coworkers [9] have also suggested that leaderless mRNAs may represent remnants of ancestral mRNAs that have acquired canonical start codons at the 5′-end, i.e. the earliest mRNA templates were simply single-stranded polynucleotides.

7.1.3
Initiation Factor 1 Binds to the Ribosomal A-site

The exact role of IF1 within the initiation complex is perhaps the least understood of the IFs. A number of roles have been described for IF1 including (i) subunit association during 70S initiation complex formation, (ii) modulating the binding and release of IF2 and (iii) blocking the binding of tRNAs to the A-site (reviewed in Refs. [10, 11]). Irrespective the role of IF1, the gene encoding IF1, *infA*, is essential for cell viability in *Escherichia coli* [12] indicating its importance in the initiation process.

The structure for IF1 has been determined by NMR spectroscopy and revealed to contain a secondary structure characteristic of the oligomer binding (OB) fold family of proteins, termed because of their ability to bind oligonucleotides and oligosaccharides [13]. The architecture of a classic OB-fold motif includes a five-stranded β-sheet coiled to form a closed βbarrel, and capped by a α-helix as exemplified by IF1 (Fig. 7.1-2A). A number of other translational proteins are members of this family including ribosomal proteins S1, S17, and L2 (reviewed in Refs. [14, 15]), tRNA synthetases, IF5A and eIF2a, as well as the central region of eIF1A (Fig. 7.1-2A; [16]). The presence of domains additional to the common OB component in higher organisms, namely archeal and eukaryotic eIF1A, at least partly correlates with the ability to form binary complexes with eIF5B (see following).

Interestingly, a number of the cold shock protein (Csp) family have high structural homology to IF1 (although little sequence homology). In fact, some strains, predominantly Gram-positive, for example *Bacillus stearothermophilus*, have no obvious IF1 homolog [17]. It has been postulated based on the structural similarity between the Csp and IF1 families that in these strains one of the often many Csps may have assumed this role. In this regard, it is interesting that a double deletion CspB–CspC

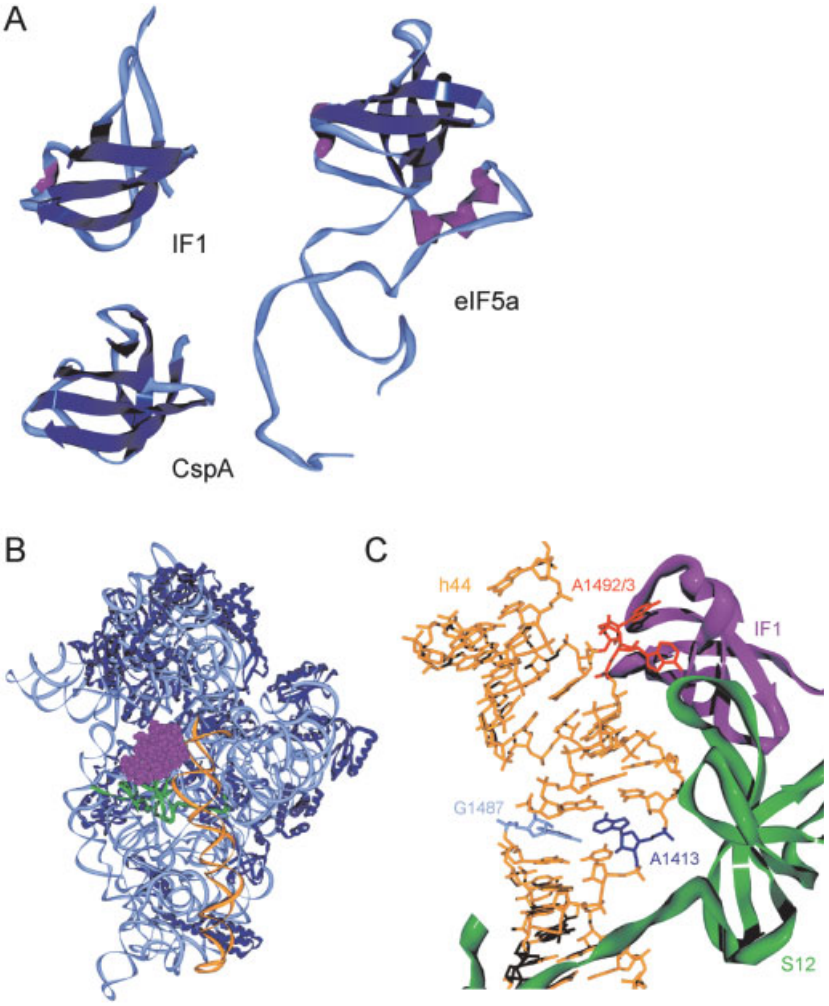

Figure 7.1-2 The binding site of IF1 on the 30S subunit and homology with other factors. (A) The solution structures of IF1 (pdb1ah9; [99]), CspA (pdb1mjc; [100]) and eIF1a (pdb 1d7q; [16]), all shown in ribbon representation with strands (dark blue), helices (purple) and random coil (light blue). (B) Overview of the IF1 binding site on the 30S subunit (pdb1hr0; [19]). Ribbon representation of the 16S rRNA (pale blue) including ribosomal proteins (dark blue) with h44 (yellow) and ribosomal protein S12 (green) highlighted. IF1 (purple) is shown as spacefill representation. (C) Close-up view showing that IF1 (purple ribbons) binding, causes A1492 and A1493 (red) to be flipped out of helix 44 (yellow) and the base-pair between A1413 (dark blue) and G1487 (light blue) to be broken.

in *Bacillus subtilis* led to alterations in protein synthesis, cell lysis upon entry into stationary phase, and the inability to sporulate [18]. Deletion of all three Csp proteins was lethal suggesting the importance of having at least one of this family present. Intriguingly, the defects caused by the double knock-out could be cured by the heterologous overexpression of *E. coli* IF1, suggesting that IF1 could assume some of the chaperone activities normally performed by the Csps. This raises the question if under some conditions the reverse could be true, especially for strains lacking the *infA* gene. Certainly, there is some evidence that members of the Csp family co-purify with ribosomes; however, this may be related simply to their chaperone activity and reflect their tendency to interact with RNA rather than their involvement in the initiation of protein synthesis.

Despite the low-sequence similarity between OB-fold family members, secondary-structure similarity is striking, as well as the localization of basic residues on one face of the OB-fold. The recent crystal structure of *T. thermophilus* IF1 bound to the 30S subunit [19] demonstrates that IF1 is no exception. Interactions with the 30S subunit associate with the highly basic surface of IF1, where conserved arginine residues (Arg46 and Arg64) stabilize RNA-binding interactions through stacking and electrostatic interactions. The IF1-binding site on the 30S subunit consists of a cleft formed by h44, the 530 loop and protein S12 (Fig. 7.1-2B; [19]). The loop between strands β3 and β4 is inserted into the minor groove of h44 and flips out residues A1492 and A1493 from their stacked position in h44 (Fig. 7.1-2C). This is reminiscent of the situation where these residues are flipped out due to binding of the antibiotic paromomycin to the decoding site (see Chap. 12) and also due to a cognate tRNA at the A-site (see Chap. 8.2). The major distinction being that during decoding, A1492 and A1493 are critically involved in direct monitoring of correct Watson–Crick pairing of the first two positions of the anticodon–codon duplex [20], whereas within the IF1:30S structure these residues are inaccessible, being protected by IF1 and S12. This suggests that although the binding sites of the A-site tRNA and IF1 overlap, there is little mimicry in their interaction.

Despite the expectation that IF1 would sterically occlude tRNA binding at the A-site [21], it is unlikely that this is the role of IF1 during initiation as there is only one tRNA-binding site on the 30S subunit, that of the prospective P-site [22, 23]; reviewed in Ref. [24]. It seems more probable that IF1 binding at the A-site induces conformational changes that promote subunit association during 70S initiation complex formation. Indeed, the flipping out of A1493 disrupts a base-pair with A1408, destabilizing the top of h44 and allowing lateral movement of bases C1412 and A1413 such that the base-pair between A1413 and G1487 is broken (see Fig. 7.1-2C). This lateral shift moves one strand of h44 with respect to the complementary strand generating "long distance" (up to 70 Å from the IF1-binding site) conformational changes within h44 [19]. The minor groove of h44 makes extensive contacts with the 50S subunit, one per helical turn, forming intersubunit bridges B3, B5 and the largest contact point between subunits, bridge B2a [25]. Thus, it is possible that these changes induced by IF1 binding may be responsible for the observed increase in association rates between 30S and 50S subunits [26]. The activation energy associated

with 70S formation is large, estimated at 80 kJ mol^{-1}, and is involved only in adaptation of the 30S subunit (not 50S subunit), rather than the association step itself [27]. Therefore it is tempting to speculate that the initiation factors, particularly IF1 because of the changes it induces in the 30S subunit, help to overcome the free-energy barrier for 50S subunit association with the 30S [28]. The functionally active 30S conformations are obtained by heat activation [29] and have been visualized by cryo-EM, which revealed that they bear a closer resemblance to the 50S-subunit-bound state than to the inactivated state [30]. This heat-activated "intermediate" state may reflect a physiological state [29], such as that induced *in vivo* by translational factors such as IF1. Indeed, the crystal structure of the IF1-bound 30S subunit [19] also exhibits more similarity to the 50S bound state [25, 31], than to that of the free 30S subunit [32].

Mutation of A1408G eliminates all indicators associated with IF1 binding to the 30S subunit, such as the "tell tale" footprints at A1492 and A1493, yet retains wild-type growth characteristic [33]. This is perplexing as IF1 interaction with the 30S subunit is essential for competent 70S formation [34] and cell survival [12]. The A1408G mutation would also be expected to disrupt the base pair with A1493, tempting speculation that by doing so it enables the 30S subunit to adopt a conformation mimicking that of the initiation complex, thus making IF1 dispensable for cell viability [33]. If this hypothesis would be correct, then direct interaction of IF1 and IF2 may not be necessary and that the 30S conformational change induced by IF1 is sufficient to stimulate IF2 binding.

7.1.4
The Domain Structure of Bacterial IF2

IF2 is the largest of all eubacterial translation factors and can be divided into three major domains based on primary sequence homology (Fig. 7.1-3A), an N-terminal domain (NTD) that is not conserved in sequence or length among bacteria, a central domain containing the guanine-nucleotide-binding motif (termed the G domain), and a C-terminal domain (CTD), which contains the entire fMet-$tRNA^{fmet}$-binding site (reviewed in Ref. [11]). *E. coli* IF2 has been divided further into subdomains by Sperling-Petersen and co-workers [35], such that the NTD consists of subdomains I–III, the G domain encompasses IV–VI-1 and the CTD, VI-2. In *E. coli*, the IF2 gene, *infB*, encodes three isoforms of IF2, termed IF2-1, -2 and -3 [36]. The latter two isoforms are smaller and result from translation at alternative initiation sites near the beginning of domain II (as indicated by arrows in Fig. 7.1-2A). The cellular level of all three isoforms is similar and the presence of all three isoforms has been shown in *E. coli* to be optimal for growth. However, the absence of multiple isoforms in the most of the bacteria suggests that they are not essential for survival; indeed many extremophilic species in bacteria, such as *Thermus,* or in Archea, such as *Sulfolobus* or *Methanococcus,* do not even have this NTD region [37]. A fragment consisting of subdomains I and II (but not subdomain I alone) was capable of binding the 30S subunit and IF2 lacking this region showed low binding affinity, suggesting the importance of this region for factor binding [38, 39]. Interestingly, this

same fragment has been shown to bind to the *infB* mRNA, hinting at the existence of an autoregulatory mechanism for IF2 [40]. NMR studies of the NTD subdomain I have revealed that residues 2–50 form a compact structure containing three short α-helices and three antiparallel twisted β-strands (Fig. 7.1-3A), the following residues 51–97 were unstructured and the rest of subdomain I (98–157) was of a highly helical nature [41]. The latter was suggested to act like a linker, much like that found between domains VI-1 and VI-2 of aIF5B (see the following). The compact core of subdomain I (IF2-DI) has structural similarity to the SC-fold domain of class Ia aminoacyl-tRNA synthetases (RS), such as that found in GlnRS (Fig. 7.1-3B). In the crystal structure of Gln-tRNA bound to GlnRS, the SC-fold domain contacts the inner side of the L-shaped tRNA, where it provides a connection between the RS domains that interact with the acceptor (green) and anticodon (red) of the tRNA (yellow in Fig. 7.1-3B). This suggests that the NTD of IF2 is probably associated with positioning of the anticodon stem loop of the fMet-tRNA into the P-site of the 30S subunit. Consistent with such a suggestion is the crosslink found between subdomain II of IF2 and the anticodon stem of fMet-tRNA as well as the similarity in the footprinting pattern found within this region in the presence of IF2 or MetRS.

The G domain and CTD of IF2 (IV–VI) are the most highly conserved regions, having homology across all kingdoms. In fact, IF2 from *Mycoplasma genitalium* and

Figure 7.1-3 The domain structure of *E. coli* initiation factor IF2. (A) Schematic diagram of the domain structure of *E. coli* IF2. There are two alternative initiation sites (arrowed) within subdomain II marked with IF2-2 and IF2-3. The structure of part of subdomain I of the N-terminal domain (NTD) of *E. coli* IF2 has been determined (pdb1euq; [101]) and the central (G domain) and CTD encompassing subdomains IV–VI have almost 50% similarity to the archeal IF2 homologue aIF5B, whose structure (pdb 1g7t; [102]) is also shown. (B) Part of the NTD of IF2 (residues 2–50; subdomain I) has structural homology with the SC-fold domain of Gln (and Met) aminoacyl-tRNA synthetases (GlnRS-SC). Within the complex GlnRS structure, this region contacts the anticodon stem of the tRNA (pdb1euq; [101]). The tRNA is colored yellow with the anticodon (red) and CCA end (green) highlighted for reference. The homologous region to domain I of IF2 in the GlnRS is colored purple. (C) Domain VI-2 of IF2 has structural homology with domain III of EF-Tu, leading to the proposal that IF2 recognition of the fMet of an initiator tRNA utilizes the equivalent surface. Shown here is domain VI-2 of IF2 (IF2-DVI-2; pdb 1d1n; [43]) compared with domain III of EF-Tu.Cys-tRNA^{Cys} (pdb1b23; [45]). In the latter structure, the Glu271 (red; stacks with A76) and His273 (green)/ Arg274 (purple) are in close proximity to the terminal adenine (A76) of the CCA end of tRNA (yellow) and the attached cysteine residue respectively. The equivalent positions are not conserved in IF2 suggesting that the details of recognition differ, however, residues on the equivalent surface as that used by EF-Tu to recognize tRNA predicted to participate in fMet recognition are indicated in red [43].
(D) Topology of IF2 (middle) on the 30S (left) and 50S subunit (right). Positions of IF2 used for site-directed hydroxyl-radical probing are shown on the structure of the aIF5B at the equivalent locations: cleavages from the pale and dark blue positions on IF2 map to the 30S subunit and include positions G35/G38-C40 and A397 of h3/h4 (brown), G423 (green; h16) and residues in h17/h18 (C443 and A498/A537, purple/red). Residues A1418 and A1483 (cyan) exhibited reactivity upon IF2 binding. On the 50S subunit, the L11-binding region (brown), the sarcin-ricin loop (purple) and H89 (green) have been also footprinted. The small and large subunits (shown as if the 70S ribosomes were opened like a book) are shown in ribbon format with rRNA and ribosomal proteins colored in pale and dark blue, respectively. Helix 44 (yellow) on the 30S subunit and the A- (red) and P-site (yellow) CCA-end substrates are highlighted for reference positioning.

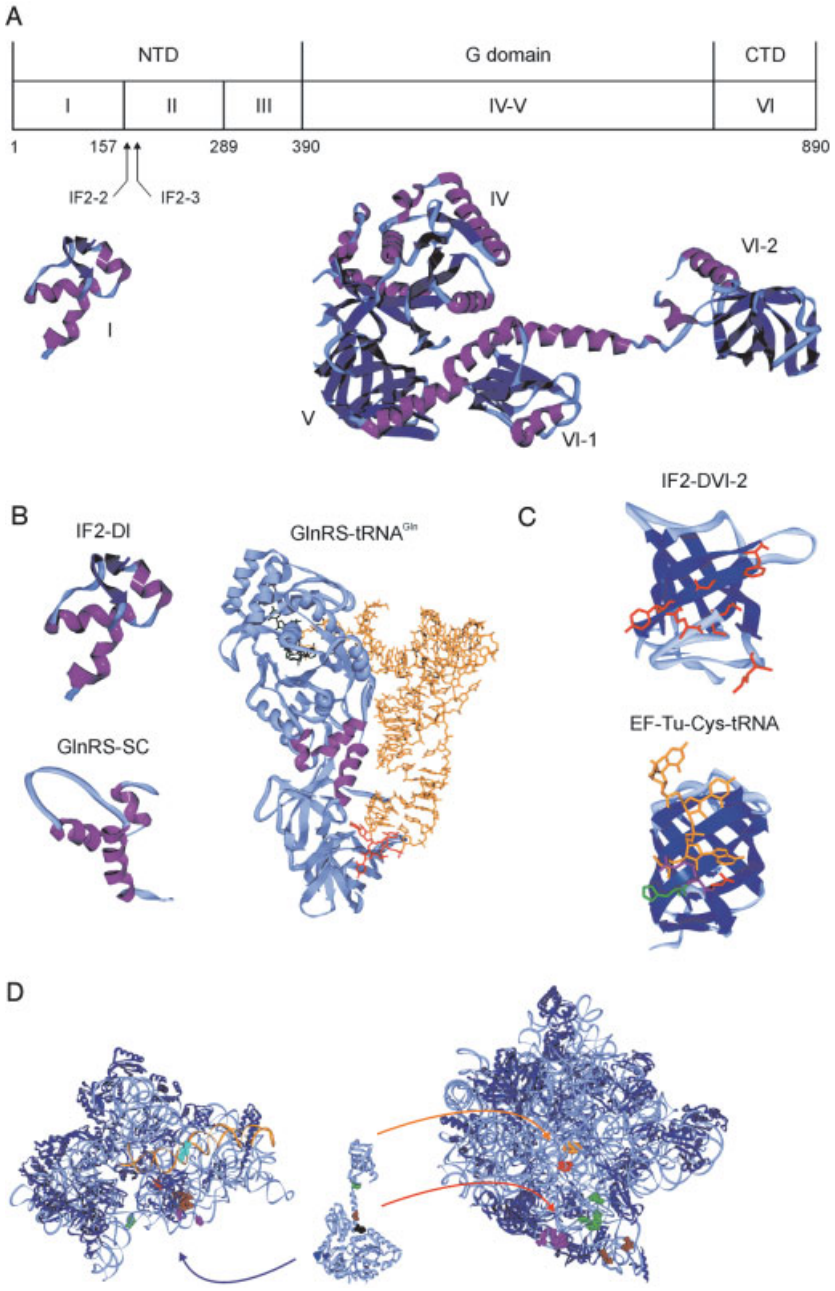

Figure 7.1-3

T. thermophilus are unusually small, consisting of only ~600 amino acids (rather than the usual 800–1000), the missing residues being absent from the NTD. Similarly, the IF2 homologs found in eukaryotes and archaea, termed eIF5B and aIF5B, respectively, are also smaller than their eubacterial counterparts and by comparison with their eubacterial counterparts contain only the G and CTD domains. The crystal structure of aIF5B from *Methanobacterium thermoautothrophicum* has been solved therefore providing a good homology model for the C-terminal region of IF2 (Fig. 7.1-3A). The crystal structure is described as being "chalice-shaped", where the "cup" region containing the G domain is identical to the corresponding regions in EF-Tu•GTP and EF-G•GDP. The stem of the chalice constitutes an α-helical linker region separating the G domain by over 40 Å from the base of the chalice (VI-2 in Fig. 7.1-3A). The structure of aIF5B was solved in the GTP, GDP and nucleotide-free state; however, surprisingly there was little significant difference between them and no observable change within domain IV, the formyl-methionine (fMet)-binding domain, relative to the functional state. This is consistent at least with the stable binding of fMet-tRNA^{fMet} observed with bacterial IF2 regardless of whether in the GTP or GDP form [42].

Recently, domain VI-2 of the CTD from *B. stearothermophilus* IF2 containing all the molecular determinants necessary and sufficient for fMet-tRNA^{fMet} recognition and binding [42] was determined by NMR [43] (Fig. 7.1-3C). The β-barrel structure of this domain shows remarkable similarity to domain II of EF-G and EF-Tu (Fig. 7.1-3C), despite having low-sequence identity (13%) and homology (17%). This high structural homology to EF-Tu and the availability of structures for two different aminoacyl–tRNA•EF–Tu complexes [44, 45] enabled a model to be proposed to define an IF2 recognition site for the fMet moiety and the acceptor stem (CCA-end) of the initiator tRNA [46, 43]. Although the mechanisms probably differ in their details since there is little comparative conservation in residues at equivalent positions between EF-Tu and IF2, it seems probable, however, that the same surfaces are used and a number of residues conserved within the IF2 family, such as R654, Q655, F657, G667 and E713, constitute the fMet-CCA-binding site (colored red in Fig. 7.1-3C).

7.1.5
Interaction Partners of IF2

On the ribosome, IF2 accelerates codon–anticodon base-pairing between the initiator fMet-tRNA^{fMet} and the start codon of the mRNA in the ribosomal P-site [47]. The specificity of the reaction is governed by the exclusive recognition of the fMet moiety of the initiator fMet-tRNA^{fMet} [48, 49]. In bacteria, IF2 can form a ternary complex with fMet-tRNA and GTP [50], whereas no evidence for the equivalent interaction between eIF5B and Met-tRNA has been found, although eukaryotes have an additional factor eIF2, which assumes this delivery role (see Sect. 7.2.7.4). Since the majority of the interactions of tRNA with programed 30S subunits depend on codon–anticodon interaction [51], the stimulation of this reaction by IF2 is probably due to the corresponding increase in stability of the initiator tRNA on the ribosome. In the presence of IF1, binding of the ternary complex is additionally stimulated,

suggesting some interplay between the factors. However, unlike the situation in eukaryotes, where eIF1A and eIF5B form a stable interaction in the absence of the ribosome [52], no evidence for such an interaction has been observed between bacterial IF1 and IF2. Consistent with this, the binding interface between eIF1A and eIF5B was recently determined to use the C-terminal region of each factor, i.e., regions that are not present in bacterial IF1 and IF2 [53]. Therefore, if an interaction between the bacterial counterparts exists it seems to occur only on the ribosome: IF2 has been crosslinked to IF1 on the ribosome [54] and subdomain II of IF2 has been proposed to interact with IF1 [38].

Manual sequence alignment of IF2 against EF-G suggested that IF2 could be aligned against all of EF-G, with the exception of the very N-terminal domain and the terminal region of domain IV of EF-G, i.e., the region mimicking the tRNA anticodon stem loop. Interestingly, this latter region was found to have similarity to IF1, leading to the suggestion that IF2 and IF1 may together mimic the structure of EF-G, thus extending the structural mimicry found between elongation factors EF-G and the ternary complex EF-Tu•tRNA•GTP (reviewed in [55]; see Chap. 8.2.5) to encompass the initiation factors [21]. However, the subsequent structure of IF1 bound to the 30S subunit does not support a direct structural mimicry of either domain IV of EF-G or the anticodon stem loop of a tRNA [19]. This aside, it does seem probable that the general topographies of the factors is consistent with this idea, since IF1 does bind in the A-site and interact with the bases A1492 and A1493 involved intimately in the decoding process. Furthermore, the strong homology between G domains of IF2/eIF5B and EF-G/EF-Tu and the ribosome-dependent activation of their GTPase activities suggests that IF2, in particular the G domain, is likely to occupy a similar position to EF–G, EF-Tu ternary complex and EF-1α at the A-site of the ribosome as visualized by a multitude of cryo-EM studies [56–62].

Early attempts to map the position of IF2 on the ribosome using chemical modification approaches have been relatively unsuccessful [63, 64]. The former study identified a large number of residues of the 16S rRNA spread throughout the 30S subunit [64], suggesting a weak or disperse association of IF2 with the 30S subunit or perhaps predominantly with ribosomal proteins. Recent base-specific probing studies also detected no protections of the 16S rRNA resulting from the binding of IF2 to 30S subunits; however, in loose couple ribosomes, binding of IF2 led to a decrease in reactivity of residues A1418 and A1483. Since these residues are located in the lower portion of h44 that makes contacts with the 50S subunit, the changes in reactivity are probably indirect and might indicate that IF2 has a "tightening effect" on the interaction between the subunits [65]. Site-specific hydroxyl-radical probing experiments suggested that the G domain (V) is in close proximity to the 16S rRNA, since cleavages of the 16S rRNA were observed from two positions in this region. The cleavages were localized to residues in h3/h4 (positions G35/G38-C40, A397), h16 (G423) and h17/h18 (C443, A498/A539), suggesting that the G domain of IF2 is in a similar position as that of EF-G. Consistently, cleavage of some 16S rRNA residues was observed when equivalent positions in EF-G to those in the IF2 study were used [66]. This raises the question as to why no protections

are observed when IF2 binds to the 30S subunit and invites the speculation that IF2 may undergo conformational changes upon 50S subunit association, such that stronger contacts are then made with the rRNA component of the 30S subunit in the 70S ribosome.

Two distinct regions of the 23S rRNA become protected from chemical probing upon binding of IF2 to 70S ribosomes; these include positions in the sarcin-ricin loop (G2655, G2661 and A2665 as well as an enhancement in the reactivity of A2660) and the loop at the end of H89, specifically positions A2476 and A2478 [65]. Residues in H89 (A2482 and U2474) were also cleaved using site-directed hydroxyl-radical probing when tethers were placed at positions within the CTD (VI-1) [67]. In addition, these tethers produced cleavages of nucleotides within the L11-binding region (G1068 and weakly at C1076 in H43). This set of protection and cleavage patterns for IF2 on the 50S subunit are similar to those determined for EF-G and EF-Tu [68], but not identical. This is certainly consistent with the observation that IF2 and EF-G compete for overlapping binding positions on the 70S ribosome [69]. Interestingly, in this study, the antibiotic micrococcin, which interacts with the L11 binding region, was shown not only to inhibit EF-G-dependent GTPase, but also to stimulate the IF2-dependent GTPase activity. These observations suggest that, although both factors interact with this region, they probably do so in a distinct manner. One of the largest differences is the implication of H89 in IF2 binding, since this region is not considered part of the binding site for the other elongation factors. Indeed the antibiotic evernimicin, which footprints within H89, has been proposed to act as an IF2-dependent translation-initiation inhibitor ([70]; see Chap. 12).

7.1.6
The Role of the IF2-dependent GTPase Activity

Early experiments suggested that the GTP form of IF2 was required for 70S ribosome formation by association of the component subunits and that hydrolysis of GTP released IF2 from the ribosome allowing translation to enter the elongation cycle by the binding of the ternary complex to the A-site [71, 72]. The situation was found to be the same in eukaryotes, where the GTP form of eIF5B was essential for subunit association and that hydrolysis of GTP releases eIF5B allowing peptide-bond formation to occur [73, 74]. This harmony was challenged when it was reported that the association of bacterial pre-initiation complexes with 50S subunits to form a post-initiation complex capable of peptide-bond formation required the same length of the time regardless of whether GTP or GDP was used [75]. The interpretation from these experiments was that the GDP form of IF2 catalyzes subunit association as efficiently as the GTP form and that GTP hydrolysis does not stimulate (i) the adjustment of fMet-tRNA in the P-site, (ii) the ejection of IF2 from the ribosome, or (iii) the formation of the initiation dipeptide (see Ref. [10]). However, an elegant series of experiments from Ehrenberg and co-workers [76] conclusively demonstrated that, in fact, the GTP form of IF2 (or with the non-hydrolyzable analog GDPNP), but not the GDP form, promotes rapid association of the ribosomal subunits during initiation (the K_a in the presence of GTP was over 20 times higher than

with GDP). In this study, the binding of GTP to IF2 was the most efficient in the presence of both fMet-tRNA and 30S subunits (with mRNA, IF1, and IF3), suggesting that the GTP form of IF2 stabilizes the binding of fMet-tRNA to the 30S subunit (and *vice versa*) and this promotes association. Furthermore, formation of the first dipeptide was also fast for IF2-GTP, but not IF2-GDP or IF2-GDPNP, indicating that GTP hydrolysis is necessary for rapid release of IF2 from the ribosome and therefore for dipeptide formation [76].

These observations led Ehrenberg and co-workers to propose a two-state model for IF2 action during initiation: the free form of IF2 is the GDP form, which has a low affinity for both the pre-initiation complex and 70S ribosomes. The presence of 30S subunits with *both* fMet-tRNA and mRNA promote nucleotide exchange, and stabilizes the pre-initiation complex since IF2 is now in the GTP form. The GTP form of IF2 has a high affinity for the 50S subunit and thus rapid association between the pre-initiation complex and the 50S subunit ensues. In this manner, only fully competent 30S pre-initiation complexes are converted into 70S initiation complexes. The high affinity of the GTP form of IF2 is consistent with the slow dissociation of IF2-GDPNP from the 70S ribosome. Subsequent to 70S association, GTP hydrolysis occurs and the low-affinity IF2-GDP dissociates from the ribosome, leaving the A-site free for the binding of the ternary complex. Interestingly, ternary complex binding was demonstrated to be possible in the presence of IF2, at least temporarily [76], which is consistent with the observation that ternary complex can bind to the 70S ribosome with the same kinetics in the presence or absence of IF2-dependent GTP hydrolysis [75]. Understanding of the exact binding position of IF2 will help to address the extent to the overlap in position with the ternary complex.

7.1.7
The Mystery of the IF3-binding Site on the 30S Subunit

IF3 was originally identified as an anti-association factor because it binds with high affinity to the 30S subunit (an association constant greater than 10^7 M^{-1} [77]) and thereby prevents re-association of the 30S and 50S subunits [26]. In addition to this function, IF3 is known in conjunction with IF2 to be involved in the discrimination between aminoacyl tRNAs, thereby permitting only the presence of an initiator tRNA at the P-site [34, 78]. Discrimination is based on recognition by IF3 of the anticodon loop and three base-pairs of the anticodon stem [79] and may even involve recognition of the start codon itself [80]. IF3 is encoded by the *infC* gene located at 37.5 min on the *E. coli* chromosome [81, 82], and has been shown to be essential for cell viability [83] and for protein synthesis [84]. IF3 consists of two distinct domains separated by a 20-residue-long (~45 Å) lysine-rich linker region [85]. It has been speculated that the two different IF3 functions described above could be attributable to each of the domains [86]. However, a number of other functions for IF3 have been assigned, such as the (i) adjustment of the mRNA from a so-called standby site to the P-site, (ii) stimulation initiator tRNA binding to the P-site, and (iii) dissociation of fMet-tRNA from the start codon of leaderless initiator tRNAs (see Ref. [87] and references therein).

The complete intact structure of IF3 has not been determined, but those of both NTD (with linker region) and CTD have been solved by X-ray crystallography [88] and NMR [89, 90] (Fig. 7.1-4A). The CTD has been shown to be capable of independently inhibiting 30S and 50S association, although it requires much higher excess over ribosomes compared with the full-length factor [90, 87]. *Thermotoga maritima* IF3 bound to the *T. thermophilus* 30S subunit has been visualized by cryo-EM at 27 Å resolution [91]. Density correlating to the CTD was found to locate to a region of the 30S subunit involved in forming bridges with the 50S subunit, suggesting that IF3 prevents subunit association by physically blocking the docking sites [91] in agreement with protection studies [63]. In contrast, recent X-ray crystallographic data of the CTD of *T. thermophilus* IF3 bound to the *T. thermophilus* 30S subunit revealed that IF3 was not bound at the subunit interface but at the upper end of platform on the solvent side [92] (Fig. 7.1-4B), where it makes contacts with h23, h26 and the 3′-proximal end of h45. In this position, the anti-association activity of IF3 cannot result from physically blocking subunit association, but probably derives from indirectly moderating the mobility of h45. Support for the latter model comes from an observation that a double mutant in h45 of the 16S rRNA reduces IF3 binding to the 30S subunit [93]. Furthermore, IF3 cannot dissociate 70S ribosomes carrying this double mutation even though the affinity of IF3 for the 70S ribosome is enhanced 30-fold over the wild-type 70S ribosomes [93]. A number of other biochemical data are more consistent with the platform localization of IF3, for example, regions in h45 (1506–1529) and h26 (819–859) have been crosslinked to IF3 [94], as have ribosomal proteins S7, S11, and S18 [95]. Docking the NTD of IF3 based on both the constraints of the position of the CTD on the 30S subunit and available biochemical data places the NTD in close proximity to the P-site [92]. This led to a model where the codon–anticodon recognition operates by space restrictions such that only correct-binding orientations are permissible, rather than by a direct interaction of the P-site tRNA with the NTD of IF3.

However, recent evidence has cast doubt of on both the position of the CTD of IF3 determined from the crystallographic analysis and the involvement of the NTD in any of the IF3 functions. It has been noted that 30S subunits are arranged within the crystal lattice such that they contact each other at the region where the cryo-EM has localized the CTD, leading to the suggestion that this could have masked the physiological binding site during the soaking of the crystals with the IF3 domain [96]. Furthermore, a comprehensive set of site-directed hydroxyl-radical probing experiments suggest that IF3 binds on the interface side of the 30S subunit and not on the solvent side as seen in the crystal structure. The model presented from these experiments places the CTD of IF3 at the subunit interface making contact with helices 23, 24 and 45 (cleavages colored red in Fig. 7.1-4C), whereas the linker and NTD were oriented towards the platform (colored yellow). This position for IF3 is in closer agreement with the cryo-EM localization but also the location of eukaryotic IF3 (eIF3) on the rat liver 40S ribosomal subunit to the interface surface by immuno-EM [97]. Indeed, mutation of G791A in h24 leads to a 10-fold decrease in the affinity of IF3 for the 30S subunit [98].

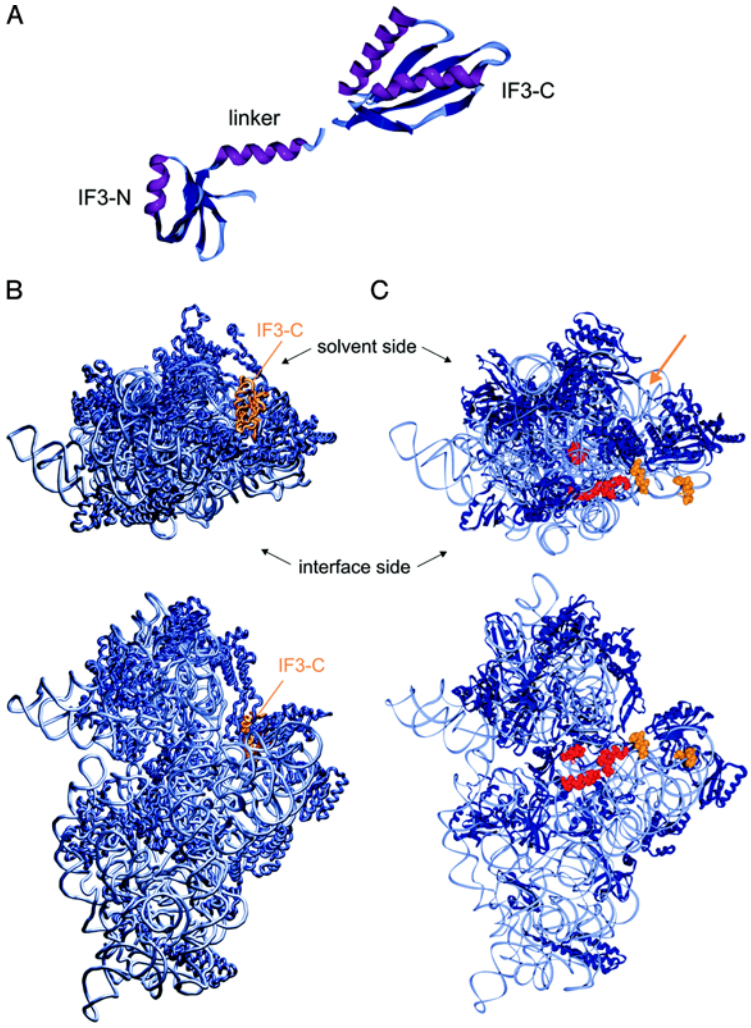

Figure 7.1-4 Where does IF3 really bind on the small ribosomal subunit? (A), IF3 is composed of an N-terminal domain linked by a long α-helix linker region (pdb 1TIF) to the C-terminal domains (pdbTIG) [88]. Both domains have a similar α/β topology with an exposed β-sheet that is reminiscent of several ribosomal and other RNA-binding proteins. (B), The CTD of IF3 was found to bind to the solvent side of the *T. thermophilus* 30S subunit by crystallography (pdb 1i96; [92]). Two views are shown: (i) a view from above looking down onto the head of the 30S subunit, with IF3C shown in orange, the 16S rRNA in light blue and ribosomal proteins in dark blue. (ii) View from 50S side onto the interface surface of the small subunit such that the IF3-C binding site is clearly on the back or solvent side. (C), Chemical cleavage of the 16S rRNA from specific sites on the C-terminal (cleavages colored red; locate mainly to 790 loop (h24) and 1400 region of h44) and linker region (yellow; found in predominantly in h23) of IF3 suggest that IF3 binds on the interface side of the 30S subunit [103], in contrast with the crystallography results. In the view from above the position of IF3-C found in the crystallography study is indicated.

Perhaps the most important observation is the recent report that the CTD of IF3 can perform all of the aforementioned activities attributed to the full-length molecule, when added in amounts (10–40 times) compensating for the reduced binding affinity [87]. In fact, the NTD alone displayed no affinity for the ribosome and no detectable functions even with high excess of protein, suggesting that the NTD is only stabilizing the interaction of the CTD with the 30S subunit. Since no conformational changes in the 30S subunit were observed upon binding of the CTD of IF3 in the crystal structure of the complex, it is difficult to envisage how IF3 can perform all its functions from a remote position on the solvent side of the 30S subunit. Certainly, further experiments need to be performed to address this issue, since if there is a second binding site for IF3, what is the function of this site?

References

1 J. Shine, L. Dalgarno, *Proc. Natl. Acad. Sci. USA* **1974**, *71*, 1342–1346.
2 J. A. Steitz, K. Jakes, *Proc. Natl. Acad. Sci. USA* **1975**, *72*, 4734–4738.
3 A. Hui, B. H. A. De, *Proc. Natl. Acad. Sci. USA* **1987**, *84*, 4762–4766.
4 M. Brink, H. de Boer, *Meth. Mol. Biol.* **1998**, *77*, 117–128.
5 G. Z. Yusupova, M. M. Yusupov, J. H. Cate et al., *Cell* **2001**, *106*, 233–241.
6 B. Larsen, N. M. Wills, R. F. Gesteland et al., *J. Bacteriol.* **1994**, *176*, 6842–6851.
7 R. B. Weiss, D. M. Dunn, J. F. Atkins et al., *Cold Spring Harbor Symp. Quant. Biol.* **1987**, *52*, 687–693.
8 V. Marquez, D. N. Wilson, K. H. Nierhaus, *Biochem. Soc. Trans.* **2002**, *30*, 133–140.
9 I. Moll, S. Grill, C. O. Gualerzi et al., *Mol. Microbiol.* **2002**, *43*, 239–246.
10 R. Boelens, C. O. Gualerzi, *Curr. Protein Pept. Sci.* **2002**, *3*, 107–119.
11 C. Gualerzi, L. Brandi, E. Caserta et al.: in *The Ribosome, Structure, Function, Antibiotics, and Cellular Interactions*, eds R. A. Garrett, S. R. Douthwaite, A. Liljas et al., ASM Press, Washington, DC 2000, 477–494.
12 H. S. Cummings, J. W. B. Hershey, *J. Bacteriol.* **1994**, *176*, 198–205.
13 A. Murzin, *EMBO J.* **1993**, *12*, 861–867.
14 D. E. Draper, L. P. Reynaldo, *Nucleic Acids Res.* **1999**, *27*, 381–388.
15 V. Ramakrishnan, S. W. White, *Trends Biochem. Sci.* **1998**, *23*, 208–212.
16 J. L. Battiste, T. V. Pestova, C. U. T. Hellen et al., *Mol. Cell* **2000**, *5*, 109–119.
17 A. Kay, M. Grunberg-Manago, *Biochim. Biophys. Acta* **1972**, *277*, 225–230.
18 M. H. Weber, C. L. Beckering, M. A. Marahiel, *J. Bacteriol.* **2001**, *183*, 7381–7386.
19 A. P. Carter, W. M. Clemons, Jr., D. E. Brodersen et al., *Science* **2001**, *291*, 498–501.
20 J. M. Ogle, D. E. Brodersen, W. M. Clemons Jr et al., *Science* **2001**, *292*, 897–902.
21 S. Brock, K. Szkaradkiewicz, M. Sprinzl, *Mol. Microbiol.* **1998**, *29*, 409–417.
22 A. Gnirke, K. H. Nierhaus, *J. Biol. Chem.* **1986**, *261*, 14506–14514.
23 D. Hartz, D. S. Mc Pheeters, L. Gold: in *The Ribosome: Structure, Function and Evolution*, eds W. E. Hill, A. Dahlberg, R. A. Garrett et al., American Society of Microbiology, Washington, DC 1990, 275–280.
24 K. H. Nierhaus, *Biochemistry* **1990**, *29*, 4997–5008.
25 J. H. Cate, M. M. Yusupov, G. Z. Yusupova et al., *Science* **1999**, *285*, 2095–2104.
26 M. Grunberg-Manago, P. Dessen, D. Pantaloni et al., *J. Mol. Biol.* **1975**, *94*, 461–478.
27 G. Blaha, N. Burkhardt, K. H. Nierhaus, *Biophys. Chem.* **2002**, *96*, 153–161.
28 I. Gabashvili, R. Agrawal, R. Grassucci et al., *EMBO J.* **1999**, *18*, 6501–6507.

29 A. Zamir, R. Miskin, D. Elson, *J. Mol. Biol.* **1971,** *60,* 347–364.
30 R. K. Agrawal, R. K. Lata, J. Frank, *Int. J. Biochem. Cell Biol.* **1999,** *31,* 243–254.
31 M. M. Yusupov, G. Z. Yusupova, A. Baucom et al., *Science* **2001,** *292,* 883–896.
32 B. T. Wimberly, D. E. Brodersen, W. M. Clemons et al., *Nature* **2000,** *407,* 327–339.
33 K. D. Dahlquist, J. D. Puglisi, *J. Mol. Biol.* **2000,** *299,* 1–15.
34 D. Hartz, D. S. McPheeters, L. Gold, *Genes Dev.* **1989,** *3,* 1899–1912.
35 K. K. Mortensen, J. Kildsgaard, J. M. Moreno et al., *Biochem. Mol. Biol. Int.* **1998,** *46,* 1027–1041.
36 N. R. Nyengaard, K. K. Mortensen, S. F. Lassen et al., *Biochem. Biophys. Res. Commun.* **1991,** *181,* 1572–1579.
37 J. M. Moreno, H. P. Sorensen, K. K. Mortensen et al., *IUBMB Life* **2000,** *50,* 347–354.
38 J. M. Moreno, L. Drskjotersen, J. E. Kristensen et al., *FEBS Lett.* **1999,** *455,* 130–134.
39 J. M. Moreno, J. Kildsgaard, I. Siwanowicz et al., *Biochem. Biophys. Res. Commun.* **1998,** *252,* 465–471.
40 B. S. Laursen, de, A. S. S. A. et al., *Genes Cells* **2002,** *7,* 901–910.
41 B. S. Laursen, K. K. Mortensen, H. U. Sperling-Petersen et al., *J. Biol. Chem.* **2003,** *278,* 16320–16328.
42 R. Spurio, L. Brandi, E. Caserta et al., *J. Biol. Chem.* **2000,** *275,* 2447–2454.
43 S. Meunier, R. Spurio, M. Czisch et al., *EMBO J.* **2000,** *19,* 1918–1926.
44 P. Nissen, M. Kjeldgaard, S. Thirup et al., *Science* **1995,** *270,* 1464–1472.
45 P. Nissen, S. Thirup, M. Kjeldgaard et al., *Struct. Fold Des.* **1999,** *7,* 143–156.
46 M. Guenneugues, E. Caserta, L. Brandi et al., *EMBO J.* **2000,** *19,* 5233–5240.
47 C. O. Gualerzi, C. L. Pon, *Biochemistry* **1990,** *29,* 5881–5889.
48 U. L. RajBhandary, M. C. Chow: in *tRNA: Structure, Biosynthesis, and Functions,* eds D. Söll and U. L. RajBhandary, American Society for Microbiology, Washington, DC 1995, 511–528.
49 E. Schmitt, J. M. Guillon, T. Meinnel et al., *Biochimie* **1996,** *78,* 543–554.
50 C. Mayer, A. Stortchevoi, C. Kohrer et al., *Cold Spring Harb. Symp. Quant. Biol.* **2001,** *66,* 195–206.
51 M. A. Schäfer, A. O. Tastan, S. Patzke et al., *J. Biol. Chem.* **2002,** *277,* 19095–19105.
52 S. K. Choi, D. S. Olsen, A. Roll-Mecak et al., *Mol. Cell. Biol.* **2000,** *20,* 7183–7191.
53 A. Marintchev, V. G. Kolupaeva, T. V. Pestova et al., *Proc. Natl. Acad. Sci. USA* **2003,** *100,* 1535–1540.
54 G. Boileau, P. Butler, J. W. B. Hershey et al., *Biochemistry* **1983,** *22,* 3162–3170.
55 P. Nissen, M. Kjeldgaard, J. Nyborg, *EMBO J.* **2000,** *19,* 489–495.
56 R. Agrawal, P. Penczek, R. Grassucci et al., *Proc. Natl.. Acad. Sci. USA* **1998,** *95,* 6134–6138.
57 R. K. Agrawal, A. B. Heagle, P. Penczek et al., *Nat. Struct. Biol.* **1999,** *6,* 643–647.
58 M. G. Gomez-Lorenzo, C. M. T. Spahn, R. K. Agrawal et al., *EMBO J.* **2000,** *19,* 2710–2718.
59 H. Stark, M. V. Rodnina, J. Rinkeappel et al., *Nature* **1997,** *389,* 403–406.
60 H. Stark, M. V. Rodnina, H. J. Wieden et al., *Cell* **2000,** *100,* 301–309.
61 H. Stark, M. V. Rodnina, H. J. Wieden et al., *Nat. Struct. Biol.* **2002,** *15,* 15–20.
62 M. Valle, J. Sengupta, N. K. Swami et al., *EMBO J.* **2002,** *21,* 3557–3567.
63 D. Moazed, R. R. Samaha, C. Gualerzi et al., *J. Mol. Biol.* **1995,** *248,* 207–210.
64 H. Wakao, P. Romby, S. Laalami et al., *Biochemistry* **1990,** *29,* 8144–8151.
65 A. La Teana, C. O. Gualerzi, A. E. Dahlberg, *RNA* **2001,** *7,* 1173–1179.

66 K. S. Wilson, H. F. Noller, *Cell* **1998**, *92*, 131–139.
67 S. Marzi, W. Knight, L. Brandi et al., *RNA* **2003**, *9*, 958–969.
68 D. Moazed, J. M. Robertson, H. F. Noller, *Nature* **1988**, *334*, 362–364.
69 D. M. Cameron, J. Thompson, P. E. March et al., *J. Mol. Biol.* **2002**, *319*, 27–35.
70 L. Belova, T. Tenson, L. Q. Xiong et al., *Proc. Natl. Acad. Sci. USA* **2001**, *98*, 3726–3731.
71 R. Benne, N. Naaktgeboren, J. Gubbens et al., *Eur J. Biochem.* **1973**, *32*, 372–380.
72 J. Dubnoff, A. Lockwood, U. Maitra, *J. Biol. Chem.* **1972**, *247*, 2884–2894.
73 J. Lee, T. Pestova, B. Shin et al., *Proc. Natl. Acad. Sci. USA* **2002**, *99*, 16689–16694.
74 T. V. Pestova, I. B. Lomakin, J. H. Lee et al., *Nature* **2000**, *403*, 332–335.
75 J. Tomsic, L. A. Vitali, T. Daviter et al., *EMBO J.* **2000**, *19*, 2127–2136.
76 A. Antoun, M. Y. Pavlov, K. Andersson et al., *EMBO J.* **2003**, *22*, 5593–5601.
77 J. Weiel, J. W. Hershey, *Biochemistry* **1981**, *20*, 5859–5865.
78 G. Risuleo, C. Gualerzi, C. Pon, *Eur. J. Biochem.* **1976**, *67*, 603–613.
79 D. Hartz, J. Binkley, T. Hollingsworth et al., *Gene Dev.* **1990**, *4*, 1790–1800.
80 J. K. Sussman, E. L. Simons, R. W. Simons, *Mol. Microbiol.* **1996**, *21*, 347–360.
81 C. Sacerdot, P. Dessen, J. W. B. Hershey et al., *Proc. Natl. Acad. Sci. USA* **1984**, *81*, 7787–7791.
82 C. Sacerdot, G. Fayat, P. Dessen et al., *EMBO J.* **1982**, *1*, 311–315.
83 C. L. Olsson, M. Graffe, M. Springer et al., *Mol. Gen. Genet.* **1996**, *250*, 705–714.
84 Y. Shimizu, A. Inone, Y. Tomari et al., *Nat. Biotechnol.* **2001**, *19*, 751–755.
85 J. H. Kycia, V. Biou, F. Shu et al., *Biochemistry* **1995**, *34*, 6183–6187.
86 E. de Cock, M. Springer, F. Dardel, *Mol. MicroBiol.* **1999**, *32*, 193–202.
87 D. Petrelli, A. LaTeana, C. Garofalo et al., *EMBO J.* **2001**, *20*, 4560–4569.
88 V. Biou, F. Shu, V. Ramakrishnan, *EMBO J.* **1995**, *14*, 4056–4064.
89 C. Garcia, P. L. Fortier, S. Blanquet et al., *Eur. J. Biochem.* **1995**, *228*, 395–402.
90 C. Garcia, P. L. Fortier, S. Blanquet et al., *J. Mol. Biol.* **1995**, *254*, 247–259.
91 J. P. McCutcheon, R. K. Agrawal, S. M. Philips et al., *Proc. Natl. Acad. Sci. USA* **1999**, *96*, 4301–4306.
92 M. Pioletti, F. Schlunzen, J. Harms et al., *EMBO J.* **2001**, *20*, 1829–1839.
93 M. A. Firpo, M. B. Connelly, D. J. Goss et al., *J. Biol. Chem.* **1996**, *271*, 4693–4698.
94 C. Ehresmann, H. Moine, M. Mougel et al., *Nucleic Acids Res.* **1986**, *14*, 4803–4821.
95 L. A. MacKeen, L. Kahan, A. J. Wahba et al., *J. Mol. Biol.* **1980**, *255*, 10526–10531.
96 V. Ramakrishnan, *Cell* **2002**, *108*, 557–572.
97 S. Srivastava, A. Verschoor, J. Frank, *J. Mol. Biol.* **1992**, *226*, 301–304.
98 W. Tapprich, D. Goss, A. Dahlberg, *Proc. Natl. Acad. Sci. USA* **1989**, *86*, 4927–4931.
99 M. Sette, P. vanTilborg, R. Spurio et al., *EMBO J.* **1997**, *16*, 1436–1443.
100 H. Schindelin, W. Jiang, M. Inouye et al., *Proc. Natl. Acad. Sci. USA* **1994**, 91.
101 L. Sherlin, T. Bullock, K. Newberry et al., *J. Mol. Biol.* **2000**, *299*, 431–436.
102 A. Roll-Mecak, C. Cao, T. E. Dever et al., *Cell* **2000**, *103*, 781–792.
103 A. Dallas, H. F. Noller, *Mol. Cell* **2001**, *8*, 855–864.
104 H. U.Petersen, A.Danchin, M.Grunberg-Manago, *Biochemistry*, **1976**, *15*, 1357–1362.
105 K.Saito, L. C. Mattheakis, M. Nomura, *J. Mol. Biol.*, **1994**, *235*, 111–124.
106 A. G. Balakin, E. A. Skripkin, I. N. Shatsky, A. A. Bogdanov, *Nucl. Acids Res.*, **1992**, *20*, 563–571.
107 T. Udagawa, Y. Shimizu, T. Ueda, *J. Biol. Chem.*, **2004**, *279*, 8539–8546.
108 S. O'Donnell, G. Janssen, *J. Bacteriol.*, **2002**, *184*, 6730–6733.
109 M. A. Schäfer, A. O. Tastan, S. Patzke et al., *Biol. Chem.*, **2002**, *277*, 19095–19105.

110 M. M. Yusupov, G. Z. Yusupova, A.Baucom et al., *Science,* **2001,** *292,* 883–896.
111 S. Grill, I. Moll, D. Hasenohrl et al., *FEBS Lett.,* **2001,** *495,* 167–171.
112 I. Moll, U. Bläsi, *Biochem. Biophys. Res. Comm.,* **2002,** *297,* 1021–1026.
113 K.Tedin, A. Resch, U. Blasi, *Mol. Microbiol.,* **1997,** *25,* 189–199.
114 J. Sengupta, R. Agrawal, and J. Frank, *Proc. Natl Acad. Sci. USA.,* **2001,** *98,* 11991–11996.

7.2 Mechanism and Regulation of Protein Synthesis Initiation in Eukaryotes

Alan G. Hinnebusch, Thomas E. Dever, and Nahum Sonenberg

7.2.1 Introduction

7.2.1.1 Overview of Translation-initiation Pathways in Eukaryotes and Prokaryotes

The decoding of an mRNA transcript and synthesis of a protein by the ribosome requires the assistance of two highly conserved translation-elongation factors known as EF1A and EF2 in eukaryotes (and archaea) and EF-Tu and EF-G in eubacteria (reviewed by Gualerzi et al. [1] and in Chap. 7.1). Studies on the structure and mechanics of the ribosome and the roles of the elongation factors have revealed the intricate functions of these enzymes, and the complex reactions required for efficient protein synthesis of high fidelity. Prior to the elongation phase of translation, the ribosome must be loaded with the initiator methionyl tRNA (Met-tRNA$_i^{Met}$) and assembled on an mRNA at the start codon in a process referred to as initiation. The general scheme of translation initiation seems to be conserved throughout evolution, and a core set of *trans*-acting initiation factors that promote these reactions are similarly conserved. In eukaryotes, several embellishments to the core initiation pathway have evolved, and these new steps require the functions of additional initiation factors. The eukaryotic-specific factors not only increase the rate and fidelity of the process, but also provide a means to regulate protein synthesis in response to cellular or environmental signals.

The general schemes of translation initiation in prokaryotes and eukaryotes, summarized in Fig. 7.2-1A and B is based largely on the biochemical activities of the purified factors and other components of the protein synthesis machinery. (The relevant literature supporting the depiction of this pathway is not cited in this introductory note, but can be found in the body of this chapter for the eukaryotic pathway.) The small and large ribosomal subunits have distinct roles in protein synthesis. The small subunit is responsible for decoding and contains binding sites for the tRNAs and the mRNA, whereas the large subunit contains the active site of the peptidyltransferase. In both kingdoms, the starting point for assembly of the initiation complex is the production of free small ribosomal subunits. In eukaryotes, binding of the initiation factors (eIFs) 1, 1A and 3 to the small ribosomal subunit prevents its coupling with the large subunit. The initiation complex is then assembled on the free small subunit as follows.

The first step is the binding of Met-tRNA$_i^{Met}$ to the P-site of the small subunit. The Met-tRNA$_i^{Met}$ does not bind alone, rather it is delivered to the ribosome by eIF2. eIF2, similar to IF2 in eubacteria, is a GTP-binding (G) protein; however, only eIF2 requires GTP to bind Met-tRNA$_i^{Met}$. The eIF2 forms a stable ternary complex with

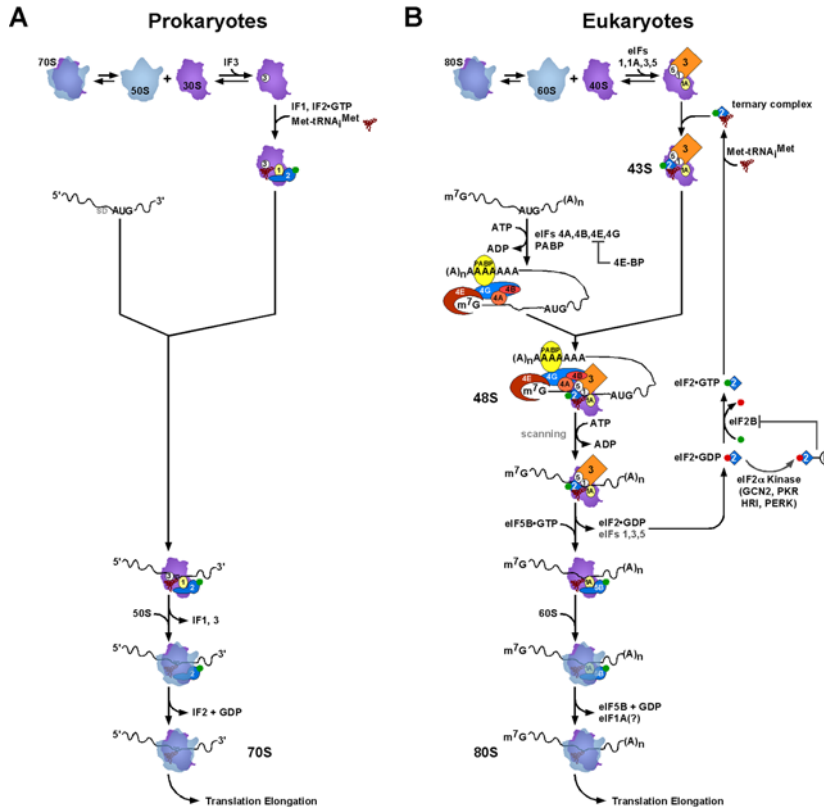

Figure 7.2-1 Pathways of translation initiation in prokaryotes and eukaryotes. The individual steps in the prokaryotic (A) and eukaryotic (B) pathways have been aligned to reflect the conservation of the reactions and functions of the factors. The three initiation factors (IF1-IF3) in prokaryotes and the various eukaryotic initiation factors (eIFs) are labeled. Biochemical studies have suggested that an alternate pathway in which mRNA binding to the 30S subunit precedes Met-tRNA$_i^{Met}$ binding may also function in prokaryotes (see Chap. 7.1). At the completion of the initiation pathway, Met-tRNA$_i^{Met}$ is bound to the ribosomal P site and the A site is vacant waiting for binding of the first elongating tRNA in an eEF1 A/EF-Tu•GTP•aminoacyl-tRNA ternary complex. The green dot represents GTP and the red dot is GDP.

GTP and Met-tRNA$_i^{Met}$, and this eIF2•GTP•Met-tRNA$_i^{Met}$ ternary complex (TC) binds to the 40S subunit. The factors eIF1, eIF1A, and eIF3 all stimulate binding of the TC to the 40S ribosome to form a 43S preinitiation complex. Binding of Met-tRNA$_i^{Met}$ to IF2 in bacteria is dependent on formylation of the methionine, a modification that does not occur in eukaryotes.

The next step in the pathway entails binding of the small ribosomal subunit to mRNA. Biochemical studies on translation initiation in prokaryotes revealed no fixed order of binding by fMet-tRNA$_i^{Met}$ and mRNA to the 30S subunit; however, genetic studies support the scheme shown in Fig. 1A wherein tRNA binding precedes mRNA binding (1). The 3′ end of 16S rRNA in the 30S ribosomal subunit binds dierctly to the Shine-Dalgarno (SD) sequence located just upstream of the start codon (see Chap. 7.1). In the cap-dependent initiation pathway found in eukaryotes, formation of the 43S preinitiation complex containing Met-tRNA$_i^{Met}$ is a prerequisite for mRNA binding and the formation of a 48S preinitiation complex (Fig. 7.2-1B). The m^{7}GpppN (where N is any nucleotide) cap structure at the 5′-end of the mRNA is the entry point for 40S ribosomes, and the start site is selected as the ribosome scans along the mRNA. Multiple initiation factors mediate the 5′-cap-binding specificity of the 48S complex. The eIF4F cap-binding complex consists of the cap-binding protein eIF4E, the ATP-dependent RNA helicase eIF4A, and the scaffold/adaptor protein eIF4G. The eIF4G is thought to facilitate ribosome binding near the 5′-cap by forming a bridge between the eIF4E•cap complex and eIF3, a constituent of the 43S complex. The eIF4G also has a binding domain for the poly(A)-binding protein (PABP) and thus can mediate binding of both ends of the mRNA to eIF3 and the 43S complex (Fig. 7.2-1B).

Following the formation of the eukaryotic 48S complex near the cap, the 40S ribosome scans in an ATP-dependent reaction in search of a start codon. It is generally thought that ATP is consumed by eIF4A in the removal of RNA secondary structures that impede sliding of 40S subunits along the mRNA. The eIF4B greatly stimulates the RNA helicase activity of eIF4A. Typically, translation initiates at the first AUG codon encountered during scanning from the cap, and several factors (eIF1, eIF1A eIF4G, and eIF2) play important roles in scanning and AUG recognition. Pairing of the anticodon of Met-tRNA$_i^{Met}$ with the AUG codon triggers GTP hydrolysis by eIF2, stimulated by the concerted action of the GTPase activating protein (GAP) eIF5 and the 40S ribosome itself. The eIF2•GDP and many, if not all, of the other initiation factors are subsequently released from the 48S complex (Fig. 7.2-1B).

In prokaryotes, IF1 and IF3 dissociate from the ribosome following AUG recognition, whereas IF2 remains bound (Fig. 7.2-1A). eIF5B, the eukaryotic homolog of bacterial IF2, promotes joining of the large ribosomal subunit to the preinitiation complex. Subunit joining triggers GTP hydrolysis by eIF5B, and release of these factors. (As eIF1A interacts with eIF5B, it is possible that these factors are released as a complex following GTP hydrolysis by eIF5B (Fig. 7.2-1B).) Finally, the 80S initiation complexes are ready to enter the elongation phase of protein synthesis and produce a protein. The eIF2•GDP must be recycled to eIF2•GTP by the guanine nucleotide exchange factor (GEF) eIF2B to permit a new round of initiation (Fig. 7.2-1B). In contrast, eIF5B (and IF2) are thought to recycle to the GTP-bound state without the assistance of a GEF.

A fraction of eukaryotic mRNAs is translated by an alternative mechanism, known as internal initiation, in which the 40S ribosome, with or without the assistance of eIFs, binds directly to an internal sequence in the mRNA upstream of the start codon. The 40S subunit is transferred from this internal ribosome entry site (IRES)

to the start codon either directly or through a short period of scanning. This mode of ribosome binding is similar to the SD/30S subunit interaction in bacteria. Consistently, IRES-dependent translation mechanisms dispense with some, or even all, of the canonical eukaryotic initiation factors.

7.2.1.2 Conservation and diversity of translation-initiation factors among bacteria, archaea and eukaryotes

Comparison of the translation-initiation factors in bacteria (Fig. 7.2-1A and Chap. 7.1) and in eukaryotes (Fig. 7.2-1B) reveals only three initiation factors in bacteria against at least 12 factors in eukaryotes. Several of the eukaryotic factors are composed of multiple polypeptides, and the 28 polypeptides that comprise the full complement of eukaryotic factors are listed in Tables 7.2-1 and 7.2-2, highlighting their functions and the conservation of sequences among human, plant and yeast homologs. Examination of the genome sequences from several archaea reveals orthologs of a subset of the eukaryotic factors, suggesting that archaea possess an initiation mechanism, which is intermediate in complexity between the prokaryotic and eukaryotic pathways.

The three bacterial factors IF1, IF2, and IF3 are functionally or structurally conserved in all three kingdoms, interact directly with the ribosome, and promote conserved steps in the initiation pathways (Fig. 7.2-1 and 7.2-2). The bacterial factors IF1 and IF2 perform analogous roles to the eukaryotic factors eIF1A and eIF5B, consistent with the structural conservation of these factors through evolution. Pairwise alignments among the bacterial, archaeal, and eukaryotic IF1/aIF1A/eIF1A factors reveal sequence identities ranging from 21 to 38% [2], and the solution structures of IF1 and eIF1A contain homologous oligonucleotide/oligosaccharide binding (OB) folds [3, 4]. The bacterial, archaeal and eukaryotic IF2/aIF5B/eIF5B sequences are 27–39% identical with aIF5B, excluding the nonconserved N-terminal domain (NTD) present in prokaryotic and eukaryotic factors [5]. Both IF2 and eIF5B have been implicated in promoting Met-tRNA$_i^{Met}$ binding to the ribosome and in subunit joining. In addition, IF2 and eIF5B physically and functionally interact with the homologous factors IF1 and eIF1A, respectively, although probably only on the ribosomes in the bacterial situation [6, 7]. Both bacterial IF3 and eukaryotic eIF1 play important roles in translation start site recognition. Intriguingly, eIF1 and the C-terminal domain (CTD) of IF3 have similar α/β-fold structures with a four- or five-stranded β-sheet packed against two α-helices (see Ref. [8]). The presence of a highly conserved (25–30% sequence identity) eIF1-like protein, distinct from IF3, in some, but not all, bacteria indicates that additional investigations are necessary to determine whether IF3 and eIF1 are true homologs.

The eIF5A in eukaryotes and EF-P in bacteria share approximately 20% sequence identity [2], and both proteins have been implicated in translation. They both have stimulatory activities in model assays of first-peptide-bond formation, especially the synthesis of methionyl puromycin; however, their precise roles in protein synthesis are unknown [9]. As depletion of eIF5A in yeast only slightly impaired protein

Table 7.2-1 Initiation factors from mammalian, plant, and yeast cells [a]

Molecular weight[b]						
Name	**Human**	**Arabidopsis**	**Saccharomyces**	**Yeast gene**	**% identity[c]**	**Functions[d]**
eIF1	12.6	12.6	12.3	*SU11*	58	AUG recognition; promotes TC and mRNA binding to 40S; 80S anti-association, binds eIF3c, eIF3a, and eIF5
eIF1A	16.5	16.6	17.4	*TIF11*	65	Promotes TC and mRNA binding to 40S; 80S anti-association; binds RNA, eIF5B, eIF2, eIF3, and eIF5B
eIF2α	36.2	41.6	34.7	*SUI2*	58	TC component; AUG recognition; mediates inhibitory interaction with eIF2B on phosphorylation of Ser^{51}, binds eIF2γ, binds eIF2B $\alpha/\beta/\delta$ subcomplex when phosphorylated
eIF2β	39.0	26.6	31.6	*SUI3*	42	TC component; GTP/Met-tRNA$_i^{Met}$ binding; AUG recognition; binds eIF2γ, eIF2Bε, eIF5, eIF3a, mRNA
eIF2γ	51.8	50.9	57.9	*GCD11*	71	TC component; GTP/Met-tRNA$_i^{Met}$ binding; GTPase; AUG recognition; binds eIF2α and eIF2β
eIF2Bα	33.7	39.8	34.0	*GCN3*	42	Nonessential in yeast; regulatory subunit that helps bind eIF2(αP) and inhibit GEF function; forms subcomplex with eIF2B β/δ
eIF2Bβ	39.0	43.6	42.6	*GCD7*	36	Regulatory subunit; helps bind eIF2(αP) and inhibit GEF function; forms subcomplex with eIF2B α/δ
eIF2Bγ	50.4		65.7	*GCD1*		Promotes GEF function of catalytic subdomain; forms subcomplex with eIF2Bε
eIF2Bδ	57.8	29.4	70.9	*GCD2*	36	Regulatory subunit; helps bind eIF2(αP) and inhibit GEF function; forms subcomplex with eIF2B α/β
eIF2Bε	80.2	81.9	81.2	*GCD6*	30	GEF catalytic subunit; forms subcomplex with eIF2Bγ
eIF4AI	44.4	46.7	45.1	*TIF1*	65	ATPase, RNA helicase
eIF4AII	46.3	46.8	44.6	*TIF2*		ATPase, RNA helicase

Name	Molecular weight[b] Human	Arabidopsis	Saccharomyces	Yeast gene	% identity[c]	Functions[d]
eIF4B	69.2	57.6	48.5	*TIF3*	22	Binds RNA and eIF3g; stimulates eIF4A helicase activity; nonessential in yeast
eIF4E	25.1	26.5	24.3	*CDC33*	33	Binds m^7G-cap of mRNA and eIF4G
eIFiso4E		22.5				
eIF4GI	175.6	153.2	107.1	*TIF4631*	22	Binds eIF4E, eIF4A, eIF3, eIF5, PABP, and kinase MNK1
eIF4GII	176.6	176.5	103.9	*TIF4632*	21	Binds eIF4E, eIF4A, eIF3, eIF5, PABP, and kinase MNK1
eIFiso4G		87.0				
eIF5	48.9	48.6	45.2	*TIF5*	39	AUG recognition; stimulates eIF2 GTPase in conjunction with 40S subunit; promotes TC and eIF3 binding to 40S; binds eIF2β, eIF1, and eIF3c
eIF5B	139.0		112.3	*FUN12*	70	Nonessential in yeast; GTPase; promotes subunit joining; stabilizes Met-$tRNA_i^{Met}$ binding to 40S; binds eIF1A
PABP	70.7	68.7	64.2	*PAB1*	59	Binds poly(A) tail of mRNA and eIF4G.
eIF3[e]						5 of 6 subunits essential in yeast; 10 subunits in human factor; 80S anti-association; promotes TC and mRNA binding to 40S; binds eIF5, TC, and eIF1 simultaneously in the MFC; binds eIF4G, eIF4B, and multiple 40S ribosome components

a Adapted from Ref. [174].
b The masses in kDa pertain to human or rat, Arabidopsis thaliana, and Saccharomyces cerevisiae proteins.
c Percent sequence identity shared by yeast and human proteins (from Ref. [174]).
d Some functions have been demonstrated only for the mammalian or yeast factor (see text for details).
e See Table 7.2-2 for detailed information on each subunit.

Table 7.2-2 eIF3 subunits from mammalian, plant, and yeast cells

Subunit	Human		Arabidopsis	Saccharomyces			Motifs/functions/comments[c]
	Name	MW[a]	MW	Name	Gene	MW	
eIF3a	p170	166.6	114.3	p110	*TIF32/ RPG1*	110.3	Contains PCI motif[b]; binds eIF3 subunits b, c, and j, eIF4B[d], eIF2*β*, eIF1, RPS0, RPS10, and 18S rRNA; promotes eIF2-eIF3 and eIF1-eIF3 interactions and 40S binding of eIF3; promotes TC and mRNA binding to 40S subunits in conjunction with eIF3b/c, plus a step(s) post-48S assembly
eIF3b	p116/ p110	92.4	81.9	p90	*PRT1*	88.1	Contains RRM; binds eIF3 subunits a, c, e[d], j, i, and g; promotes TC and mRNA binding to 40S subunits
eIF3c	p110	105.3	102.9	p93	*NIP1*	93.2	Contains PCI motif; binds eIF3 subunits a, b, and e[d], eIF1, eIF5, and RPS0; promotes eIF3 interactions with eIFs 1 and 5, eIF2-eIF3 interaction (via eIF5), and 40S binding of eIF3; promotes TC and mRNA binding to 40S subunits
eIF3d	p66	64.0	66.2	na[e]	na	na	Binds RNA[d], eIF3e[d]
eIF3e	p48/ INT-6	52.2	51.8	na	na	na	Contains PCI motif, binds eIF3 subunits a, b[d], c[d], d[d]
eIF3f	p47	37.6	31.9	na	na	na	Contains MDN[b] motif
eIF3g	p44	35.6	32.7	p33	*TIF35*	30.5	Contains RRM and Zn domain; binds eIF3 subunits b and i; binds RNA[d] and eIF4B
eIF3h	p40	39.9	38.4	na	na		Contains MDN[b] motif
eIF3i	p36/ TRIP-1	36.5	36.4	p39	*TIF34*	38.8	Contains 7 WD repeats; binds eIF3 subunits b and g
eIF3j	p35	29.1	na		*HCR1*	29.6	Nonessential in yeast; binds eIF3 subunits a and b; promotes MFC integrity and a step(s) post-48S assembly; 40S biogenesis
eIF3k	na	na	25.7	na	na		

a Masses in kDa calculated from deduced protein sequence.
b PCI motif has been called the PINT motif; MDN has been called the MPN motif [398, 399].
c Demonstrated for Saccharomyces subunit unless otherwise indicated.
d Demonstrated for human subunit only.
e na; not applicable, protein not found in eIF3 of this organism.

synthesis [10], the assignment of EF-P/eIF5A as a universally conserved translation-initiation factor should be viewed cautiously. This is especially true in the case of EF-P since it has been shown, using an *in vitro* translation system composed completely from purified factors, that EF-P was not necessary for translation and, furthermore, the addition of the factor did not improve the rate or efficiency of translation (T. Ueda, pers. comm.).

Building on this conserved core group of factors, the RNA-associated factor eIF4A and the Met-tRNA$_i^{Met}$-binding factor eIF2 are additionally present in archaea (Fig. 7.2-2). Whereas the translation-initiation pathway in archaea is not well understood, the identification of eIF2 and eIF4A suggests that a scanning-type mechanism for mRNA binding and AUG recognition may operate on some archaeal mRNAs. In fact, there is evidence that recognition and translation of the first open reading frame (ORF) on polycistronic mRNAs in some archaea occurs via scanning or direct binding of the ribosome to a 5′-terminal start codon, whereas subsequent ORFs are recognized by a bacterial-like SD interaction [11]. The absence of the cap-binding protein eIF4E as well as eIF4G from archaea is consistent with lack of m^{7}GpppN caps on archaeal mRNAs. Finally, several factors, including other members of the RNA-binding eIF4 family of proteins, eIF3, and the eIF2-interacting proteins eIF5 and eIF2B are restricted to eukaryotes (Fig. 7.2-2).

The presence of the GTPase eIF2, as well as the complex cap-dependent mRNA binding and scanning mechanisms in eukaryotic initiation, provide new opportunities for translational regulation. Phosphorylation of the α-subunit of eIF2 converts eIF2 from a substrate to competitive inhibitor of eIF2B, impairing the recycling of inactive eIF2•GDP to active eIF2•GTP, thereby inhibiting protein synthesis (Fig. 7.2-1B). Binding of 4E-binding proteins (4E-BPs) to eIF4E blocks eIF4E binding to eIF4G and prevents formation of the cap-binding complex eIF4F, thus impairing mRNA binding to the ribosome. Phosphorylation of the 4E-BPs prevents their binding to eIF4E and relieves translational inhibition. Regulation of translation-initiation factors has not been reported in bacteria. Thus, the appearance of new mechanisms and factors in evolution to facilitate both Met-tRNA$_i^{Met}$ and mRNA binding to the ribosome has provided powerful means to regulate initiation in eukaryotes.

7.2.1.3 Genetic assays for *in vivo* functions of eIF2

Many advances in our knowledge of the functions of eIF2, its GEF (eIF2B), and its GAP (eIF5) in recruitment of Met-tRNA$_i^{Met}$ and recognition of the start codon, have come from genetic analysis of translational control in yeast. Accordingly, these genetic systems are summarized briefly before considering the biochemical mechanisms of these steps in the pathway. As mentioned above, recycling of eIF2-GDP to eIF2-GTP by eIF2B is impaired by phosphorylation of eIF2 on Ser-51 of its α-subunit (eIF2[αP]) (Fig. 7.2-1B). As eIF2 is generally present in excess of eIF2B, and phosphorylation of eIF2-GDP increases its affinity for eIF2B, the recycling of eIF2 can be impaired by phosphorylation of only a fraction of eIF2 [12, 13]. Four eIF2α – Ser-51 kinases regulated by different signals have been identified in mammalian cells: HRI (heme deprivation), PKR (double-stranded RNA produced in virus-

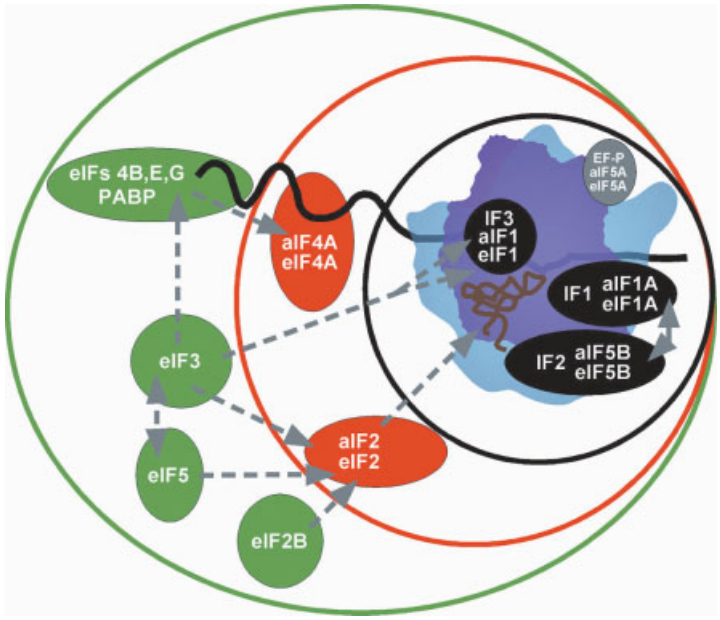

Figure 7.2-2 Conservation of a core set of translation-initiation factors through evolution. The translation-initiation factors identified in bacteria, archaea and eukaryotes are depicted based on their conservation through evolution. Depicted in black and enclosed within the innermost black circle, the three universally conserved initiation factors IF1/eIF1A, IF2/eIF5B, and IF3/eIF1 interact directly with the ribosome. The proposed grouping of IF3 and eIF1 is based on similar α/β-fold structures for the two factors, and their common function to insure accurate Met-tRNA$_i^{Met}$ and start site selection in the ribosome P-site. The factor EF-P/eIF5A, depicted in gray, is also universally conserved, however, questions have been raised regarding the assignment of this protein as a translation factor, and lowering the amount of eIF5A in yeast did not appear to impair translation initiation [10]. Building upon this core set of factors, the DEAD-box RNA helicase eIF4A and the tRNA delivery factor eIF2 were added in archaea and retained in eukaryotes (red circle). Finally, the eIF4 family of factors that function in mRNA binding, the eIF3 complex that facilitates both mRNA and tRNA binding to the 40S subunit, and the proposed GAP (eIF5) and GEF (eIF2B) for eIF2 were added in eukaryotes (green circle). Dashed gray arrows indicate protein–protein, protein–RNA (eIF2-tRNA), or factor–ribosome (eIF3-40S) interactions.

infected cells), PERK (unfolded proteins in the endoplasmic reticulum), and GCN2 (serum or amino acid starvation, UV irradiation) [14–18]. GCN2 (General Control Nonderepressible 2) is the only eIF2α kinase in *Saccharomyces cerevisiae,* where it is

activated by diverse starvation or stress conditions, including amino acid limitation. Physiological activation of GCN2 in amino acid-starved yeast cells does not generate eIF2[αP] at a level that prevents eIF2 recycling and blocks protein synthesis; instead, it specifically increases translation of *GCN4* mRNA, encoding the transcriptional activator of amino acid biosynthetic enzymes subject to the general amino acid control. The specific induction of *GCN4* translation by eIF2[αP] is mediated by four short open reading frames (uORFs) in the leader of *GCN4* mRNA [19].

According to the current model (Fig. 7.2-3), ribosomes scanning from the 5′-cap translate uORF1, and ~50% resume scanning as 40S subunits. Under nonstarvation conditions, all of these reinitiating ribosomes rebind the TC and reinitiate at uORFs 2–4, after which they dissociate from the mRNA and are prevented from translating *GCN4*. Phosphorylation of eIF2α by GCN2 in starved cells inhibits eIF2B and lowers the concentration of TC. Consequently, as many as ~50% of the 40S subunits scan-

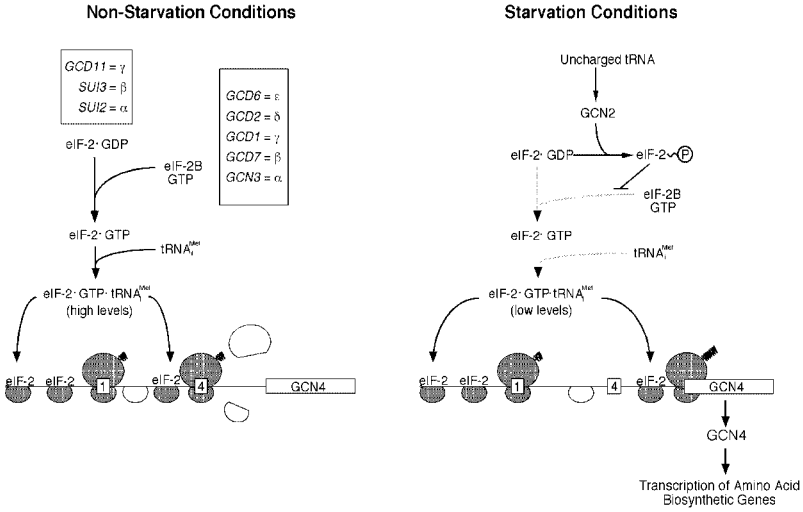

Figure 7.2-3 Molecular model for *GCN4* translational control. *GCN4* mRNA is depicted with uORF1 and 4 and the *GCN4* coding sequences shown as boxes. For simplicity, uORF2 and uORF3 were omitted because they are functionally redundant with uORF4. The 40S ribosomal subunits are shaded when associated with the ternary complex TC and competent to reinitiate at the next start codon they encounter. 80S ribosomes are shown translating uORF1, uORF4, or *GCN4* with the synthesized peptides depicted as coils. Free 40S and 60S subunits are shown dissociating from the mRNA following translation of uORF4. The three subunits of eIF2 and the five subunits of eIF2B are listed in the boxes on the left panel. Following translation of uORF1, the 40S ribosome remains attached to the mRNA and resumes scanning. Under nonstarvation conditions, the 40S quickly rebinds the TC and reinitiates at uORF4 because the TC concentration is high. Under amino acid starvation conditions, many 40S ribosomes fail to rebind the TC until scanning past uORF4, because the TC concentration is low, and reinitiate at *GCN4* instead. TC levels are reduced in starved cells due to phosphorylation of eIF2 by the kinase GCN2, converting eIF2 from substrate to inhibitor of its guanine-nucleotide exchange factor eIF2B.

ning from uORF1 reach uORF4 before rebinding the TC, and lacking Met-tRNA$_i^{Met}$, they bypass the uORF4 start codon. Most of these ribosomes rebind the TC before reaching the *GCN4* start codon. Thus, reducing TC levels by phosphorylating eIF2α allows a fraction of scanning 40S subunits to by-pass the inhibitory uORFs 2–4 and re-initiate at *GCN4* instead (see Refs. [15, 19] and references therein).

Mutants harboring lesions in eIF2γ [20] and the β, γ, δ, and ε subunits of eIF2B [19] were first isolated by their constitutive derepression of *GCN4* translation (general control derepressed, or Gcd$^-$ phenotype). These mutations also produce a slow-growth phenotype (Slg$^-$) and reduce rates of protein synthesis on rich medium, indicating nonlethal impairment of the essential functions of eIF2 or eIF2B [21–24]. Mutations in eIF2β and eIF2α can also produce Gcd$^-$ and Slg$^-$ phenotypes [25], as does reducing the copy number of *IMT* genes, encoding tRNA$_i^{Met}$ [26]. The derepression of *GCN4,* conferred by these Gcd$^-$ mutations is maintained in *gcn2Δ* cells [25, 27], suggesting that the mutations reduce TC levels independent of eIF2α phosphorylation. Consistently, overexpressing eIF2 prevents derepression of *GCN4* in starved wild-type cells (Gcn$^-$ phenotype) [26], presumably by offsetting the inhibitory effect of eIF2[αP] on TC formation (Fig. 7.2-3). Thus, the level of *GCN4* expression is a sensitive *in vivo* indicator of the functions of eIF2 and eIF2B in TC formation.

The genetic studies of Donahue and colleagues have provided a valuable entry into the mechanism of start codon selection by the TC. They have isolated mutations allowing expression of a defective *HIS4* gene harboring a non-AUG start codon. The isolation of mutations with this Sui$^-$ (suppressor of initiation codon) phenotype in one of the genes encoding tRNA$_i^{Met}$ showed that base-pairing between the start codon and Met-tRNA$_i^{Met}$ plays a dominant role in directing the 40S subunit to the initiation site [28]. The Sui$^-$ selection also yielded mutations in all three subunits of eIF2, eIF5 (the GAP for eIF2), and eIF1, implicating these factors in stringent selection of the start codon.

7.2.2 Generation of Free 40S Subunits and 40S Binding of Met-tRNA$_i^{Met}$

7.2.2.1 Dissociation of Idle 80S Ribosomes

Most ribosomal subunits that are not engaged in translation occur in idle 80S ribosomes, or "80S couples", which must be dissociated into 40S and 60S subunits to allow assembly of the 43S preinitiation complex. The eIF1A, eIF3, and eIF1 have all been implicated in this reaction, but the molecular mechanisms are unknown. The mammalian eIF3 can bind to 40S ribosomes in the absence of other factors [29], but its binding site on the 40S subunit, as visualized in EM images of negatively stained native 40S subunits, does not seem to preclude association of the 60S subunit [30, 31]. Most of the mass of eIF3 was found attached to the back lobes rather than to the 60S-interface side of the 40S subunit. Thus, eIF3 might function indirectly by

producing an allosteric change in the 40S subunit that inhibits 60S joining. It may also sterically impede 60S joining by stabilizing the binding of TC to the interface side of the 40S subunit. Consistent with the latter is a report that eIF3 does not exhibit ribosome dissociation activity alone, but can prevent 60S subunits from displacing the TC from 40S subunits in the absence of AUG or mRNA [32]. The eIF1A can augment this anti-association activity of eIF3, and can also function with eIF1 in the absence of eIF3 to prevent disruption of 43S complexes by 60S subunits [33]. The eIF3 in yeast is physically linked to eIF1, eIF5, and the TC in a multifactor complex (MFC) that can exist free of ribosomes [34]. Hence, all of these factors may bind coordinately to the 40S subunit and, together with eIF1A, produce a stable assembly that can resist displacement by a 60S subunit prior to mRNA binding. This would be consistent with previous observations that the stimulatory effect of eIF3 on TC binding to 40S subunits was greater when 60S subunits were present [35], and that binding of eIF3 itself is enhanced by simultaneous binding of the TC to 40S subunits [35–36].

7.2.2.2 Components of the eIF2/GTP/Met-tRNA$_i^{Met}$ Ternary Complex

Sequence Determinants of tRNA$_i^{Met}$ that Restrict it to the Initiation Pathway

Eukaryotic tRNA$_i^{Met}$ has sequence and structural characteristics that allow eIF2 to distinguish it from the elongator methionyl tRNA (tRNA$_e^{Met}$) and all other elongator tRNAs (reviewed in Ref. [15]). These include the A1:U72 base pair at the very end of the acceptor stem, several G:C base pairs in the anticodon stem, both of which were implicated in eIF2 binding, and (for yeast tRNA$_i^{Met}$) A54 in loop IV [39–42] (Fig. 7.2-4A). The A1:U72 base pair in tRNA$_i^{Met}$ also discriminates against its activity in elongation [40, 43], as do the A50:U64 and U51:A63 base pairs in the TΨC stem of human tRNA$_i^{Met}$, and the corresponding U50:A64 base pair in yeast tRNA$_i^{Met}$, which are believed to perturb the structure of this helix in a way that blocks eEF1α binding. The tRNA$_i^{Met}$ in fungi and plants additionally contains a unique 2′-*O*-phosphoribosyl modification of A64 in the TΨC helix that prevents elongator function [44, 45] and impedes binding to eEF1α-GTP [46]. Thus, structural perturbation of the TΨC stem seems to be a common strategy to block tRNA$_i^{Met}$ binding to eEF1α [43]. Inactivation of the yeast enzyme responsible for A64 modification (encoded by *RIT1*) showed that the modification is dispensable for initiator function and serves to block its activity in elongation [45]. This activity of RIT1 becomes essential in strains with mutations in eIF2 subunits or lacking a full complement of the *IMT* genes encoding tRNA$_i^{Met}$ [47]. The methionyl group attached to charged Met-tRNA$_i^{Met}$ may also increase the efficiency of translation initiation, as initiators charged with certain other amino acids function poorly in initiation [48, 49]. For more information about tRNA structure and modifications refer to Chap. 4.1.

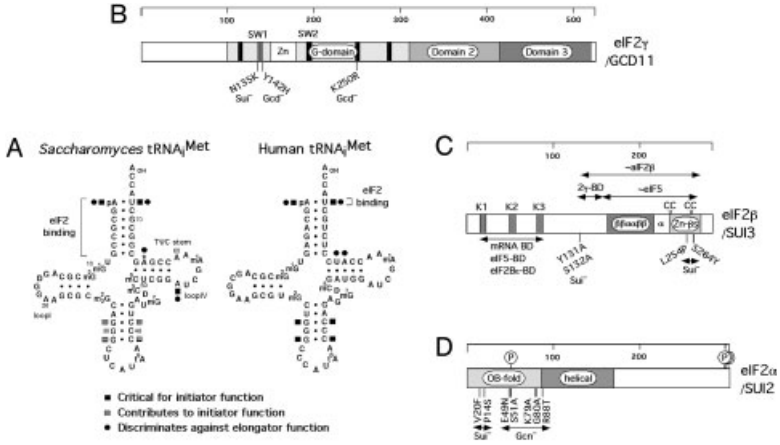

Figure 7.2-4 Schematic representations of the secondary structures of yeast and human initiator tRNA^{Met} and the primary structures of the subunits of yeast eIF2. **(A)** The sequences of the tRNAs and identities of modified bases are found in Ref. [395]. The asterisk at position 64 of yeast initiator designates the phosphoribosyl group attached to the ribose 2′-OH. See text for details. The numbering of bases shown for the yeast initiator also applies to human initiator. This figure has been adapted from RajBhandary and Chow [396] and is reprinted with permission from Ref. [15]. **(B)** The amino acid sequence of the γ subunit of eIF2 is depicted as a rectangle with amino acid positions shown above. Shading is used to depict the G-domain, and domains 2 and 3, all defined by the crystal structure of aIF2γ shown in Fig. 7.2-5(A). The four conserved motifs characteristic of G proteins are shown as black bars in the G-domain, one of which coincides with the switch 2 element (SW2). The locations and phenotypes of selected mutations are shown beneath the schematic using the one-letter code for amino acids. The abbreviation for the wild-type residue is followed by the position of the residue in the protein sequence and then the abbreviation for the substituting residue in the mutant. **(C)** The amino acid sequence of the β subunit of eIF2 is depicted with shading used to identify the lysine boxes (K1–K3) and the domains labeled $\beta\beta\alpha\alpha\beta\beta$ and Zn-βs (for Zn-binding β-sheet) whose 3D structures can be predicted from that of aIF2β shown in Fig. 7.2-5B. The four cysteine (C) residues that comprise the Zn-binding domain are indicated. Regions of similarity to eIF5 (~eIF5) or aIF2β (~aIF2β) are delimited with double-headed arrows, as are binding domains (BDs) for various factors or mRNA. The locations and phenotypes of selected mutations are shown beneath the schematic. **(D)** The amino acid sequence of the α subunit of eIF2 is depicted with shading used to identify the domains labeled OB-fold and helical whose 3D structures are shown in Fig. 7.2-5(C). The locations of the phosphorylation site for the kinases GCN2, HRI, PERK/PEK, and PKR at position 51, and the three casein kinase sites at the C-terminus are indicated with Ps. The locations and phenotypes of selected mutations are shown beneath the schematic. See text for more details.

eIF2γ Plays a Central Role in Binding Guanine Nucleotides and Initiator tRNA

The eIF2γ belongs to the superfamily of GTP-binding proteins and is closely related to the bacterial and eukaryotic elongation factors, EF-Tu and eEF1α, respectively, which deliver charged elongator tRNAs in ternary complexes with GTP to the ribosome during the elongation phase of protein synthesis. The molecular masses and sequences of eIF2γ proteins are well conserved among animals, plants, and fungi (Table 7.2-1), and orthologs also exist in archaea (Fig. 7.2-2). The sequence similarities between eukaryotic and archaeal eIF2γ proteins and EF-Tu extend throughout the G domain (domain 1), and into domains 2 and 3 [20, 50, 51] (Fig. 7.2-4B), consistent with the occurrence of binding sites for guanine nucleotides and Met-tRNA$_i^{Met}$ in eIF2γ. The crystal structure of the archaeal ortholog of eIF2γ from *P. abyssi* (Fig. 7.2-5A) shows three domains highly similar to domains 1–3 of EF-Tu, and the binding pocket for GDP-Mg^{2+} seen in the structure of the aIF2γ–GDP complex is superimposable on that of EF-Tu. Consistently, the *gcd11–K250R* mutation in yeast eIF2γ, which is predicted to alter the conserved Lys residue in the third consensus motif of the GDP-binding pocket [51] (Figs. 7.2-4B and 7.2-5A), increased the off-rates for GDP and GTP, without affecting Met-tRNA$_i^{Met}$ binding to purified eIF2. The eIF2–GTP complex is stabilized by Met-tRNA$_i^{Met}$, and addition of Met-tRNA$_i^{Met}$ overcame the GTP-binding defect of the *gcd11-K250R* lesion *in vitro* and suppressed its Slg$^-$ and Gcd$^-$ phenotypes *in vivo* [52]. Thus, there is little doubt that eIF2γ directly binds GTP.

In EF-Tu, the relative orientation of domain 1 versus domains 2 and 3 varies dramatically between the GDP-bound (inactive) and GDPNP-bound (active) states as a result of altered conformations of the switch-1 and switch-2 regions, which contact the γ-phosphate of GDPNP. In sharp contrast, the unliganded, GDP- and GDPNP-bound forms of aIF2γ all display close packing of domains 2–3 against domain 1 in the manner observed for GDPNP-bound EF-Tu. There is no difference in switch 1, and only a small conformational change in switch 2, between the GDP- and GDPNP-bound states, apparently because contacts with the γ-phosphate of GDPNP are lacking in the aIF2γ crystal structure. Therefore, it is difficult at present to account for the GTP requirement for Met-tRNA$_i^{Met}$ binding to eIF2 [51]. (It should be noted that the aIF2γ–GTP crystal structure was obtained for a mutant protein containing the G235D mutation in strand β8 of domain 2.)

A model of Met-tRNA$_i^{Met}$ docking on aIF2γ was constructed by superimposing the EF-Tu/GTP/Phe-tRNA^{Phe} complex on domains 2 and 3 of the aIF2γ–GDPNP structure. The β-hairpin in switch 1 is predicted to contact the acceptor stem and interact with the critical A1:U72 base pair in Met-tRNA$_i^{Met}$ [51]. Consistent with this model, the *gcd11-Y142H* mutation in yeast eIF2γ [24, 27], predicted to impair β-strand 2 in switch 1 [51] (Figs. 7.2-4B and 7.2-5A), produces Gcd$^-$ and Slg$^-$ phenotypes and a reduced polysome content, and is suppressed by overproducing tRNA$_i^{Met}$. Consistently, purified eIF2 containing the *gcd11-Y142H* subunit shows reduced Met-tRNA$_i^{Met}$ binding but normal off-rates for GDP and GTP [52]. The *N135K* mutation

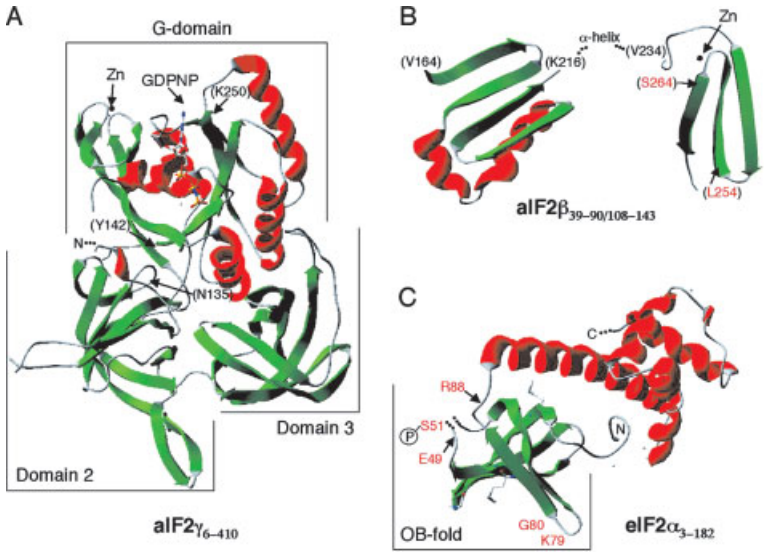

Figure 7.2-5 Ribbon diagram representations of the 3D structures of portions of aIF2γ, aIF2β, and eIF2α. **(A)** Co-crystal structure of residues 6–410 of aIF2γ from *P. abyssi* (shown with β-sheets in green and α-helices in red) in complex with GDPNP (shown in ball and stick representation) [51] (PDB ID: 1KK1). The predicted locations of selected residues in yeast eIF2γ (in parantheses) are indicated, as is the bound Zn atom and location of N-terminal residues not visualized in the structure (N...). **(B)** Solution structure of two domains of aIF2β from *M. jannaschii* joined by a predicted flexible α-helix, with a Zn atom bound to the C-terminal β-sheet domain [58] (PDB ID: 1K8B, and 1K81). The relative orientation of the two domains is unknown. The residues in yeast eIF2β corresponding to the N- and C-termini of the domains are shown in black with in parantheses. The predicted positions of two residues in yeast eIF2β which produce Sui$^-$ phenotypes when mutated are shown in red. **(C)** The crystal structure of residues 3–182 of human eIF2α [82] (PDB ID: 1KL9). The phosphorylation site at Ser^{51} is indicated in red as are the positions of residues in yeast eIF2α that produce Sui$^-$ phenotypes when mutated. All structures were drawn using the DeepView/Swiss-Pdb viewer (v. 3.7) using data obtained from the Protein Data Bank (www.pdb.org). For the NMR structures, the first of multiple solved structures stored in the PDB file was employed.

in yeast eIF2γ, isolated for its dominant Sui$^-$ phenotype [53], maps in the predicted β-hairpin of switch 1 [51] (Figs. 7.2-4B and 7.2-5A). *In vitro*, this lesion reduced TC formation, partly by increasing spontaneous GTP hydrolysis, but also by increasing the off-rate of Met-tRNA$_i^{Met}$ from eIF2 without affecting the affinity for GTP. Thus, there is strong evidence implicating switch 1 of yeast eIF2γ in Met-tRNA$_i^{Met}$ binding.

To account for the dominant Sui⁻ phenotype of this mutation, it was proposed that premature dissociation of Met-tRNA$_i^{Met}$ from the mutant eIF2–GTP complex during the scanning process allows incorrect pairing of the initiator with a near-cognate UUG codon [53].

The e/aIF2γ proteins contain some structural features not present in EF-Tu, including a disordered loop and β-hairpin in domain 2, and a zinc-binding "knuckle" containing four Cys residues appended to domain 1 [51] (Zn in Fig. 7.2-4B). Mutational analysis of yeast eIF2γ is consistent with the possibility that zinc binding to this domain is important, but not essential, for some aspect of eIF2 function [54]. However, there is no direct evidence for zinc binding by yeast eIF2γ. Moreover, only one of the four Cys residues is conserved in mammalian eIF2γ, making zinc-binding improbable for this protein. The e/aIF2γ proteins lack several residues in EF-Tu that help to clamp the 5′ phosphate group of the different elongator tRNAs [51]. Crosslinking and affinity-labeling experiments indicated that both the β and γ subunits of eIF2 are in close proximity to GTP and Met-tRNA$_i^{Met}$ in the TC [50, 55]. Moreover, an eIF2$\alpha\gamma$ dimer could bind GDP but was unable to form a stable TC with Met-tRNA$_i^{Met}$ [56]. These and other findings discussed below suggest that the β subunit contributes to Met-tRNA$_i^{Met}$ binding. The α and β subunits of both yeast and archaeal eIF2 interact directly with the γ subunit, but not with each other [51, 57], consistent with the notion that γ is the core subunit and that its functions in binding guanine nucleotides and Met-tRNA$_i^{Met}$, and in GTP hydrolysis, are augmented or regulated by the α and β subunits of eIF2.

eIF2β: Interactions with Met-tRNA$_i^{Met}$, mRNA, eIF5, and eIF3

eIF2β can be divided into three structural domains (Fig. 7.2-4C). The C-terminal half is closely related in sequence to the archaeal ortholog (aIF2β), and most probably has a two-domain structure similar to that solved by NMR for *Methanococcus Jannaschii* aIF2β [58] (Fig. 7.2-5B). The first domain in the latter consists of a four-stranded β-sheet with two helices packed against one face of the β-sheet. It is connected by an α-helical linker to the second domain, comprised of a three-stranded β-sheet with two CXXC clusters that form a Zn^{2+}-binding pocket at one end of the β-sheet. Both domains in aIF2β appear to be structurally independent units, and the C-terminal β-sheet is stabilized by Zn^{2+}. The N-terminus of eukaryotic eIF2β has an additional ~130 residues, not found in the archaeal orthologs, which contains three polylysine stretches (K-boxes 1–3) [59–61] (Fig. 7.2-4C).

Mutational analysis of yeast eIF2β (encoded by *SUI3*) shows that the Cys residues in the Zn^{2+}-binding pocket are critically required for eIF2β function *in vivo* [62]. A *SUI3* allele lacking the zinc-finger motif cannot support viability and has a dominant Gcd⁻ phenotype in otherwise wild-type cells, suggesting that the mutant protein forms an eIF2 complex defective for TC formation or 40S binding *in vivo*. Remarkably, all 13 dominant Sui⁻ alleles of *SUI3* alter conserved residues [59, 62] predicted to lie at one end or the other of the C-terminal β-sheet, in most cases near or within the loops connecting β-strands [58]. Biochemical analysis showed that two

such Sui⁻ mutations (*S264Y* and *L254P*) (Figs. 7.2-4C and 7.2-5B) increased GTPase activity by the purified TC, independent of the GAP function of eIF5 [53]. The *S264Y* mutation also led to increased dissociation of Met-tRNA$_i^{Met}$ from the TC independent of GTP hydrolysis, supporting a role for the β subunit in Met-tRNA$_i^{Met}$ binding. It was proposed that both defects increase the probability that the TC can dissociate during the scanning process and leave Met-tRNA$_i^{Met}$ inappropriately paired with a UUG start codon [53].

A segment of yeast eIF2β that is necessary and sufficient for eIF2γ binding was localized to residues 128–159 in eIF2β [63], just N-terminal to the region homologous to the well-defined structural domains in aIF2β [58] (2γ-BD (binding domain) in Fig. 7.2-4C). Alanine substitutions of the highly conserved Tyr^{131} and Ser^{132} residues in this region of yeast eIF2β (Fig. 7.2-4C) abolished *in vitro* binding to eIF2γ and impaired interaction of native eIF2β with the eIF2$\gamma\alpha$ dimer *in vivo*. The *SUI3-YS* allele containing both of these substitutions conferred Ts⁻ and Sui⁻ (or possibly Gcd) phenotypes and was synthetic lethal with the Sui⁻ *SUI3-S264Y* allele. Thus, by weakening β–γ interaction, the *SUI3-YS* mutation may exacerbate the hyperactive GTPase function of eIF2γ conferred by *S264Y*, reduce binding of Met-tRNA$_i^{Met}$ to eIF2, or both [63]. Interestingly, the C-terminal half of eIF2β shows strong similarity to the N-terminal portion of eIF5 [64] (~eIF5 in Fig. 7.2-4C), including the two CXXC clusters, raising the possibility that the homologous domains in eIF5 and eIF2β interact with one another, or compete for an interaction with the γ subunit, in a way that stimulates GTP hydrolysis by eIF2. It should be noted, however, that eIF5 lacks the major binding domain for eIF2γ between residues 128 and 159 in eIF2β [57, 63].

There are numerous reports that eIF2 binds mRNA and that this interaction can impede TC formation (reviewed in Ref. [55]) or stimulate translation [13, 65]. The β subunit has mRNA-binding activity [66] and seems to be required for mRNA binding by the eIF2 complex. A 4-thio-UTP-substituted viral mRNA was crosslinked to the C-terminal one-third of eIF2β containing the zinc-binding domain [67]; however, mutational analysis of the yeast protein suggests that the K-boxes in the NTD make an even larger contribution to mRNA binding (mRNA-BD in Fig. 7.2-4C). The third K-box was sufficient for nearly wild-type mRNA binding *in vitro*, even when altered to a run of arginine residues. Deletion of all three K-boxes was lethal, but *SUI3* alleles retaining any single K-box were viable, indicating functional redundancy for their essential function(s) *in vivo* [68].

The *SUI3* allele lacking all three K-boxes conferred dominant Slg⁻ and Gcd⁻ phenotypes, suggesting a defect in TC formation or binding to 40S ribosomes. Ostensibly at odds with this interpretation, the triple K-box mutations had no effect on TC formation by purified eIF2 *in vitro*. Moreover, eIF2 containing the β subunit lacking the K-boxes was found in 43S or 48S preinitiation complexes in yeast cells, indicating that the K-boxes are dispensable for TC formation and 40S binding *in vivo* [68]. Nevertheless, the dominant Gcd⁻ phenotype of this *SUI3* allele may signify a reduced rate of TC binding to 40S subunits that is sufficient to derepress *GCN4* translation because of the kinetic restrictions on re-initiation on *GCN4* mRNA. In fact, the K-boxes stabilize interaction between recombinant eIF2β or eIF2 holoprotein with the

catalytic subunit of eIF2B (ε/GCD6) *in vitro*, and all of the viable single and double K-box mutations in *SUI3* had a Gcd⁻ phenotype. Thus, the K-box mutations most probably impede the recycling of eIF2-GDP to eIF2-GTP by eIF2B and diminish the rate of TC formation *in vivo* [69].

The K-boxes in eIF2β promote interaction between eIF2 and eIF5 in addition to their roles in mRNA binding and interaction with eIF2B (eIF5-BD in Fig. 7.2-4C). Mammalian eIF5 copurifies with eIF2 from lysates, and a 1:1 complex was formed *in vitro* with purified eIF2 and recombinant eIF5 [70]. Mammalian eIF5 binds specifically to eIF2β *in vitro*, dependent on the second K-box [64]. Mutational analysis of yeast eIF2β showed that at least one K-box was required for interaction with yeast eIF5, and that the K-boxes had additive effects on eIF5 binding *in vitro*. Similarly, K-boxes 1 or 3 were sufficient for association of eIF5 and eIF2β *in vivo*, but at levels approximately one-third of that seen with all K-boxes intact. As with mammalian eIF2β, the C-terminal half of yeast eIF2β (related in sequence to eIF5) contributed little to its interaction with eIF5 [69].

Interestingly, the K-box domain in eIF2β promotes binding to eIF5 and eIF2Bε through interactions with a conserved bipartite motif found at the C-termini of both proteins, dubbed AA-boxes 1 and 2 for the conserved aromatic and acidic residues they contain (Figs. 7.2-6A and 7.2-8D). Alanine substitutions of multiple residues in AA-boxes 1 or 2 of yeast eIF5 (12A and 7A, respectively, in Fig. 7.2-8D) impaired its interaction with recombinant eIF2β-NTD and purified eIF2 holoprotein *in vitro*. The *tif5-7A* allele (harboring the seven Ala mutations in AA-box2) likewise abolished native eIF5-eIF2 interaction and conferred a Ts⁻ phenotype in yeast that was partially suppressed by overexpressing all three subunits of eIF2 and $tRNA_i^{Met}$. The *tif5-12A* allele (bearing the 12 Ala replacements in AA-box 1) is lethal [69]. Thus, the AA-boxes in eIF5 mediate an important interaction with TC *in vivo* that may facilitate the GAP function of eIF5 on base pairing of Met-$tRNA_i^{Met}$ with the start codon. Consistent with this idea, mutations in the AA-boxes of mammalian eIF5, which impair its interaction with eIF2β reduced the GAP activity of eIF5 *in vitro* and the eIF5-dependent formation of 80S initiation complexes [71] (M3 and M4 mutations in Fig. 7.2-8D). Surprisingly, a reduction in GAP activity *in vitro* was not observed in response to the more extensive mutations in the yeast eIF5 AA-boxes of *tif5-7A* and *tif5-12A* [72], possibly indicating that substrate binding is not rate-limiting in the model GAP assay established for yeast eIF5 [53]. As discussed below, the *tif5-7A* mutation also destabilizes a physical interaction between eIF2 and eIF3 that is bridged by the eIF5-CTD, impairing the binding of TC to 40S subunits *in vitro* and possibly impeding scanning or AUG recognition *in vivo* [34, 72].

The corresponding *12A* and *7A* mutations in the AA-boxes of eIF2Bε/GCD6 reduced its binding to the eIF2β–NTD and eIF2 holoprotein *in vitro*, just as observed for eIF5. Moreover, the corresponding *gcd6-7A* mutation reduced association between native eIF2 and eIF2B *in vivo* and conferred a Gcd⁻ phenotype that could be suppressed by overexpressing eIF2 and initiator $tRNA^{Met}$, all consistent with a reduction in GDP–GTP exchange on eIF2. The *gcd6-12A* allele, bearing substitutions in the first AA-box was lethal, suggesting that the bipartite motif in GCD6

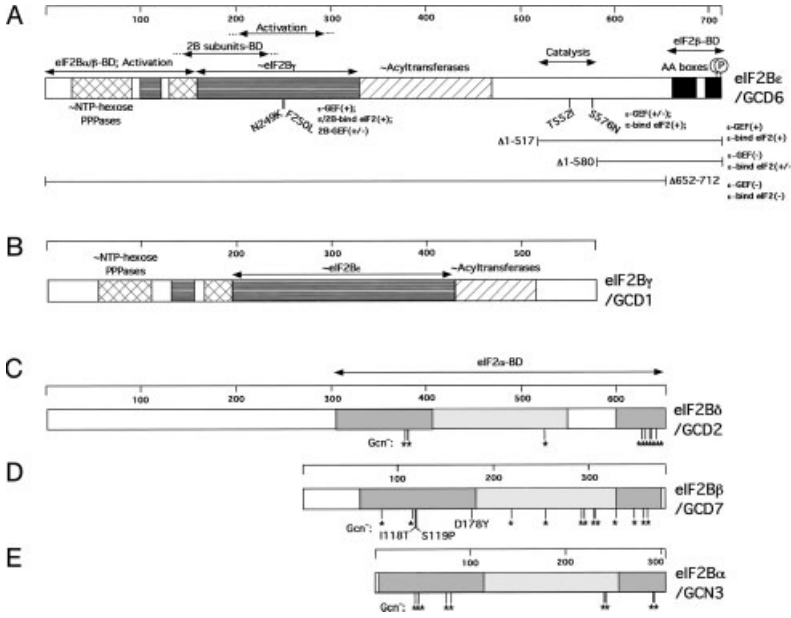

Figure 7.2-6 Schematic representations of the primary structures of the subunits of yeast eIF2B. **(A)** The amino acid sequence of the ε subunit of eIF2B is depicted as a rectangle with amino acid positions shown above. Hatching is used to depict domains with sequence similarity to the indicated proteins; the AA-boxes are shown as black boxes at the C-terminus. The boundaries of binding domains (BDs) for other factors or regions required for catalysis or activation of catalytic function (activation) are delimited with double-headed arrows. The locations and *in vitro* phenotypes of selected point mutations and deletions are shown beneath the schematic. *ε-GEF(+)* denotes wild-type GEF activity conferred by the isolated ε-subunit; *2B-GEF(+/–)* denotes reduced GEF activity conferred by the eIF2B holoprotein; *ε-* or *2B-bind eIF2(+)* denotes wild-type binding of eIF2 by the isolated ε-subunit or eIF2B holoprotein, respectively. **(B)** The amino acid sequence of the γ subunit of eIF2B depicted as for eIF2Bε in (A). **(C–E)** The amino acid sequences of the δ, β, and α subunits, respectively, of eIF2B with shading used to depict regions of similarity among the three proteins. The BD for eIF2α is delimited with a double-headed arrow. The locations of point mutations with Gcn⁻ phenotypes are shown beneath the schematic indicated with asterisks or the amino acid replacements. See text for further details.

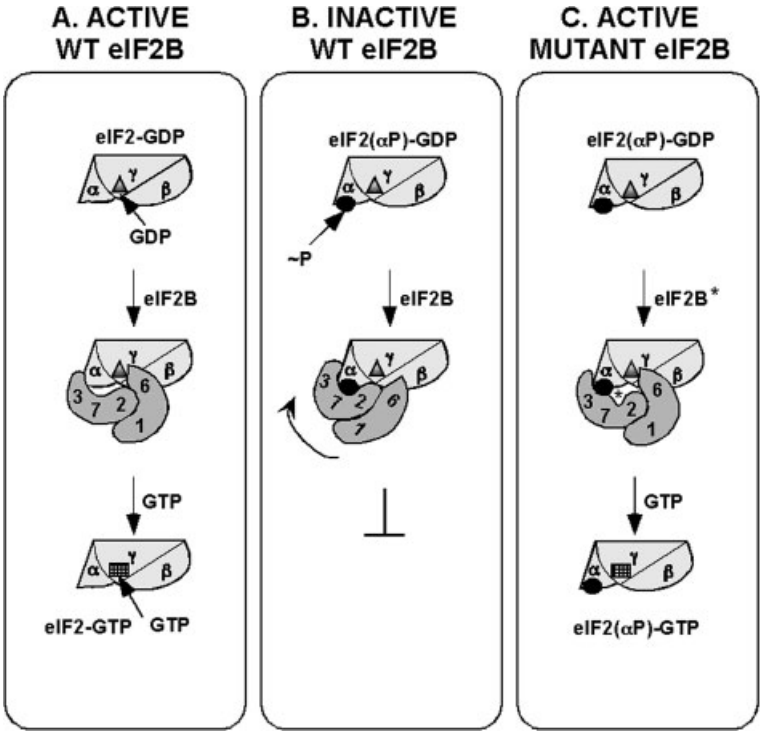

Figure 7.2-7 A mechanistic model for negative regulation of the guanine nucleotide exchange activity of eIF2B by eIF2(αP). **(A)** Unphosphorylated eIF2α promotes the GDP/GTP exchange activity of eIF2B. The heterotrimeric eIF2 (shown as different shapes labeled α, β, γ) complexed with GDP (shaded triangle) has two binding sites in eIF2B. The GCD2/δ-GCD7/β-GCN3/α regulatory subcomplex in eIF2B (labeled 2, 3, 7) binds to the α subunit of eIF2, whereas the GCD1/γ–GCD6/ε catalytic subcomplex in eIF2B (labeled 1, 6) interacts with the β and γ subunits of eIF2. Based on results with rat proteins, the GCD2 (δ) subunit of eIF2B may also interact with eIF2β. The binding interactions shown here position the catalytic subunit of eIF2B (GCD6/ε) in proximity to the bound GDP in the manner required to catalyze exchange of GDP for GTP (hatched rectangle) on eIF2. **(B)** Phosphorylated eIF2 inhibits the GDP/GTP exchange activity of wild-type eIF2B. Phosphorylation of eIF2α (●, labeled ~P in eIF2(αP)-GDP) leads to more extensive interactions between eIF2α and the eIF2B regulatory subcomplex, preventing productive interactions between GCD6/ε and the β/γ subunits of eIF2, thereby inhibiting nucleotide exchange. **(C)** A Gcn$^-$ mutation in the GCD7/β regulatory subunit of eIF2B weakens interaction between eIF2α(P) and the regulatory sub-complex of the mutant eIF2B complex (eIF2B*), permitting the productive interaction between GCD6/ε and eIF2(αP)-GDP necessary for GDP–GTP exchange. Reproduced from Ref. 84.

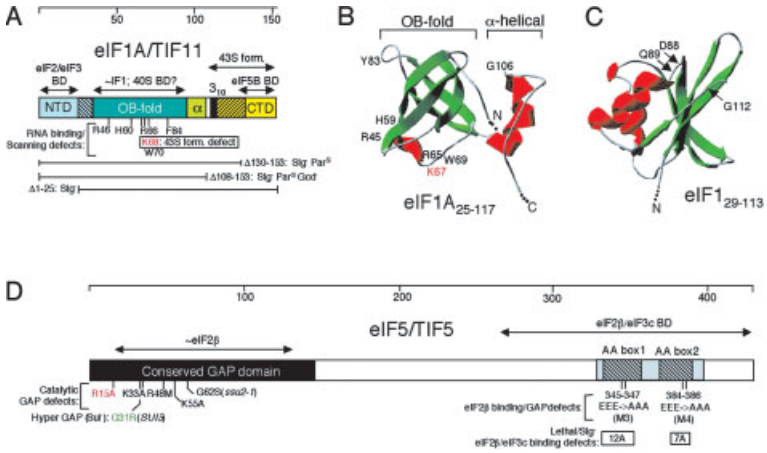

Figure 7.2-8 Schematic representations of the primary and tertiary structures of eIF1A, eIF1, and eIF5. **(A)** The amino acid sequence of yeast eIF1A (encoded by *TIF11*) is depicted as a rectangle with amino acid positions shown above. Different colors are used to depict the N-terminal (NTD), OB-fold, α-helical (α), 3_{10} helix, and C-terminal (CTD) domains, based on the 3D structure of the human protein shown in (B). The region of similarity to bacterial IF1 (~IF1) predicted to be the BD for the 40S ribosome, is delimited with a double-headed arrow, as are demonstrated BDs for eIF2, eIF3, and eIF5B, and the C-terminal region required for TC binding to 40S subunits and the formation of 43S complexes *in vivo* (43S form.) The locations and phenotypes of selected deletions are shown beneath the schematic, as are the residues homologous to those in human eIF1A whose substitution led to defects in RNA binding and AUG selection by the scanning 48S complex, and 43S complex formation (for K68 only), *in vitro*. **(B)** Solution structure of residues 25–117 of human eIF1A (191) (PDB ID: 1D7Q). **(C)** Solution structure of residues 29–113 of human eIF1 (PDB ID: 2IF1) [4]). The indicated residues D88, Q89, and G112, homologous to yeast residues 83, 84, and 107, respectively, give rise to Sui$^-$ (all three residues) and Mof$^-$ (G112 only) phenotypes when mutated in yeast. The structures in (B) and (C) were drawn using the DeepView/Swiss-Pdb viewer (v. 3.7) using data obtained from the Protein Data Bank (www.pdb.org). In each case, the first of multiple solved structures stored in the PDB file was employed. **(D)** The amino acid sequence of yeast eIF5 (encoded by *TIF5*) is depicted as a rectangle with amino acid positions shown above. Shading or hatching is used to depict the conserved N-terminal GAP domain and conserved CTD harboring AA-boxes 1 and 2 (hatched). The region of similarity to eIF2β is delimited with a double-headed arrow, as is the BD for eIF2β and eIF3c/NIP1. The locations and *in vitro* or *in vivo* phenotypes of selected point mutations are shown beneath the schematic.

is essential for the GEF function of eIF2B [69]. Interactions of the CTDs in eIF5 and eIF2Bε with the eIF2β–NTD appear to be mutually exclusive, as eIF2B and eIF5 are not found in the same complexes containing eIF2 in yeast cells [69]. The β subunit of archaeal eIF2 lacks the NTD containing the K-boxes and, consistently, archaea lack recognizable orthologs of eIF5 and eIF2Bε [73–75]. Thus, the K-boxes may have arisen during evolution, at least partly, to facilitate the interactions of eIF2 with the factors that regulate the status of its bound guanine nucleotide [69].

eIF2α Promotes and Regulates GDP–GTP Exchange by eIF2B

The α subunit of eIF2 (encoded by *SUI2* in yeast) contains the conserved Ser residue at position 51 whose phosphorylation converts eIF2-GDP from substrate to inhibitor of eIF2B [76, 77]. (Note that Ser-51 is actually the 52nd encoded residue in human and yeast eIF2α, as the N-terminal Met is removed posttranslationally; other residues in eIF2α also are typically numbered relative to the second encoded residue of the protein.) The sequence surrounding Ser^{51} is highly conserved in eukaryotic eIF2α proteins [78–80], but not in archaea [73], consistent with phosphorylation of this residue occurring only in eukaryotes. Interestingly, residues 14–93 in archaeal and eukaryotic eIF2α exhibit sequence similarities with the RNA-binding domain of *E. coli* ribosomal protein S1, a five-stranded antiparallel β-barrel called the OB-fold [81] (Fig. 7.2-4D). The crystal structure of the N-terminal segment of human eIF2α confirms the presence of the OB-fold in residues 1–87, with Ser-51 located in a long unstructured loop between β strands 3 and 4 (Fig. 7.2-5C). The OB domain of eIF2α lacks the clustered positively charged surface residues involved in RNA binding by other OB-fold proteins, and there is no evidence that eIF2α has RNA binding activity. Residues 88–182 comprise a helical domain that interacts with the OB domain, forming a highly conserved, negatively charged channel at the interface between the two domains [82] (Fig. 7.2-5C). Sui$^-$ mutations in yeast eIF2α alter residues in the NTD [78] (Fig. 7.2-4D). Thus, this region may contribute to Met-$tRNA_i^{Met}$ binding or an interaction with mRNA during scanning by eIF2. Other *sui2* mutations reduce the inhibitory effect of phosphorylated eIF2 on the GEF eIF2B (Gcn$^-$ phenotype) [83, 84] and alter residues in the eIF2α OB domain, including amino acids in the loop between β4 and β5 (G80 and K79), in the loop containing Ser-51 itself (E49), and in the loop connecting the OB-fold to the helical domain (R88) [82] (Fig. 7.2-5C). As discussed below, this portion of eIF2α most probably interacts with the regulatory subunits of eIF2B (α, β, and δ) and mediates inhibition of the GEF activity when Ser-51 in eIF2α is phosphorylated.

Recent studies of yeast eIF2α indicate that this subunit is dispensable for the essential functions of eIF2 in translation initiation and is required primarily to promote and regulate GDP–GTP exchange by eIF2B. While a *SUI2* deletion is lethal in otherwise wild-type cells, *sui2Δ* mutant cells can survive if eIF2[$\beta\gamma$] is overexpressed along with $tRNA_i^{Met}$. A nearly complete by-pass of eIF2α function was achieved by overexpressing the mutant protein eIF2γ-K250R along with eIF2β and $tRNA_i^{Met}$. The *K250R* mutation stimulates TC formation by eIF2-GDP *in vitro* in the absence of eIF2B by enhancing the spontaneous GDP–GTP exchange activity intrinsic to yeast eIF2. Consistently, overexpressing all three eIF2 subunits (with the K250R mutation in the γ subunit) and $tRNA_i^{Met}$ suppressed the lethality of deleting all four essential eIF2B subunits. These last findings imply that eIF2B has no essential functions beyond GDP–GTP exchange that cannot be by-passed by increasing the concentration of TC (85). In accordance with these genetic results, biochemical analysis of the eIF2[$\beta\gamma$] heterodimer showed that absence of the α subunit had no substantial effect on binding of guanine nucleotides, TC formation, binding of TC to purified 40S

subunits, or eIF5-catalyzed GTP hydrolysis by 43S complexes. The only defect observed was an 18-fold increase in the K_m of eIF2B for eIF2[$\beta\gamma$]-GDP versus eIF2[$\alpha\beta\gamma$]-GDP [86]. The latter suggests that eIF2α contributes to the binding of eIF2 by eIF2B, possibly through direct interactions with the eIF2B[$\alpha\beta\delta$] regulatory subcomplex [84, 87] (see below). In view of these findings, it is surprising that eIF2α is conserved in archaea, which lack eIF2B. Perhaps archaeal eIF2α performs a crucial function that is carried out redundantly by a eukaryotic-specific factor (e.g., eIF3) or a ribosomal protein.

Yeast eIF2α is phosphorylated *in vivo* on Ser residues 292, 294 and 301 at the extreme C-terminus (Fig. 7.2-4D). *In vitro* and *in vivo* results indicate that casein kinase II (CKII) phosphorylates one or all three residues. Whereas Ala substitutions of these residues did not confer any growth or Sui$^-$ phenotypes in wild-type cells, they exacerbated the growth defects of mutants in which eIF2B activity was inhibited by constitutive phosphorylation of Ser-51 in eIF2α (*GCN2^c* mutant) or by Gcd$^-$ mutations in eIF2Bα (*gcn3^c*) or eIF2Bδ (*gcd7*). Thus, lack of CKII phosphorylation reduces eIF2 activity significantly only when combined with a defect in eIF2 recycling [88]. CKII phosphorylation may promote productive interaction between eIF2-GDP and eIF2B. There is currently no evidence that this phosphorylation event is regulated in yeast cells. Mammalian eIF2α lacks the CKII sites and it is not a substrate for the mammalian kinase *in vitro* [13].

7.2.2.3 The GEF eIF2B regulates ternary complex formation

The Catalytic Function of eIF2B

1. *The mechanism of guanine nucleotide exchange*. Following recognition of the AUG codon and hydrolysis of the GTP bound to eIF2 in the TC, the resulting eIF2-GDP is released from the ribosome. At physiological Mg^{2+} concentrations, the eIF2–GDP complex dissociates slowly and the affinity of eIF2 is much greater for GDP than GTP [13]. Accordingly, the GEF eIF2B is required to displace the GDP bound to eIF2 and allow its replacement with GTP to regenerate the TC. The eIF2B contains five different subunits (α through ε), whose primary structures are well conserved between yeast and mammals (Table 7.2-1), and it occurs in a 1 : 1 complex with its substrate eIF2 in extracts [13,22].

The molecular mechanism of the exchange reaction is uncertain. Evidence supporting a substituted enzyme (ping-pong) mechanism involving a nucleotide-free eIF2B–eIF2 intermediate was presented [89]; however, it has been suggested that the high GDP concentration used in that study would have made it difficult to rule out a sequential mechanism involving a GTP–eIF2B–eIF2–GDP quaternary complex [90]. Indeed, kinetic data consistent with the sequential mechanism, have been reported for both mammalian [91] and yeast [92] eIF2B. Ostensibly at odds with the ping-pong mechanism is the fact that unlabeled GTP is required for displacement of radiolabeled GDP from eIF2 by eIF2B [91,93]. However, this would be expected for a ping-pong mechanism when eIF2B is present in catalytic amounts, as unlabeled

GTP will be needed to release eIF2B from the eIF2–eIF2B complex without reforming the starting substrate eIF2–[^{3}H]GDP. In fact, [^{3}H]GDP was released from eIF2 in the absence of GTP when stoichiometric amounts of eIF2B were employed [94]. Another observation, inconsistent with the ping-pong mechanism, namely that eIF2B cannot be displaced from eIF2 by GDP [93], also has been contradicted by the results of more recent experiments [94].

The sequential mechanism predicts that the eIF2–eIF2B complex should have two guanine nucleotide-binding sites in eIF2 and eIF2B, respectively. Dholakia and Wahba [91] reported that eIF2B binds GTP (but not GDP) with K_d of 4μM, and showed by photoaffinity labeling experiments that the β subunit of eIF2B contains a GTP-binding site. The latter was confirmed by Williams, et. al. [94], who found that eIF2Bβ (native or recombinant) can be crosslinked to GTP or ATP. Similarly, yeast eIF2B binds GTP with K_d of 1 μM [92]. The main difficulty with these last findings is that the β subunit is dispensable for GEF activity *in vitro* [87, 95]. In fact, the C-terminal ~25% of the ε/GCD6 subunit is sufficient for measurable eIF2B activity *in vitro* (see below). Manchester [96] suggested that the GTP-binding site in eIF2Bβ could increase the local concentration of the displacing nucleotide and thereby enhance the exchange reaction, effectively converting a basal ping-pong mechanism operative with eIF2Bε alone to the sequential mechanism seen for five-subunit eIF2B (holoenzyme) [91, 92]. This model seems at odds with the finding that the yeast eIF2B$\gamma\varepsilon$ binary complex and eIF2B holoenzyme were equally active [87]; however, the predicted difference in activity may be evident only at low GTP concentrations. It should also be noted that sequence motifs conserved in GTP-binding proteins do not occur in eIF2Bβ or in any other eIF2B subunit.

2. *Structures and functions of eIF2B subunits.* As indicated above, the eIF2B contains five different subunits. Recessive mutations in the yeast ε, δ, γ, and β subunits (encoded by *GCD6, GCD2, GCD1,* and *GCD7,* respectively) have Ts$^-$ and Gcd$^-$ phenotypes [19], indicative of reduced TC formation, and deleting any of these subunits is lethal. In contrast, deleting *GCN3* (encoding eIF2Bα) has a Gcn$^-$ phenotype (failure to induce *GCN4* in response to eIF2α phosphorylation) and no effect on cell growth [97]. Thus, eIF2Bα in yeast seems to be required primarily for inhibition of eIF2B by eIF2(αP). Similarly, a rat eIF2B complex devoid of the α subunit, either overexpressed in insect cell extracts or affinity-purified, had full GEF activity that was relatively insensitive to inhibition by eIF2(αP) [95, 98]. In contrast, a rabbit eIF2B complex lacking the α subunit did not co-purify with eIF2 and had only 20–25% of the activity of the five-subunit complex. Nearly full activity was recovered by adding recombinant eIF2Bα to the latter four-subunit preparation, leading to the conclusion that eIF2Bα is required for wild-type activity of rabbit eIF2B, perhaps by promoting substrate binding [94, 99].

Although four of the five subunits of yeast eIF2B are essential, the intrinsic GEF activity is lodged in the C-terminal ~25% of the ε/GCD6 subunit (Fig. 7.2-6A). The eIF2Bε from rat [95], *Drosophila* [100], and yeast [87, 101] can catalyze nucleotide exchange independently of the other subunits *in vitro*, albeit with 10–40-fold lower specific activity than that of eIF2B holoenzyme. In fact, a fragment of ε/GCD6

containing only the last 195 residues was comparable with full-length ε/GCD6 for eIF2 binding and GEF activity. Deletion of only the C-terminal 60 residues of ε/GCD6, containing the AA-boxes 1 and 2 mentioned above, destroyed eIF2 binding and GEF function by the isolated ε/GCD6 subunit, and greatly reduced the activity of the yeast eIF2B holoprotein (Fig. 7.2-6A) [101, 102]. Consistently, two serine residues in this segment of mammalian eIF2Bε S712 and S713 are phosphorylated *in vivo* and their replacement with nonphosphorylatable residues reduced both interaction of eIF2B with eIF2 and GEF activity in cell extracts. These sites are phosphorylated by casein kinase II *in vitro*, but it is unknown whether their phosphorylation is regulated as a means of controlling eIF2B activity *in vivo* [103]. A region N-terminal to the AA-boxes in ε/GCD6, between residues 518 and 581, is required for GEF activity but nonessential for eIF2 binding (Fig. 7.2-6A) [101, 102]. Hence, this region is predicted to contain the catalytic center in ε/GCD6, presumably responsible for distorting the GDP-binding pocket in eIF2γ to effect release of the bound GDP.

What are the functions of the other eIF2B subunits? As described above, mutations or deletions in the AA-boxes of ε/GCD6 do not abolish the activity of eIF2B holoprotein; hence, there must be additional contacts between eIF2B and eIF2 subunits. In fact, both the ε and δ subunits of eIF2B can interact with the C-terminal portion of mammalian eIF2β [104] and, as discussed below, the α, β, and δ eIF2B subunits form a stable subcomplex that can bind eIF2α. The yeast ε/GCD6–γ/GCD1 subcomplex has higher GEF activity than does ε/GCD6 alone, comparable with the eIF2B holoprotein [87, 95], and the stimulatory effect of γ/GCD1 is attributable partly to enhanced binding of eIF2 [87]. The ε and γ subunits have recognizable sequence similarity to one another and to NTP-hexose-pyrophosphorylases and acyltransferases [105] (Figs. 7.2-6A and B), but these similarities are of unknown significance. Point mutations in a highly conserved Asn-Phe-Asp motif at positions 249–251 in ε/GCD6 had no effect on GEF activity of the isolated subunit, but substantially reduced the activity of eIF2B holoprotein, nearly to the level of wild-type ε/GCD6 alone (Fig. 7.2-6A). These mutations did not impair complex formation with other eIF2B subunits, or eIF2 binding by the eIF2B holoprotein; hence, they seem to abrogate a stimulatory effect of γ/GCD1 or other eIF2B subunits on the catalytic function of ε/GCD6. Consistently, the mutations lie within a region of ε/GCD6 (defined by deletions Δ93–358 and Δ144–230), which is required for complex formation with other eIF2B subunits [101]. The extreme N-terminal 158 residues of rat eIF2Bε are required for association of eIF2Bα with the rest of the eIF2B holoprotein and also seem to promote GEF activity independent of their role in maintaining eIF2Bα in the complex. This segment of rat eIF2Bε also contains a strong binding site for the eIF2Bβ subunit [106] (Fig. 7.2-6A). Thus, the eIF2Bε-NTD is involved in interactions with other eIF2B subunits that influence the efficiency of the catalytic center in the C-terminal portion of the protein.

Inhibition of eIF2B by phosphorylated eIF2

The binary complex eIF2(αP)-GDP (phosphorylated on Ser^{51}) is a poor substrate for nucleotide exchange catalyzed by eIF2B in mammals [89, 93, 98, 107], *Drosophila*

[100], and yeast [87]. This does not reflect weak substrate binding, as phosphorylation of eIF2 increases its affinity for eIF2B [13], with estimates ranging from several-fold [93, 108] to more than 100-fold [89] increased affinity. It is frequently assumed that eIF2(αP)-GDP forms a nondissociable complex with eIF2B, physically sequestering eIF2B in an inactive state. At odds with this idea, it was found that eIF2B–eIF2(αP)–GDP complexes dissociate rapidly and that eIF2(αP)–GDP acts as a competitive inhibitor of eIF2B through an enhanced on-rate or decreased off-rate compared with unphosphorylated eIF2 [89]. Because eIF2 is generally present in molar excess of eIF2B, a moderate increase in affinity for eIF2B might account for the strong inhibition of translation that occurs in mammals [12, 109] and yeast [22, 77, 110] when only a fraction of eIF2 is phosphorylated. Studies in yeast showed that the degree of translation inhibition was correlated with the eIF2(αP) : eIF2 ratio instead of the absolute amount of eIF2(αP) present in cells, consistent with a competitive mode of inhibition and a relatively high dissociation rate for the inhibited eIF2B–eIF2(αP)–GDP complex [26].

As discussed above, phosphorylation of eIF2α by GCN2 in amino acid-starved yeast cells inhibits eIF2B and lowers the concentration of TC, reducing general translation initiation but specifically increasing *GCN4* translation. The fact that *gcn3Δ* mutants are defective for this response (Gcn$^-$ phenotype) [97] suggested that eIF2Bα/GCN3 mediates the inhibitory effect of eIF2(αP) on eIF2B function. The strong sequence similarity of eIF2Bδ/GCD2 and eIF2Bβ/GCD7 to α/GCN3 [111, 112] (Figs. 7.2-6C–E) suggested that δ/GCD2 and β/GCD7 also are involved in negative regulation of eIF2B by eIF2(αP). Consistently, overexpressing these three eIF2B subunits in yeast led to formation of a stable subcomplex that can reduce the toxic effect of high-level eIF2(αP) on cell growth [113] and can bind to purified eIF2 *in vitro* in a manner stimulated by eIF2α phosphorylation [87]. Hence, these authors proposed that the overexpressed subcomplex binds preferentially to eIF2(αP)–GDP and prevents it from interfering with the ability of endogenous eIF2B holoprotein to recycle the unphosphorylated eIF2-GDP. All three eIF2B subunits (α,β, and δ) are required for binding to eIF2(αP) [87]. Subsequently, it was shown that the eIF2B α/β/δ regulatory subcomplex, but not the individual subunits, can also bind recombinant eIF2α/SUI2 *in vitro*, dependent on phosphorylation of the latter at Ser^{51}. Thus, the eIF2B regulatory subcomplex directly interacts with eIF2α in a manner stabilized by phosphorylation of Ser^{51} [84]. There is genetic and biochemical evidence that the C-terminal portion of eIF2Bδ/GCD2, which is related in sequence to β/GCD7 and α/GCN3, is sufficient for complex formation with the latter two subunits *in vivo* [113]. Hence, a heterotrimeric structure comprised of the homologous segments of eIF2B α/β/δ is thought to be the binding domain for the phosphorylated NTD of eIF2α (eIF2α-BD in Figs. 7.2-6C, D and 7.2-7).

Additional genetic evidence implicating δ/GCD2 and β/GCD7 in negative regulation of eIF2B came from isolation of Gcn$^-$ point mutations in these two subunits that relieve the inhibitory effects of eIF2(αP) on translation without impairing GEF function, mimicking in both respects a *gcn3Δ* mutant [108, 114]. As these *GCD2* and *GCD7* mutations do not simply cause α/GCN3 to be lost from eIF2B, it appears that

δ/GCD2 and β/GCD7 act directly in the regulation of eIF2B [108]. The *GCD2* and *GCD7* mutations could decrease the affinity of eIF2B for eIF2(αP) or, alternatively, allow eIF2B to accept eIF2(αP)-GDP as a substrate. The latter mechanism is favored by the fact that nearly all eIF2α was phosphorylated in certain of these mutants [108], and was later confirmed biochemically for the *GCD7-S119P* and *GCD7-I118T, -D178Y* mutations in eIF2Bβ (Fig. 7.2-6D) and for the four-subunit complex lacking GCN3 (i.e., the *gcn3Δ* mutation), as follows. All three mutant eIF2B holoproteins were shown to catalyze nucleotide exchange at high levels using either phosphorylated or unphosphorylated eIF2-GDP as substrate, as did the ε/GCD6–γ/GCD1 catalytic subcomplex [87]. Based on these findings, it was proposed that the eIF2B $\alpha/\beta/\delta$ regulatory subcomplex is required to inhibit the ε/γ catalytic subcomplex when the substrate is phosphorylated. Tight binding of phosphorylated eIF2α to the eIF2B $\alpha/\beta/\delta$ subcomplex would prevent the productive interaction between the eIF2B ε/γ catalytic subcomplex and eIF2 β/γ, which is required for release of GDP from the latter (Fig. 7.2-7). Support for this model came from the fact that the Gcn– mutations *GCD7-S119P* and *GCD7-I118T,-D178Y* in eIF2Bβ decreased binding of the eIF2B $\alpha/\beta/\delta$ subcomplex, and also of eIF2B holoprotein, to phosphorylated recombinant eIF2α (Fig. 7.2-6D). These mutations also decreased interaction between the eIF2B and eIF2 holoproteins, even when the latter was unphosphorylated. Thus, contacts between the eIF2B $\alpha/\beta/\delta$ subcomplex and eIF2α probably contribute to the productive interaction of eIF2B with nonphosphorylated eIF2-GDP [84]. This is consistent with results showing that the K_m value of eIF2B for eIF2-GDP increased by an order of magnitude when the α subunit of eIF2 was missing [86]. Presumably, the presence of a phosphate group at Ser^{51} provides additional contacts with the eIF2B $\alpha/\beta/\delta$ subcomplex that interfere with the correct interaction between the eIF2B ε/γ subcomplex and the GDP-binding pocket in eIF2 β/γ (Fig. 7.2-7).

Two mutations were introduced into rat eIF2Bδ identical to substitutions in δ/GCD2 that individually rendered yeast eIF2B insensitive to eIF2(αP) *in vivo* (Gcn– phenotype) [108]. The rat eIF2B bearing the G377K, L381Q double substitution in the δ-subunit (eIF2B[δ*]) was only minimally inhibited by preincubation with eIF2(αP), similar to what occurred with the four-subunit eIF2B lacking the α-subunit. Unlike the latter, however, the eIF2B(δ*) complex was completely ineffective using eIF2(αP)-GDP as a substrate. Presumably, the eIF2B(δ*) complex escapes inhibition primarily because it binds the phosphorylated inhibitor less tightly than the unphosphorylated substrate [98].

Most of the Gcn– mutations in eIF2B fall into two clusters located in regions of strong sequence similarity among the α/GCN3, β/GCD7 and δ/GCD2 subunits (Figs. 7.2-6C–E), leading to the suggestion that the structurally homologous segments in these subunits interact to form a binding pocket for the phosphorylated NTD of eIF2α [108]. As noted above, Gcn– point mutations were also isolated in the NTD of yeast eIF2α that eliminate the inhibitory effect of eIF2(αP)-GDP on eIF2B activity [83] (Fig. 7.2-4D). Consistently, a number of these mutations weaken binding of recombinant phosphorylated eIF2α to the eIF2B $\alpha/\beta/\delta$ subcomplex or eIF2B holoprotein [84], suggesting that at least some portion of the OB domain in eIF2α

(Fig. 7.2-5C) binds directly to the eIF2B $\alpha/\beta/\delta$ subcomplex (Fig. 7.2-7). The Ala substitution of Ser-48 has the same phenotype in mammalian cells when eIF2α is phosphorylated by PKR, HRI, or in response to heat shock [115–120]. Interestingly, addition of eIF2α-S48A to inhibited RRL reduced the abundance of 15S complexes containing eIF2, thought to represent inactive eIF2B-eIF2(αP)–GDP complexes [121]. This last finding supports the idea that Ala-48 reduces the affinity of eIF2(αP)–GDP for eIF2B [120]. Consistently, the Ala-48 mutation in yeast eIF2α partially suppressed growth inhibition by hyperactive GCN2c kinases without lowering Ser51 phosphorylation [77].

Interestingly, mutations in each of the five subunits of eIF2B have been associated with the human genetic disease leukoencephalopathy with vanishing white matter (VWM) [122, 123]. It is unknown whether these mutations lead to defects in eIF2B function or its regulation.

Additional Functions for eIF2B?

It was found that *gcd1* and *gcd2* mutations in yeast eIF2B subunits led to accumulation of eIF2 in 43–48S complexes [22, 23], implying that initiation was blocked at a step in the pathway following TC binding to the 40S subunit, rather than at TC formation. Similarly, in rabbit reticulocyte lysates (RRL) inhibited by eIF2α phosphorylation, the eIF2(αP) and exogenously added mRNA and $tRNA_i^{Met}$ accumulated in 48S complexes [124]. Other workers observed accumulation of 48S complexes and halfmer polysomes containing Met-$tRNA_i^{Met}$ in inhibited RRL that could be reversed by exogenous eIF2B. Because the 48S complexes lacked eIF2 and halfmers did not appear immediately, it was proposed that 80S initiation complexes could not proceed to elongation and dissociated into mRNA-bound 40S subunits (halfmers) [125, 126]. Several groups have observed eIF2-GDP bound to 60S [121, 125–128] or 40S subunits [129], which might represent physiological intermediates in the initiation pathway. Ribosome-bound eIF2-GDP could have a positive role in subunit joining, or it could arise following GTP hydrolysis and release of eIF2-GDP from the P-site on AUG recognition. In either case, eIF2B may be required to remove eIF2-GDP from the ribosome in addition to exchanging GDP for GTP, and phosphorylation of eIF2α could convert ribosome-bound eIF2-GDP into an inhibitor of subunit joining. Interestingly, deletion of the 40S protein RPS31/UBI3 in yeast suppressed the Gcd- and Ts- phenotypes of *gcd2* and *gcd1* mutations in eIF2B, prompting the suggestion that elimination of RPS31 partially overcomes a requirement for an eIF2B function on the 40S ribosome [130]. Consistently, eIF2B accumulated in 40S complexes in the *gcd1-101* mutant [22]. It has also been proposed that eIF2B stimulates TC formation [131] and TC binding to 40S subunits in the context of an eIF2B-eIF2-GTP-Met-$tRNA_i^{Met}$ quaternary complex [132]. As noted above, elimination of eIF2B is not lethal in yeast cells that are overexpressing the TC [85]; hence, all of these putative additional functions of eIF2B would have to be by-passed in yeast by artificially increasing the TC concentration.

7.2.2.4 Binding of Ternary Complex and mRNA to the 40S Ribosome is Stimulated by eIF3

eIF3 Promotes Ternary Complex Binding to 40S Ribosomes

The TC can bind to purified 40S subunits in the absence of other factors, and this interaction is stimulated by high, nonphysiological Mg^{2+} concentrations (greater than 2 mM) and the AUG triplet [36]. (Use of AUG in place of mRNA obviates the need for factors required for mRNA binding to the ribosome.) The stimulatory effect of the AUG triplet suggests that base pairing between the start codon and Met-$tRNA_i^{Met}$ stabilizes TC association with 40S ribosomes. High-level binding of the TC to 40S subunits under more physiological conditions requires eIF1, eIF1A and eIF3 [32, 33, 37, 133–135]. TC binding to purified 40S ribosomes can be stimulated by a factor of 2–3 by the addition of purified eIF3. The eIF3 can bind to 40S ribosomes in the absence of other factors, although this association is enhanced by simultaneous binding of the TC [35–38]. The majority of native free 40S subunits in mammalian extracts contain eIF3 [136]. Based on these results, it is generally considered that eIF3 binds to 40S subunits first and then helps to recruit the TC (Fig. 7.2-1). Consistently, a Ts$^-$ lethal mutation in the yeast eIF3b subunit (encoded by *PRT1*) produced a severe initiation defect *in vivo* [137] and heat-treated *prt1-1* extracts were defective for TC binding to 40S subunits in a manner rescued by purified wild-type eIF3 [138, 139]. Relatively little is known about how eIF3 stimulates TC binding, although the physical connections linking yeast eIF3 to eIF2 in a MFC (described below) may permit cooperative binding of both factors to adjacent sites on the 40S subunit.

A Subunit Interaction Model for eIF3

Mammalian eIF3 is a complicated factor, containing 11 nonidentical subunits (Table 7.2-2). Purified plant eIF3 contains orthologs of 10 of these proteins, lacking only eIF3j/p35, and contains an 11_{th} subunit (eIF3l/p67) not found in the mammalian factor [140]. The eIF3 purified from budding yeast contains orthologs of only five mammalian eIF3 subunits as stoichiometric components (eIF3a/TIF32, eIF3b/PRT1, eIF3c/NIP1, eIF3g/TIF35, and eIF3i/TIF34) [139], all of which are essential proteins required for translation initiation *in vivo* [140–147]. A sixth ortholog, eIF3j/HCR1, is a nonessential, substoichiometric subunit of yeast eIF3 that promotes interactions between eIF3 and other eIFs in the 43S complex, and also has an independent function in 40S ribosome biogenesis [148–150]. A possible budding yeast ortholog of human eIF3e subunit, called PCI8, was found to interact with eIF3 holoprotein *in vivo* when overexpressed, and also can bind to recombinant eIF3b/PRT1 *in vitro*, as did human eIF3e/Int-6; however, a *pci8Δ* mutation had no effect on translation *in vivo* [151]. Together, these findings suggest that the essential yeast eIF3 subunits (a, b, c, g and i) constitute a conserved core that can execute the critical functions of this factor. Consistent with this idea, the eIF3g and eIF3i subunits are also essential in fission yeast, whereas the "non-core" subunits, Moe1/d and Int6/e,

are dispensable [152-155]. Deletion of the latter two proteins reduces the stability of the eIF3 complex in fission yeast extracts [156], but produces only a modest reduction in translation rates *in vivo* [152, 153, 156]. The *moe1Δ* and *int6Δ* mutations produce an assortment of phenotypes [152, 153, 156] that could arise from reduced translation of a subset of mRNAs or from a possible involvement of these noncore subunits in other biological processes.

When purified by its ability to stimulate Met-puromycin synthesis [157], yeast eIF3 preparations contained two additional proteins of 135 and 62 kDa, subsequently identified as TIF31 [147] and GCD10 [158] in addition to the core eIF3 subunits. Affinity purification of eIF3 confirmed the association of TIF31 with the complex [144], and recombinant TIF31 interacted with TIF35/eIF3g in several assays [147]. However, *TIF31* is nonessential and its deletion has no effect on cell growth or polysome profiles [147]. It was not possible to confirm a direct association of GCD10 with eIF3 by affinity purification or co-immunoprecipitation with tagged eIF3 subunits from cell extracts [139, 159, 160]. Moreover, GCD10 resides in a nuclear complex with the product of *GCD14* that is required for the formation of 1-methyladenosine at position 58 (m^1A58) in all tRNAs containing this modification, including $tRNA_i^{Met}$ [159, 161]. It is unclear whether GCD10 contributes to eIF3 function in the cytoplasm, and the requirement for GCD10 in translational repression of *GCN4* mRNA [27] can be explained at the level of $tRNA_i^{Met}$ biogenesis and TC formation.

Pairwise interactions among the yeast core eIF3 subunits have been studied extensively by yeast two-hybrid and *in vitro* binding assays, leading to a subunit interaction model for the complex (Fig. 7.2-9A) [139, 145–147, 149]. Many aspects of this model have been confirmed and refined *in vivo* by making deletions of predicted binding domains in affinity-tagged forms of the three largest eIF3 subunits and determining the subunit compositions of the resulting subcomplexes that were affinity-purified from yeast. In the latest model, each of the three largest subunits (TIF32/a, PRT1/b, and NIP1/c) contains separate binding domains for the other two proteins, whereas the smaller subunits (TIF34/i and TIF35/g) bind only to the CTD of PRT1/b and to one another. HCR1/j binds to both PRT1/b and TIF32/a [162]. In accordance with this model, PRT1/b can form two distinct subcomplexes *in vivo*, one containing TIF32/a, PRT1/b, and NIP1/c (a/b/c), and the other comprised of PRT1/b, TIF34/i and TIF35/g (b/i/g) (Fig. 7.2-9A). Whereas the larger a/b/c subcomplex could restore 40S binding of Met-$tRNA_i^{Met}$ and mRNA, and translation of a luciferase reporter mRNA in a *prt1-1* extract, the smaller b/i/g subcomplex was relatively inert for all three activities [163]. Consistent with the subunit interaction model, expression of N-terminally truncated PRT1/b lacking the predicted RNA recognition motif RRM; *Δ*RRM, Fig. 7.2-9D) sequestered TIF34 and TIF35 in an inactive subcomplex lacking TIF32/a and NIP1/c that could not associate with ribosomes in extracts and had a dominant-negative effect on cell growth [149, 164]. Similarly, overexpression of a truncated form of PRT1/b lacking the extreme C-terminus (*Δ7*, Fig. 7.2-9D) sequestered TIF32 and NIP1 in a defective subcomplex lacking TIF34/i and TIF35/g [162]. The deleterious effect on cell growth of producing the latter subcomplex underscores the fact that TIF34/i and TIF35/g are essential *in vivo* even though they are dispensable for measurable eIF3 activity *in vitro*.

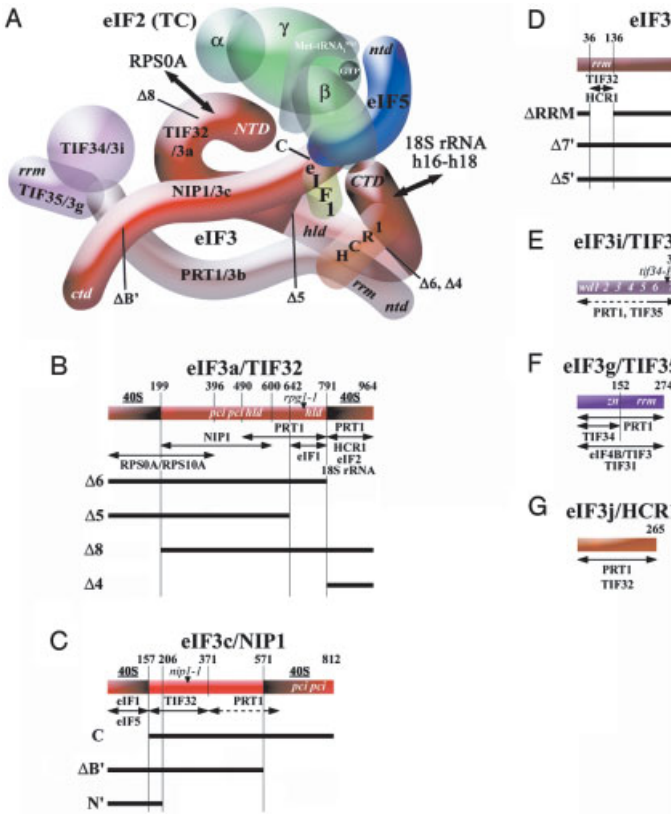

Figure 7.2-9 Schematic representations of the MFC and primary structures of eIF3 subunits of yeast. **(A)** A 3D model of the yeast MFC based on binary interactions between isolated recombinant subunits and affinity purifications of MFC subcomplexes produced by His_8-tagged subunits harboring deletions of predicted binding domains for other components of the complex. The various subunits of eIF3 (orange, red, and purple shapes) are labeled with their yeast (e.g., TIF32) and universal (e.g., 3a) designations. The subunits of eIF2 (green) are labeled α, β, and γ, with GTP and Met-tRNA$_i^{Met}$ bound (primarily) to eIF2γ to comprise the TC. The protein subunits and Met-tRNA$_i^{Met}$ are shown roughly in proportion to their molecular weights. The eIF5, NIP1, and termini of TIF32 are depicted as solid rather than partially transparent shapes to emphasize their importance in binding to 40S ribosomes. Specific inter-actions detected of eIF3 subunits with RPS0A and helices 16-18 of 18S rRNA are depicted (186). The locations of relevant deletion endpoints also are indicated. *NTD,* N-terminal domain; *CTD*, C-terminal domain; *hld*, HCR1-like domain; *rrm*, RNA recognition motif. **(B)–(G)** The amino acid sequences of the yeast eIF3 subunits are depicted as rectangles using the same color schemes as in (A) with selected amino acid positions and locations of selected point mutations shown above, and the locations of selected deletions shown below. The locations of binding domains for other MFC components, other eIFs, 40S ribosomal proteins RPS0A and RPS10A, and 18S rRNA are all indicated below the schematics with double-headed arrows. The locations of PCI homology domains in TIF32 and NIP1 (*pci*), the HCR1-like domain in TIF32 (*hld*), WD repeats in TIF34 (*wd 1, 2,..., 7*), predicted RNA recognition motifs (*rrm)* in PRT1 and TIF35, and a predicted Zn-binding domain in TIF35 (*zn*) are also indicated in the colored rectangles. See text for further details.

Although the PRT1/b CTD contains a NIP1/c-binding site (Fig. 7.2-9D), PRT1/b must interact with both TIF32/a and NIP1 for efficient incorporation into the eIF3 complex [162]. This can explain why a stable PRT1/b–NIP1/c binary complex was not formed *in vivo* by overexpressing these two subunits alone. By contrast, a stable TIF32/a–PRT1/b binary complex was purified from yeast and found to have low-level activity in promoting 40S binding of Met-tRNA$_i^{Met}$ and mRNA in a *prt1-1* extract [163]. Additionally, TIF32/a and NIP1/c can form a stable subcomplex in the absence of other eIF3 subunits [162]. The results of yeast two-hybrid and *in vitro* binding experiments suggest that the "noncore" eIF3 subunits eIF3e/INT-6 and eIF3d/Moe1 interact with one another and that eIF3e additionally binds to the three largest core subunits that comprise the stable a/b/c subcomplex described above [151, 165–167]. Consistently, disruption of eIF3d/Moe1 reduced the level of eIF3e/INT-6 in *S. pombe* extracts [167].

eIF3 Resides in a Multi Factor Complex with eIF1, eIF2, and eIF5

The eIF3 is physically associated with other essential eIFs in yeast. It co-purified with eIF1 [139, 168] and contained nearly stoichiometric amounts of eIF5 when purified by affinity chromatography [139]. *In vitro*, eIF1 and the eIF5-CTD can bind simultaneously to the NIP1/c-NTD [34, 69, 139]. Consistently, yeast eIF1 and eIF5 co-purified with the eIF3 a/b/c subcomplex, but not with the b/i/g subcomplex described above [163] (Fig. 7.2-9A). Interactions of eIF1 and eIF5 with eIF3c have also been observed for the mammalian factors [4, 169]. Interestingly, the yeast eIF5-CTD can interact simultaneously with NIP1/c and the β-subunit of eIF2 *in vitro* [34, 69], suggesting that eIF5 can bridge a physical interaction between eIFs-2 and -3. Indeed, a MFC containing eIF1, eIF2, eIF3, eIF5 and Met-tRNA$_i^{Met}$ (Fig. 7.2-9A) was shown to exist free of ribosomes and could be purified from yeast extracts. The seven alanine substitutions in AA-box 2 of the eIF5-CTD in the *tif5-7A* allele (described above) disrupt interactions of eIF5 with both eIF2β and the NIP1-NTD *in vitro* and dissociate eIF2 from eIF3 *in vivo*. This mutation confers a diminished rate of translation initiation and Slg$^-$ phenotype providing evidence that the MFC is an important initiation intermediate *in vivo* [34, 69]. Recent work indicates that TIF32/a mediates a second, direct contact between eIF3 and eIF2 in the MFC. The CTD of TIF32/a can bind to recombinant eIF2β *in vitro* and to eIF2 holoprotein *in vivo* in the absence of all other MFC components (Fig. 7.2-9B, Δ4). Consistently, a truncated form of TIF32/a lacking this binding domain (TIF32-Δ6) forms a MFC *in vivo* that lacks only eIF2. Overexpression of TIF32-Δ6 confers a dominant Slg$^-$ phenotype in otherwise wild-type cells and it exacerbates the translation-initiation defect in *tif5-7A* cells. Thus, the direct connection between eIF2β and eIF3 involving the TIF32-CTD and the indirect contact between eIF2β and NIP1/c via the eIF5-CTD seem to have additive stimulatory effects on a common step of translation initiation *in vivo* [162].

Formation of the MFC Stimulates Multiple Steps of Initiation

The presence of eIF2 and eIF3 in the MFC might be expected to enhance TC binding to ribosomes by cooperative binding of both factors to the 40S subunit. Three observations are consistent with this idea. First, TC binding to 40S subunits was defective in *tif5-7A* extracts in a manner rescued by purified wild-type eIF5 [72]. Second, the Slg⁻ phenotypes of *tif5-7A* and high-copy *TIF32-Δ6* were partially suppressed by overexpression of the TC [69, 162]. Thus, at least one consequence of disrupting MFC integrity seems to be a reduction in TC binding to 40S subunits. Third, overexpression of the NIP1-NTD sequesters eIF2, eIF1 and eIF5 in a nonribosomal subcomplex lacking all eIF3 subunits (Fig. 7.2-9C, N) and produces a Gcd⁻ phenotype. This phenotype is exacerbated by overexpressing eIF1 and eIF5, which enhances formation of the NIP1-NTD/eIF5/eIF1/eIF2 subcomplex *in vivo*, and also by overexpressing the TIF32-CTD, which sequesters eIF2 in a distinct binary complex. Because the Gcd⁻ phenotype of the NIP1-NTD was suppressed by simultaneously overexpressing TC, it was concluded that TC binds to the 40S subunit inefficiently when it resides in the NIP1-NTD/eIF5/eIF1/eIF2 or the TIF32-CTD/eIF2 subcomplexes compared with intact MFC [162].

Paradoxically, no Gcd⁻ phenotype was observed in *tif5-7A* mutant cells, even when the TIF32-Δ6 protein was being overexpressed. Moreover, there was an accumulation of 48S complexes containing eIF1, eIF2 and eIF3 but lacking eIF5 in *tif5-7A* cells [72]. These observations have been interpreted to indicate that the physical contacts among eIF2, eIF5 and eIF3 in the MFC are most critically required *in vivo* for a step(s) subsequent to TC binding to 40S subunits, such as scanning, AUG recognition, or GTP hydrolysis by eIF2. In this view, impairing one of the latter steps reduces the rate at which 48S complexes are consumed to produce 80S initiation complexes, compensating for the reduced rate of TC binding to 40S subunits that results from disrupting the MFC and suppressing the depletion of 43S complexes. The eIF5 stimulates GTP hydrolysis by eIF2 at AUG start codons and this reaction may be inhibited by eIF1 at non-AUG codons [53, 170] (see below). In addition, there is evidence that eIF1 promotes scanning and can destabilize 48S complexes at near-cognate start codons or at AUG triplets in a suboptimal sequence context [171]. As shown in Fig. 7.2-9(A), eIF1 is tethered to the MFC by interactions with the eIF5-CTD, the NIP1-NTD, and a C-terminal segment in TIF32 [34, 69, 139, 162, 163]. Thus, it is possible that MFC integrity is critically required to juxtapose eIF1, eIF2 and eIF5 in relation to one another and the P-site of the ribosome in a manner required for efficient scanning, AUG recognition, or GTP hydrolysis at the start codon.

To explain the absence of a Gcd⁻ phenotype in the *tif5-7A* and *TIF32-Δ6* mutants, it could be proposed that a delay in scanning or GTP hydrolysis at the uORF4 start codon produced by these mutations would impede the progression of all 40S ribosomes scanning from uORF1, compensating for the reduced rate of TC binding expected to occur in these mutants. This would restore efficient reinitiation at uORF4 and suppress the Gcd⁻ phenotype that normally results from a decreased rate of TC binding. By contrast, overexpressing the NIP1/c-NTD or TIF32/b-CTD

sequesters eIF2 in defective subcomplexes and reduces the concentration of intact MFC, but does not generate MFC subcomplexes with the defects in scanning, AUG recognition or GTP hydrolysis postulated above. Hence, overexpressing the NIP1/c-NTD or TIF32/b-CTD has the same outcome as mutations in eIF2B, merely reducing the rate of TC binding to 40S subunits, thus yielding a Gcd⁻ phenotype [162]. An alternative possibility that cannot be discounted is that TC binding during reinitiation on *GCN4* mRNA does not involve eIF3 and the MFC, and that sequestering eIF2 in the subcomplex with eIF5, eIF1, and the NIP1/c-NTD interferes with its recycling by eIF2B or formation of the TC, rather than delaying TC binding to 40S subunits.

Possible Functions of eIF3 in mRNA Binding

In addition to its role in Met-tRNA$_i^{Met}$ recruitment, eIF3 also stimulates mRNA binding to the 40S subunit in mammalian and yeast extracts [29, 37, 133, 163]. Because TC binding stimulates mRNA binding to the 40S ribosome [37, 133], eIF3 could act indirectly through its role in TC recruitment. However, eIF3 also seems to have an additional function in mRNA binding independent of TC [133]. The latter is generally attributed to interactions between eIF3 and the mRNA-associated factors eIF4G [172] or eIF4B [173]. Whereas mammalian eIF4B interacts directly with the eIF3a/p170 subunit [174], the yeast homolog of eIF4B (encoded by *TIF3*) interacts with yeast TIF35/eIF3g [147] (Fig. 7.2-9F). Mammalian eIF3 contains three subunits that can bind RNA as isolated proteins (eIF3a/p170, eIF3d/p66, and eIF3g/p44) [144, 175–178] (Table 7.2-2) and thus eIF3 could interact directly with mRNA in the initiation complex. Indeed, the b, c, and d subunits of mammalian eIF3 were found crosslinked to globin mRNA in 48S preinitiation complexes [175]. RNA-binding activities of certain eIF3 subunits could mediate direct interactions with the 18S rRNA, as suggested by UV-crosslinking experiments for human eIF3d/p66 [179]. Deletion of the RRM from yeast eIF3g/TIF35 was not lethal but produced a Slg⁻ phenotype. The nature of the RNA that interacts with this RRM is unknown.

Mammalian eIF3 can bind to the hepatitis C virus (HCV) and classical swine fever virus IRES elements, and the eIF3a/p170, eIF3b/p116, eIF3d/p66 and eIF3f/p47 subunits were found crosslinked to these mRNA sequences [180, 181]. The binding region for eIF3 in the HCV IRES has been localized to domains IIIa–b [180, 182] and the cryo-EM map of the IRES–40S complex places this domain extending from the platform side of the 40S subunit just below the mid-line of the particle [183]. This location is consistent with the binding site for eIF3 on 40S subunits visualized in three-dimensional (3D) reconstructions of electron micrographs of negatively stained native 40S subunits [31, 184]; however, eIF3 also makes extensive contacts with the solvent side of the 40S subunit in the model of Lutsch et al [184]. It is unclear whether conventional mRNAs translated by the scanning mechanism will interact with eIF3 in the same manner utilized by the HCV IRES, as the latter bypasses the requirement for the eIF4 factors in forming the 48S complex [185].

Binding of eIF3 to the 40S Ribosome

Recently, domains in eIF3 required for binding to 40S ribosomes were identified by investigating whether the MFCs formed by mutant versions of TIF32/a and NIP1/c, many of which lack numerous MFC components, can compete with native MFC for stable 40S binding *in vivo*. The results showed that the N-terminal half of TIF32, NIP1 and eIF5 comprise a minimal 40S binding unit (MBU) sufficient for 40S binding *in vivo* and *in vitro*. The N- and C-termini of NIP1 and the TIF32-NTD were required for 40S binding by otherwise intact MFC complexes (*TIF32-Δ8* mutation, Fig. 7.2-9B; *NIP1-ΔB′*, Fig. 7.2-9C), suggesting that these eIF3 segments make direct contact with the 40S ribosome. Consistently, the TIF32-NTD interacted specifically with 40S subunit proteins RPS0A and RPS10A, and NIP1 interacted with RPS0A and 18S rRNA *in vitro*. The NIP1-NTD may also contact the 40S subunit in addition to its role in tethering eIF5 to the MFC. eIF5 was necessary for 40S binding only when the TIF32-CTD was absent. Thus, whereas the *tif5-7A* mutation did not reduce 40S binding by any MFC components except eIF5, it reduced binding by the mutant subcomplexes formed by the C-terminally truncated proteins TIF32-Δ6 (lacking only eIF2) and TIF32-Δ5 (Δ5 and Δ6; Fig. 7.2-9B). Interestingly, a 140 nt segment of domain I in rRNA, encompassing helices 16–18, is necessary and sufficient for specific binding of 18S rRNA to the TIF32-CTD *in vitro*. Hence, the 40S binding activity of the TIF32-CTD may involve direct interaction with domain I of rRNA [186].

In the cryo-EM model of the yeast 40S subunit [187], RPS0A is on the solvent side of the 40S subunit between the protuberance (pt) and beak (bk). Hence, binding of the TIF32-NTD and NIP1 to RPS0A would place this portion of eIF3 on the solvent side of the subunit, consistent with the EM analyses of 40S–eIF3 complexes [31, 184] and the location of the HCV IRES (and its eIF3-binding domain) on the 40S subunit [180, 182]. Interaction between the TIF32-CTD and helices 16 and 18 of the rRNA would provide eIF3 with access to the 60S-interface side, as these helices are accessible from both sides of the 40S subunit. It was proposed that the bulk of eIF3 would bind to the solvent side of the 40S whereas the TIF32-CTD and NIP1-NTD would wrap around helix 16 or penetrate the cleft between the beak (bk) and shoulder (sh), respectively, gaining access to the interface side of the subunit. The P-site is located on the interface side ~50–55 Å from the binding sites for TIF32-CTD and NIP1-NTD predicted in this model [186]. This separation is comparable with the dimensions of the γ-subunit of eIF2 [51], making it reasonable to propose that the NTD of eIF2β can remain connected to the TIF32-CTD and the NIP1-NTD/eIF5 subassembly of the MFC while Met-tRNA$_i^{Met}$ is bound to the P-site. In contrast, the connections between eIF1 and the TIF32-CTD and NIP1-NTD might have to be severed to allow eIF1 to bind near the P-site [171].

7.2.2.5 eIF1A Stimulates Ternary Complex Binding to 40S Subunits and Participates in AUG Selection During Scanning

The ~17 kDa factor eIF1A has been implicated in ribosome dissociation, binding of TC and mRNA to 40S subunits, and also in scanning. The yeast and mammalian

eIF1A are similar in sequence and functionally interchangeable in supporting production of 80S initiation complexes and Met-puromycin synthesis using all mammalian components [188]. Yeast eIF1A is an essential protein *in vivo* and its depletion from cells impairs general translation initiation and leads to accumulation of 40S dimers [189]. The latter suggests that eIF1A is bound to native 40S subunits and prevents their dimerization *in vivo*. In early studies, mammalian eIF1A seemed to be less active than eIF3 in promoting TC binding to 40S subunits [37, 133], although a greater stimulation could be observed in the presence of 60S subunits and was attributed to a ribosome anti-association activity of eIF1A [190]. In a more recent study, purified eIF1A stimulated TC binding in the absence of mRNA or AUG triplet by almost 20-fold, whereas purified eIF3 conferred only a 3-fold stimulation [32, 134]. The eIF1 was found to augment the stimulatory effect of eIF1A on TC binding in the absence of AUG, even though it had little activity on its own, and the greatest level of TC binding occurred when eIF1, eIF1A and eIF3 were present simultaneously [33]. Studying the corresponding yeast factors in a reconstituted system, Lorsch et al. found that eIF1A could function in the absence of eIF3 to stimulate TC binding to 40S subunits in the presence of a model 43-nt unstructured mRNA and 60S subunits. In this system, eIF1A was strongly dependent on eIF1 for promoting TC binding, whereas eIF3 had no stimulatory activity in the presence or absence of eIF1 and eIF1A [135]. Thus, the relative importance of eIF1, eIF1A and eIF3 in promoting 43S complex formation *in vitro* seems to vary with the source and pre-paration of factors, ribosomes and assay conditions.

Maitra et al. [32] reported that eIF1A cannot stimulate TC binding in the presence of 60S subunits under conditions that promote subunit joining. The eIF3, by contrast, could function in the presence of 60S subunits, but its stimulatory effect disappeared with the addition of an AUG triplet. To account for these findings, they proposed that both eIF1A and eIF3 are required to form a stable 43S complex, with eIF1A catalyzing transfer of TC to 40S subunits harboring eIF3. The eIF3, in conjunction with TC, protects the 43S complex against disruption by a 60S subunit prior to mRNA binding but becomes dispensable for this function once Met-$tRNA_i^{Met}$ is base-paired to the AUG codon [32]. As mentioned above, they found more recently that eIF1A can enhance the anti-association activity of eIF3, and that eIF1A and eIF1 function together as effectively as eIF3 does alone in preventing disruption of 43S complexes by 60S subunits in the absence of AUG. As in the case of TC binding, the combination of all three factors conferred the greatest anti-association activity of all. Consistently, it was found that eIF3 (strongly) and eIF1A (moderately) enhanced stable 40S binding by eIF1, and that eIF1 (strongly) and eIF3 (moderately) enhanced 40S binding by eIF1A. Hence, eIF1, eIF1A and eIF3 probably cooperate in the formation of a stable 43S complex containing all three factors and TC prior to mRNA binding *in vitro* [33].

The eIF1A has an ortholog in Archaea and exhibits significant sequence similarity (21% identity) to bacterial initiation factor IF1 [2]. The three-dimensional structures of *E. coli* IF1 [3] and mammalian eIF1A [191] both contain the five-stranded antiparallel β-barrel known as the OB domain [3], whereas eIF1A contains an additional

α-helical domain and unstructured N- and C-terminal extensions not present in bacterial IF1 [191] (Fig. 7.2-8B). The archaeal orthologs of eIF1A contain abbreviated N- and C-terminal extensions and may lack the α-helical domain. As IF1 binds directly to the A-site of the 30S ribosome [192, 193], the OB-fold in eIF1A most probably binds to the A-site of 40S subunits in eukaryotes. The eIF1A shows nonspecific RNA-binding activity *in vitro* [194] with a K_d of ~15 mM [191], and NMR analysis has identified residues in the OB-fold and α-helical domains of eIF1A whose chemical shifts change in the presence of various RNAs, and thus may contact RNA directly. Consistently, mutations of several such residues reduced RNA binding by eIF1A. Interestingly, a *K67D* mutation of Lys^{67} also impaired eIF1A-stimulated TC binding to 40S subunits *in vitro*, leading to the suggestion that this residue is required for eIF1A binding to the rRNA in the 40S subunit (Figs. 7.2-8A and B) [191].

A C-terminal deletion that removes all of the unstructured CTD and a predicted 3_{10} helix in the helical domain of yeast eIF1A produced a Gcd^- phenotype in addition to the Slg^- phenotype observed for a smaller deletion that removes the eIF5B-binding domain (see below) (Fig. 7.2-8A). The fact that this Gcd^- phenotype was suppressed by overexpressing the TC suggests that it reflects diminished TC binding to 40S subunits scanning the *GCN4* mRNA leader after translating uORF1 [195]. The delayed rebinding of TC to these 40S subunits would allow a fraction of the latter to by-pass uORFs 2–4 and reinitiate at *GCN4* instead [19]. This provides the first *in vivo* evidence that eIF1A enhances TC binding.

Pestova et al. showed that eIF1A also acts in conjunction with eIF1 in the presence of TC, eIF3, and the mRNA-associated factors eIF4A, eIF4B and eIF4F, to promote formation of a stable 48S complex with the ribosome positioned at the AUG codon, as judged by toeprint analysis. In the absence of eIF1 and eIF1A, an unstable complex was formed close to the 5′-end, whereas addition of eIF1, in a manner enhanced by eIF1A, led to dissociation of this complex and the formation of the more stable, correctly positioned 48S complex. For EMCV RNA, where ribosome binding to the start codon is directed by an IRES, eIF1 could direct 40S ribosomes to the correct AUG without eIF1A. Thus, eIF1 may possess the critical activity for positioning a 40S ribosome at the start codon [196]. Interestingly, mutations in residues on the RNA-binding surface of eIF1A did not impair its ability to disrupt incorrect 48S complexes formed at the cap, but led to the stabilization of incorrect complexes located upstream from the start site [191] (Fig. 7.2-8A). These data are consistent with the idea that eIF1A acts from the A-site in conjunction with eIF1 to play a role in AUG selection by initiator tRNA during the scanning process.

eIF1A Interacts with the IF2 Ortholog eIF5B

As discussed above, eIF1A and eIF5B are structural and functionally similar to bacterial IF1 and IF2, respectively. In accordance with evidence that IF1 and IF2 interact on the 30S ribosome, eIF5B and eIF1A from yeast interact directly *in vitro* and are stably associated in cell extracts. The last 24 amino acids in the unstructured acidic tail of eIF1A and the C-terminal 153 residues in the eIF5B CTD are necessary and sufficient for strong interaction between the yeast factors [6, 195]. Concurrently,

NMR analysis showed that the C-terminal 14 residues of human eIF1A are sufficient for binding to the eIF5B-CTD *in vitro*, and provided evidence that the last five residues of eIF1A lie in a shallow hydrophobic groove between helices 13 and 14 in the eIF5B CTD [197]. This portion of eIF5B corresponds to the last 32 residues of the protein and is located in domain IV of the crystal structure of archaeal eIF5B that forms the base of the chalice-like molecule [198] (Figs. 7.2-16A and B). A deletion of the last 87 residues of yeast eIF5B impairs its function *in vivo* and *in vitro* [6], and deletion of the eIF5B-binding domain in eIF1A also reduces translation initiation *in vivo* [185, 195]. Thus, it seems likely that eIF1A–eIF5B association through their extreme C-termini enhances an important aspect of initiation. This interaction seems to be restricted to eukaryotes as the relevant domains in eIF1A and eIF5B are missing in bacterial IF1 and IF2, and archaeal eIF1A lacks the eIF5B-binding domain at the extreme C-terminus of eIF1A. There is evidence that the nonconserved NTD of yeast eIF5B makes an additional contact with eIF1A that can be observed only when both factors are bound to the same ribosome [195].

Overexpression of eIF1A exacerbated the growth defect of *fun12* mutants which either lack eIF5B entirely or contain a C-terminally truncated form of eIF5B. To explain this genetic interaction, it was suggested that eIF1A is partially dependent on eIF5B for release from the 80S initiation complex, such that eIF1A overexpression in a *fun12* mutant would prolong binding of eIF1A to the ribosome and impede entry of the first eEF1A-GTP–aminoacyl-tRNA complex into the A-site [6]. Given that IF1–IF2 association mutually stabilizes binding of these factors to the 30S ribosome [199, 200], interaction between the C-termini of eIF1A and eIF5B might also enhance their association with the 40S ribosome early in the pathway. Suggestive evidence for this possibility stems from the finding that deleting the eIF1A C-terminus confers sensitivity to paromomycin (Par^S phenotype) in a manner exacerbated by deleting the NTD of eIF5B [195]. This drug binds to the A-site of prokaryotic ribosomes in a region overlapping the binding site for IF1 [193]; hence, it may compete with eIF1A for A-site binding. In the absence of a strong interaction with eIF5B, eIF1A may compete less effectively with paromomycin for the A-site.

Wagner and co-workers [197] presented an intriguing structural model for eIF5B and eIF1A bound to the 40S ribosome (summarized in Fig. 7.2-16B, right), in which the IF1-related central domain of eIF1A is bound to the A-site and makes contact with domain II of eIF5B, in the manner proposed for bacterial IF1–IF2 interaction. The extreme C-terminus of eIF1A binds to domain IV in eIF5B, as described above, and the remainder of the unstructured eIF1A CTD is stretched out to span the 50 Å separating the eIF5B domains II and IV. Domain IV in eIF5B additionally makes contact with the methionine and accepter stem of Met-tRNA$_i^{Met}$ located in the P-site, as proposed for bacterial IF2 [197]. This model is consistent with the known physical interactions between eIF5B and eIF1A, and the genetic evidence that eIF5B enhances Met-tRNA$_i^{Met}$ binding to the P-site [201] and promotes the release of eIF1A from the A-site [6]. Interestingly, the helical domain of yeast eIF1A is oriented towards the P-site in the model of Wagner et al, consistent with its role in TC binding. It was shown that the unstructured basic NTD of eIF1A mediates direct interaction with eIF2 and

eIF3 *in vitro*, although these interactions appear to be confined to the surface of 40S subunits *in vivo*. Deleting this domain had a Slg$^-$ phenotype, especially at low growth temperatures, but did not confer Par^S or Gcd$^-$ phenotypes. Hence, its interactions with eIF2 or eIF3 may be most important for a step following recruitment of TC that involves isomerization of factors in the 43S or 48S complex [195]. If present in an extended conformation, the eIF1A NTD may be long enough to permit physical contact between eIF1A in the A-site and TC in the P-site (Fig. 7.2-16B, right).

7.2.3 Binding of Ribosomes to mRNA

7.2.3.1 The Ends of Eukaryotic mRNAs Contain Distinctive Conserved Structures

All nuclear-transcribed eukaryotic mRNAs contain the m^{7}GpppN cap structure (in which m is a methyl group and N is any nucleotide) [202]. The cap is added to the nascent pre-mRNA early during transcription, and plays important roles in mRNA metabolism in the nucleus and the cytoplasm, including splicing, nucleo-cytoplasmic export, translation and stability (see Ref. [203] for review). The cap is critical for efficient translation, being the primary mRNA structure recognized by the translation-initiation machinery, via eIF4E, for assembly of the 48S preinitiation complex. Some viral mRNAs do not contain a cap structure, and, thus, are not recruited to ribosomes via eIF4E, but use an alternative mechanism involving direct binding of the 40S ribosome to a specialized IRES (see below). A poly(A) tail is present on most eukaryotic cellular mRNAs (except for mammalian histones), and several viral mRNAs. The poly(A) tail plays an important role in mRNA stabilization and translation. Translation initiation is stimulated by the PABP, which binds to eIF4G and thus brings about circularization of the mRNA (see below).

7.2.3.2 Ribosome Binding to mRNA is Stimulated by the eIF4 Factors

The recruitment of ribosomes to eukaryotic mRNAs is catalyzed by the eIF4 group of factors, which includes eIF4A, eIF4B, eIF4G, and eIF4H, and requires the energy provided by hydrolysis of ATP (see Refs. [174, 204] for reviews). The eIF4A, eIF4E and eIF4G form a stable complex in mammalian cells, termed eIF4F, which interacts directly with the cap through eIF4E (Fig. 7.2-10A). In other species, including yeast, eIF4A is bound loosely to the eIF4F complex. The eIF4A is an RNA-dependent ATPase and RNA helicase, and these activities are stimulated by eIF4B and eIF4H. eIF4G is a large, modular scaffolding protein, containing binding sites for many other initiation factors (Fig. 7.2-11A).

In the most general mechanism for ribosome binding to mRNA, eIF4F binds directly to the cap structure via eIF4E. The 43S preinitiation complex is then recruited to the mRNA by an interaction between eIF4G and eIF3, to form the 48S pre-initiation complex (Figs. 7.2-10A and 7.2-1B). As discussed earlier and below, a

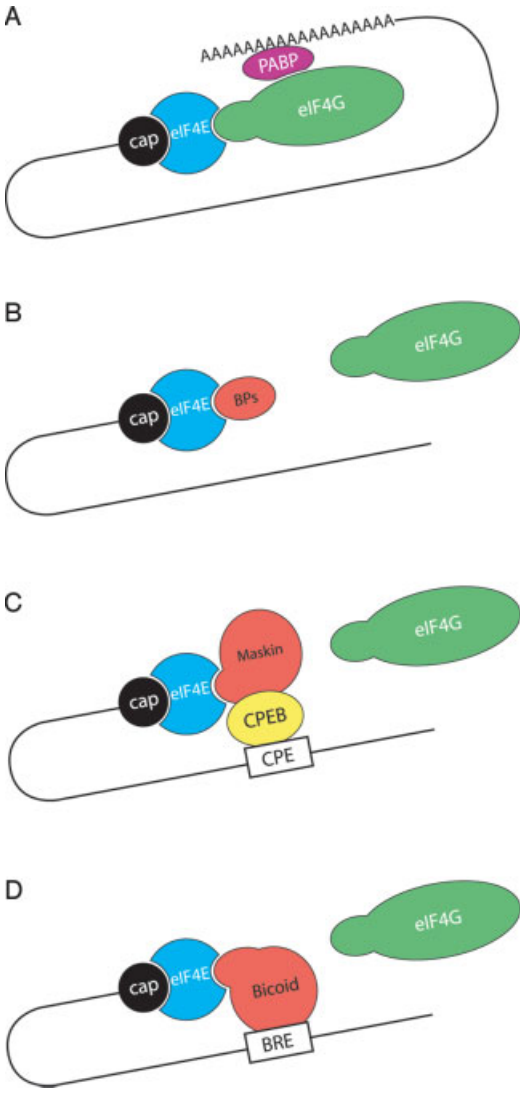

Figure 7.2-10 Regulation of translation via interactions with the mRNA 5′ cap structure **(A)** General model for 5′–3′ interactions. **(B)** Inhibition of cap-dependent by 4E-BPs binding to eIF4E and displacement of eIF4G. **(C)** CPEB-dependent displacement by maskin of eIF4G. CPEB interacts with the cytoplasmic polyadenylation element (CPE), which resides in the 3′-UTR and with eIF4E. This interaction results in inhibition of translation. **(D)** Bicoid binds directly to the Bicoid response element (BRE) in the 3′-UTR of *caudal* mRNA and displaces eIF4G from eIF4E, resulting in inhibition of translation. The common mechanism by which eIF4G is displaced from eIF4E by 4E-BPs, Maskin and Bicoid is competition for binding to eIF4E through the common motif YXXXXLΦ.In Maskin the tyrosine is substituted by threonine. Adapted with permission from Niessing et al. [293].

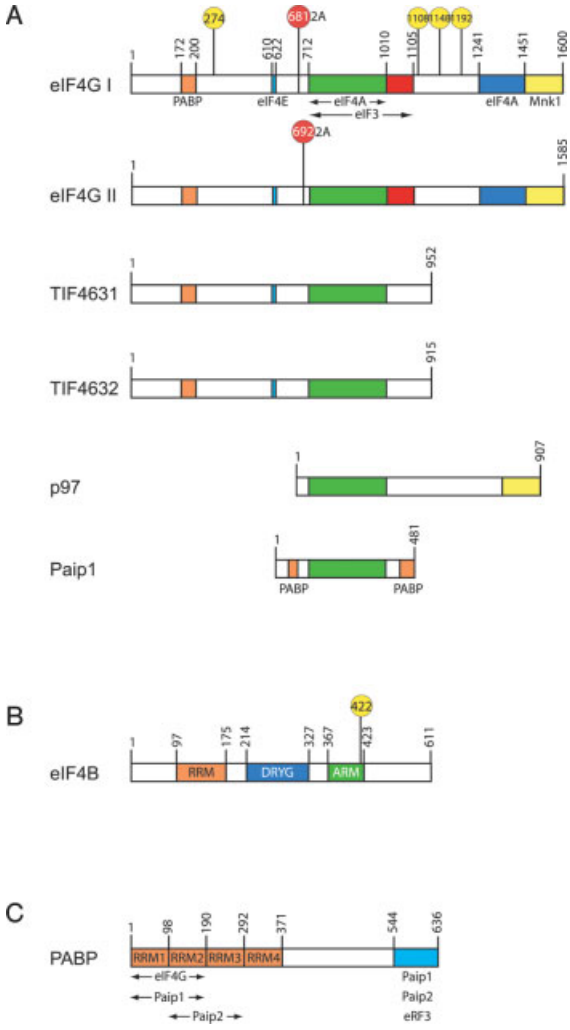

Figure 7.2-11 Schematic representations of the primary and domain structures of eIF4 factors and PABP. **(A)** Protein-binding domains in eIF4G family members are indicated by different colors. eIF4GI, eIF4GII, p97, and Paip1 are mammalian proteins, whereas TIF4631 and TIF4632 are the yeast eIF4G homologs. Phosphorylation sites in eIF4GI are indicated by their amino acid position (yellow circle), and the major cleavage site by the poliovirus 2A protease is also shown. **(B)** Functional domains in human eIF4B. RRM (RNA recognition motif) binds weakly to nonspecific RNA. DRYG (a region rich in aspartic acid, arginine, tyrosine and glycine) is important for dimerization and interaction with eIF3. ARM (arginine-rich motif) binds strongly non-specific RNA and is required for stimulation of eIF4A helicase activity. The S6 kinase phosphorylation site is indicated (yellow circle). Adapted from Methot, et. al. [271]. **(C)** Domain structure of human PABP. The boundaries of the conserved four RRM domains and the CTD (PABC) are shown. Also indicated are the binding sites of different proteins as described in the text.

number of other factors in the 43S complex participate in 48S complex assembly. It is noteworthy that a direct interaction between eIF4G and eIF3 has not been demonstrated in yeast, although eIF4G–eIF5 association has been detected and eIF5 may bridge an association between eIF4G and eIF3 in yeast cells [72]. In the following sections, structure–function relationships for the eIF4 initiation factors, followed by a discussion of alternative mechanisms of ribosome binding, ending with a discussion of the regulation of eIF4 activity are described.

eIF4E

eIF4E is the ~24 kDa cap-binding subunit of eIF4F. It was first identified by its ability to cross link to the cap structure [205] and was subsequently purified from a RRL [206]. eIF4E is essential for growth in yeast, and is highly conserved in primary sequence from yeast to human [207] (Table 7.2-1). Human and yeast eIF4E are 32% identical, and mammalian eIF4E can functionally substitute, albeit inefficiently, for yeast eIF4E [207]. The 3D structures of mammalian and yeast eIF4E bound to a cap analogue (m^7GDP) were solved by X-ray crystallography and NMR, respectively [208, 209] (Fig. 7.2-12). The protein resembles a cupped hand or baseball glove. It consists of a single α/β domain composed of an eight-stranded, antiparallel curved β-sheet, backed on its dorsal surface by three long α-helices. m^7GDP occupies a narrow slot on the concave surface of eIF4E, where m^7GDP binding is mediated by π–π stacking interactions between the base and indole side chains of two tryptophans, Trp^{56} and Trp^{102} in mammals or Trp^{58} and Trp^{104} in yeast. This binding is further stabilized by other interactions including hydrogen bonds, van der Waals contacts and electrostatic interactions. The amino acids involved in cap binding are conserved phylogenetically, demonstrating that the mechanism of cap-binding to eIF4E is also highly conserved.

eIF4E is phosphorylated on a single serine residue, Ser^{209} in mammals, which is conserved in all metazoans. Based on the mouse eIF4E-m^7GTP co-crystal structure, it was suggested that phosphorylated Ser^{209} forms a salt bridge with Lys^{159} [210]. The salt bridge was postulated to act as a clamp that brackets the proposed trajectory of the mRNA to stabilize mRNA–eIF4E interaction. However, two recent papers [211–212] demonstrated that eIF4E phosphorylated on Ser^{209} exhibits reduced, rather than increased, affinity (2–4-fold) for cap analogs. A recently described human eIF4E-m^7GpppA co-crystal structure might help to resolve some of these questions. It shows that the distance between the Cα positions of Ser^{209} and Lys^{159} is ~19 Å, which is too large for salt-bridge formation, thus arguing against a clamping mechanism [213, 214]. It was suggested that electrostatic repulsion between the penultimate adenosine of the cap structure and phosphorylated Ser^{209} might reduce eIF4E binding [211]. However, the distance might be too great (7 Å) for such a repulsion to take place. Thus, the mechanism by which phosphorylation of Ser^{209} lowers cap affinity is still in question. Regardless, the phosphorylation might stimulate the release of eIF4E from the cap structure so that the initiation complex could scan

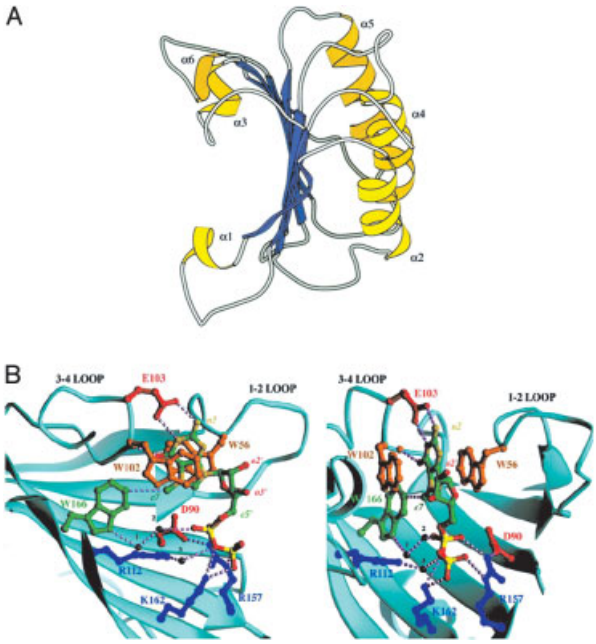

Figure 7.2-12 Ribbon diagram drawings of the 3D structure of yeast and murine eIF4E. **(A)** Solution structure of yeast eIF4E determined by NMR spectroscopy (shown with β sheets in blue and α helices in yellow). The cap structure binds to the convex surface of eIF4E, whereas the 4E-BP and eIF4G bind to a shared motif on the convex dorsal surface of eIF4E [209] (PDB ID: 1AP8). **(B)** X-ray co-crystal structure of eIF4E with m^7GDP. Only the cap-binding slot and the surrounding region of eIF4E is shown. The amino acids, which participate in m^7GDP binding, are indicated. Salt bridges, hydrogen bonds and van der Waals interactions are shown as dotted lines. Bridging water molecules are drawn in black (from Ref. [208]; PDB ID: 1EJ1). The two views of the molecule are rotated 90° relative to each other.

towards the initiation codon, in analogy to promoter clearance following phosphorylation of transcription complexes [211].

eIF4G

eIF4G is a modular scaffolding protein, and plays a major role in recruiting the ribosome to mRNA and coordinating the assembly of the 48S pre-initiation complex (Table 7.2-1). All eukaryotes contain two related eIF4G proteins (eIF4GI and eIF4GII in mammals are 46% identical; TIF4631 and TIF4632 in yeast are 53% identical). Neither TIF4631 nor TIF4632 is essential in yeast, but deletion of both is lethal [215]; hence, they execute partially overlapping functions. Mammalian cells

contain one additional, more distantly related eIF4G homologue p97/NAT1/DAP5 (see below). eIF4G is traditionally divided into three regions, which correspond to separate structural and functional domains connected by unstructured hinge regions that are sensitive to proteases (Fig. 7.2-11A). This stems from early reports on the cleavage by eIF4G into three fragments of roughly equal size by the picornavirus 2A protease [172]. The hinge regions are also susceptible to cleavage by the HIV-1 viral protease [216] and cellular proteases, such as the caspases involved in programed cell death (apoptosis) [217]. It is likely that the hinge regions provide the necessary flexibility to the independent domains to interact with each other and control eIF4G function [218].

The N-terminal fragment of eIF4G in all species examined contains binding sites for PABP and eIF4E [219–221] and the middle fragments contain the interaction domains for eIF4A, eIF3 and mRNA [222–224]. The C-terminal region, which exists only in metazoans (even in plants it is much shorter), contains an additional binding site for eIF4A [172, 224] and a binding domain for the serine–threonine protein kinases Mnk1 and Mnk2 [225, 226] (Fig. 7.2-11A).

It is well established that eIF4A binding to the mammalian eIF4G middle domain is sufficient for ribosome binding [227, 228]. Thus, a 43S pre-initiation complex can be assembled efficiently on an IRES-containing mRNA with only the eIF4G middle domain [228], or with the middle domain plus the eIF4E-binding site on a capped mRNA [218]. What then is the function of the second, C-terminal eIF4A binding site? Most evidence suggests that only one eIF4A molecule at a time interacts with one eIF4G molecule. This was initially suggested based on the finding that a mutant eIF4G defective for eIF4A binding to the C-terminal region exhibits a 3–4-fold reduction in translation, whereas deletion of the entire C-terminal fragment reduced translation by only 2-fold. It was therefore proposed that one molecule of eIF4A interacts with both the middle and C-terminal domains of eIF4G through two separate surfaces. This model was subsequently corroborated by showing that two differentially epitope-tagged eIF4A molecules failed to co-immunoprecipitate, consistent with nonsimultaneous binding of two molecules of eIF4A to the same eIF4G molecule [229]. Notwithstanding these conclusions, analysis of the ratio of eIF4A to eIF4G in the eIF4F complex led Korneeva et al. to conclude that the stoichiometry of eIF4A to eIF4G is 2:1 [230]. Clearly, further experiments are needed to resolve this disagreement. Why is there a requirement for two eIF4A-binding sites in eIF4G in mammals but not in plants or fungi? As noted above, the C-terminus might play a modulatory role in translation, which could involve phosphorylation of eIF4G via signaling pathways that affect growth and proliferation. Thus, in mammals, the CTD might mediate rearrangements of eIF4G interactions with other initiation factors following phosphorylation (see below). Recent findings show that the middle domain of eIF4G in yeast also interacts with eIF5 and this interaction could underlie the role of eIF5 in promoting 48S complex formation [72].

Several additional proteins have been reported to interact with eIF4G and could exert important physiological effects on translation or mRNA stability. However, these novel interactions have been less rigorously characterized in biochemical

assays than those described above. Pdcd4 is a tumor-suppressor protein that interacts with both eIF4A and eIF4G and inhibits cap-dependent translation [231]. The interaction site of Pdcd4 on eIF4G is in the middle domain. CBP80, together with CBP20, forms the nuclear cap-binding protein complex (nCBP) that is conserved from yeast to humans [232]. CBP20 interacts directly with the cap structure, whereas CBP80 was reported to interact with eIF4G both in yeast and in mammals [233, 234]. The interaction domain in yeast was mapped to the region between the eIF4E- and eIF4A-binding sites. There is evidence that the nCBP–eIF4G complex functions in the first round of translation [233, 235], and it was proposed that this "pioneer round" of translation is critical for degradation of mRNAs harboring premature stop codons by the nonsense-mediated mRNA decay (NMD) pathway [235]. Finally, the yeast decapping enzyme DCP1 was reported to interact with eIF4G and stimulate decapping of the mRNA [236]; however, the mechanism and characteristics of this interaction are yet to be determined.

The 3D structures of portions of the N-terminal and middle domains of eIF4G were resolved by X-ray crystallography and NMR spectroscopy. The structure of the eIF4E-binding site in the NTD of eIF4G was determined by NMR spectroscopy in yeast [237] and X-ray crystallography for mouse eIF4G [238]. In both species the eIF4E-binding domain is unfolded and becomes structured by an induced fit mechanism upon binding to eIF4E. A small unfolded fragment of mouse eIF4G (28 amino acids) assumes an α-helical structure with two turns when bound to eIF4E [238] (Fig. 7.2-13). A similar finding was made for an unstructured sequence of 88 amino acids in yeast eIF4G that becomes structured and resistant to proteases upon binding to eIF4E [237]. Strikingly, 4E-BPs, which are negative regulators of eIF4E, contain a closely related unstructured sequence, which interacts with the eIF4G-binding site on eIF4E and competes with eIF4G for binding to eIF4E (Fig. 7.2-10B). The sequence motif YXXXXLΦ (where Φ is a hydrophobic amino acid) is shared between 4E-BP and the 4E-binding domain in eIF4G. This motif is required for eIF4E binding by both proteins and makes direct contacts with amino acids in eIF4E. Consequently, the 3D structures of the 4E-binding domains in 4E-BP and eIF4G are superimposable (Fig. 7.2-13). Thus, 4E-BP competes with eIF4G by a *par-exellence* mechanism of molecular mimicry and inhibits the formation of eIF4F [239, 240]. This is a major pathway for regulating eIF4F function (see below).

The 3D structure of the middle domain of eIF4G, which binds eIF4A, eIF3 and RNA, also has been solved. This crescent-shaped domain consists of five HEAT repeats (Fig. 7.2-14A). Mutational analysis based on the structure has identified two adjacent patches of amino acids that bind eIF4A and the EMCV RNA, respectively [222].

p97/DAP5/NAT1[241–243], which plays a role in regulation of translation during apoptosis [241], exhibits homology to the C-terminal two-thirds of eIF4G. Consistently, p97 interacts with eIF3, eIF4A and Mnk1, but not with eIF4E or PABP [204] (Fig. 7.2-11A). Thus, p97 resembles the C-terminal fragment of eIF4G, which is generated during picornavirus infection and stimulates IRES-mediated translation (see below and Ref. [244]). In accordance with this, a fragment derived from p97 during

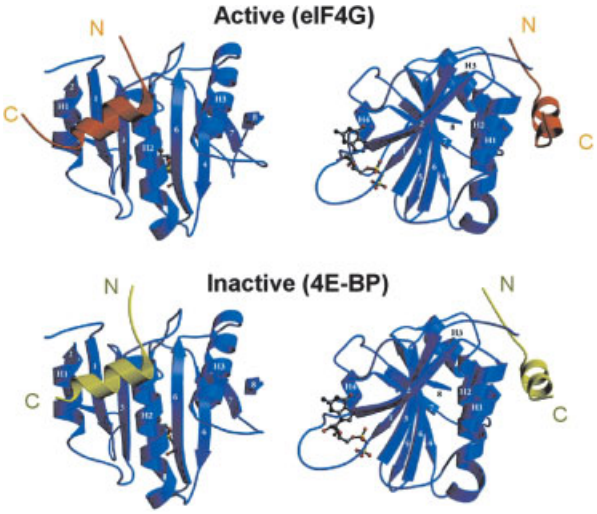

Figure 7.2-13 4E-BP1 is a molecular mimic of eIF4G. Ribbon diagrams of murine eIF4E (blue) in a complex with peptides of eIF4GII (orange), representing the active form of eIF4E, or 4E-BP1 (yellow), representing the inactive form of eIF4E, as determined by X-ray crystallography [238] (PDB IDs: 1EJ4 [4E-BP1] and 1EJH [eIF4GII]). m^7GDP is shown as a ball-and-stick representation bound to the convex surface of eIF4E. The structures on the right are rotated 90° vertically relative to each other.

apoptosis stimulates translation of IRES-containing mRNAs encoding proteins that function during apoptosis, including c-Myc, Apaf-1, XIAP, and p97 itself [204, 245, 246]. It is surprising that p97 inhibits, rather than stimulates, translation from the viral EMCV IRES [241–243]. It is therefore important to understand the different modes of action of p97 on the EMCV IRES (and perhaps other viral IRESs) versus the IRESs in cellular mRNAs.

eIF4A

The eIF4A is a ~45 kDa polypeptide that, is highly conserved in evolution (65% identity between yeast and human) (Table 7.2-1). Two different yeast genes (*TIF1* and *TIF2)* encode the same eIF4A protein, and either gene can provide the essential function of eIF4A *in vivo* [247]. The eIF4A is the most abundant translation-initiation factor, present at ~ 3 copies per ribosome as compared with 0.2–0.5 for other initiation factors [248, 249]. eIF4A is the prototype of the family of DEAD-box RNA helicases, named after one of the eight conserved motifs (D-E-A-D or Asp-Glu-Ala-Asp) shared amongst the family members. The DEAD-box family of proteins belongs to a much larger family, whose members contain the motif DExH/D (where x is any amino acid) [250]. Many of the DEAD-box proteins exhibit RNA-

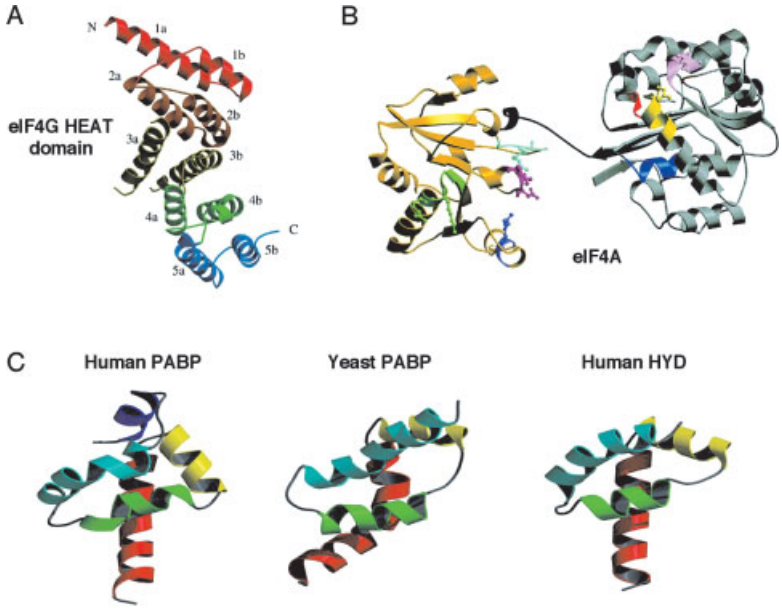

Figure 7.2-14 3D structures of mRNA binding factors. **(A)** Middle-region HEAT domain of eIF4G. Ribbon drawing of the HEAT domain of eIF4GII, which binds eIF4A and the EMCV IRES. The molecule is crescent shape, with the convex surface on the right and the concave on left. The view is along the cylindrical axis of the α helices. The HEAT domain consists of two antiparallel α helices, which are repeated in tandem five times. Unlike α helices in other HEAT domains, which are bent because they contain proline residues, those in eIF4G are predominantly straight. Each pair of helices is labeled by a different color [222]. **(B)** Model of eIF4A. The structure is shown as a ribbon diagram. The structure was constructed based on the separate crystallographic structures of the N- and C-terminal domains using molecular replacement [267]. According to the model, eIF4A, unlike other helicases, assumes a dumb-bell conformation, which consists of two compact domains. The two domains are connected through an extended, 11-residue linker. Conserved motifs are colored. **(C)** Comparison of the three PABC domains of human and yeast PABPs and human HYD. Ribbon diagrams of the 3D structures as determined by NMR spectroscopy for PABP, and X-ray crystallo-graphy for HYD. The α helices are differentially colored. Note that human PABP consists of five α helices, whereas yeast PABP and HYD contain only four helices. Adapted from Refs. [284, 285, 397]. (PDB IDs: 1GL9 (human PABC); 1IFW (yeast PABC); 1I2T (HYD)).

dependent ATPase activity, and a few show ATP-dependent RNA helicase activity. eIF4A has both activities [251, 252]; however, these activities are weak and (especially, the helicase activity) markedly stimulated by eIF4B or eIF4H [253, 254] The

mechanism of eIF4B stimulation is not well understood. eIF4A is a nonprocessive helicase, and unwinds by itself only 3–5 basepairs, but eIF4B prevents the reassociation of the unwound RNA, and thus promotes the unwinding of larger duplexes. Thus, the eIF4A (and subsequently all DEAD-box proteins) was hypothesized to function as a translocating motor, which removes mRNA secondary structure from the 5′-UTR to create a ribosome landing pad, and subsequently facilitate ribosome scanning [250, 253]. This is consistent with findings that secondary structures in the mRNA 5′-UTR potently inhibit translation [255, 256]. Also, inhibition of translation by dominant-negative mutants of eIF4A is directly proportional to the degree of secondary structure in the mRNA 5′-UTR [257]. There are three different eIF4A proteins in metazoans (eIF4AI, eIF4AII, and eIF4AIII). eIF4AI and eIF4AII are very similar in sequence (89% identity), and function [258]. eIF4AIII is 66% identical to eIF4AI in humans, but there is no evidence that eIF4AIII functions in translation [259]. It cannot substitute for eIF4AI in ribosome initiation complex formation. This might be explained by its ability to bind only to one of the eIF4A-binding sites on eIF4G (middle domain) [259]. A more distantly related eIF4A homolog, which functions in translation, is the yeast DED1 protein and its mouse homolog PL10. The *DED1* gene was initially isolated in a genetic screen using a temperature-sensitive mutant of eIF4E [260], and was subsequently shown to be required for translation initiation [260, 261]. DED1 is an RNA helicase, which functions independent of eIF4B [262]. Importantly, the murine homolog of DED1 (PL10), which is required for spermatogenesis [263], can substitute for its yeast counterpart [260]. An intriguing possibility is that DED1/PL10 is required for translation of a subset of mRNAs, perhaps those that contain extensive secondary structure. For example, Noueiry et al. [264] identified a mutant allele of *DED1*, which affects selectively the translation of a brome mosaic virus mRNA.

The eIF4A is composed of two domains, which were separately crystallized from yeast eIF4A fragments [265, 266]. A complete structure was assembled, based on results from the two studies [267] (Fig. 7.2-14B). A complete X-ray crystal structure of an eIF4A-like protein from *Methanococcus jannaschii* was also obtained [268]. This protein is similar in size to eIF4A. The eIF4A structure reveals that domain 1 contains the ATP-binding motifs, which are facing the cleft in the linker region separating the two domains. Domain 2 contains the binding site for RNA. The linker region also contains a motif (III), which links ATP binding with helicase activity. It is thought that the helicase activity is effected by conformational changes in the protein.

eIF4B

eIF4B was purified based on its ability to stimulate translation in an *in vitro* reconstituted rabbit reticulocyte translation system [133]. The best documented biochemical activity of eIF4B is its ability to stimulate the ATPase and RNA helicase activities of eIF4A in a highly specific manner (Table 7.2-1), as other RNA helicases are not stimulated by eIF4B. Also, genetic evidence demonstrated that eIF4A and eIF4B functionally interact [174, 269]. This striking biochemical and genetic specificity is all the

more surprising since there is no evidence that eIF4B interacts physically with eIF4A.

eIF4B is a 68 kDa polypeptide in mammals, but smaller in other species, and is conserved through evolution from yeast to humans [174]. However, the degree of sequence conservation is weak relative to other initiation factors (22% identity between yeast and human) (Table 7.2-1). Also, in contrast with most other initiation factors, eIF4B is not essential, as a yeast strain lacking the gene for eIF4B (*TIF3*) is viable [269]. Consistent with this, ribosome binding and translation are reduced, but not abrogated in the absence of eIF4B. Mammalian eIF4B is a dimer, whose dimerization is mediated by a region in the middle of the molecule called the DRYG domain (rich in aspartic acid, arginine, tyrosine and glycine) [173] (Fig. 7.2-11B). The DRYG region also interacts with eIF3 in mammalian cells and yeast, through eIF3g/p44, but an interaction was also reported with p170 in mammalian cells [270]. eIF4B also interacts strongly with RNA [271, 272]. A C-terminal arginine-rich motif (ARM) binds strongly to RNA in a sequence-independent manner. A second RNA-binding domain in the N-terminus containing an RRM [271] binds weakly to RNA in a sequence-independent manner. It was suggested that the RRM binds to the 18S rRNA, whereas the ARM binds to the mRNA [273]. Binding of eIF4B to the IRES of FMDV or EMCV is critical for translation [274, 275]. Thus, in addition to stimulating eIF4A helicase activity, eIF4B may promote mRNA–ribosome interaction during ribosome scanning, consistent with the finding that eIF4B exhibits RNA-annealing activity [276].

Mammalian cells contain an eIF4B-related protein termed eIF4H [277], which is 39% identical to eIF4B. eIF4H exhibits biochemical activities similar to eIF4B in that it stimulates the ATPase and helicase activities of eIF4A, and eIF4H can partially substitute for eIF4B in a highly fractionated rabbit reticulocyte translation system. The eIF4H is much smaller than eIF4B (~25 kDa), and lacks the DRYG domain, which mediates eIF4B dimerization. Consistent with this, eIF4H is a monomer. eIF4H contains an RRM, which is 45% identical to that of eIF4B, and binds weakly to RNA.

PABP

Although the PABP has not been traditionally viewed as an initiation factor, it is becoming clear that it plays an important role in translation initiation, primarily through its interaction with eIF4G. PABP is a phylogenetically conserved ~70 kDa polypeptide that is essential in yeast [278] (Table 7.2-1). PABP is an abundant protein, occurring in 6-fold excess of ribosomes, comparable with eIF4A levels [279]. A large number of studies have implicated PABP in mediating the stimulatory effects of the poly(A) tail on translation initiation (see e.g. Ref. [280]; see also review [281]).

An oligonucleotide of 12 adenosines (oligo $[A]_{12}$) is sufficient for binding to PABP, yet one PABP protects covers 27 adenosines on a poly(A) tail. PABP contains four highly conserved RRMs at the N-terminus (Fig. 7.2-11C). RRM1 and RRM2 form a contiguous binding site for oligo $(A)_{12}$ and can bind to poly(A) with an affinity equal

to that of wild-type PABP [282]. In addition, they are also bound by proteins (see below). By contrast, RRM3 and RRM4 bind to poly(A) with lower affinity (~10-fold), and exhibit weak affinity for non-poly(A) RNA. The proline-rich, C-terminal one-third of PABP serves as a docking site for several proteins, including PABP-interacting proteins 1 and 2 (Paip1 and Paip2) (Fig. 7.2-11C) (see below) [283–285].

Several distinct fragments of PABP stimulate translation in *Xenopus oocytes*, independent of their poly(A)-binding activity [280]. A fragment containing RRM1 and RRM2 of PABP, which binds eIF4G, strongly stimulates translation. RRM3, RRM4 and the C-terminus of PABP also stimulate translation, but to a lesser degree [280]. The mechanism by which RRM1 and RRM2 stimulate translation can be explained most probably through interaction with eIF4G, as discussed below. However, it is not clear how the other fragments stimulate translation.

The solution structure of the conserved ~75 amino acids at the C-terminus of PABP was determined by NMR spectroscopy [284]. The motif consists of five α-helices, which are arranged as an arrowhead (Fig. 7.2-14C). A deep hydrophobic pocket is formed between helices 2 and 3. This surface serves as binding site for Paip2, based on the chemical shift pattern induced upon ligand binding. Since these sequences are very highly conserved it is most probable that all proteins which interact with the PABP C-terminal conserved motif, such as Paip1 and eRF3, interact in a manner similar to Paip2. Consistent with this, Paip1 and Paip2 compete for binding to the CTD of PABP [283]. Similarly, Paip2 and eRF3 compete for binding (A. Kahvejian and N. Sonenberg, unpublished results). Surprisingly the human protein HYD (hyperplastic discs), which is unrelated to PABP in sequence, is structurally very similar to the PABP C-terminal conserved domain [285].

7.2.3.3 Circularization of mRNA via eIF4G–PABP Interaction

The cap and poly(A) tail of eukaryotic mRNAs are physically brought together by interactions between eIF4E and PABP with eIF4G to generate a circular mRNA (Fig. 7.2-10A). This was initially documented in yeast [219], and later shown for plants and mammals [220, 221]. Circularization of the mRNA provides a satisfactory explanation for the reported synergism between the cap structure and the poly(A) tail in stimulating translation initiation [286]. The eIF4G-binding site was mapped to the phylogenetically conserved RRM2 in yeast [287] and human PABP [220] (Fig. 7.2-11C), and the reciprocal binding site for PABP was mapped to the eIF4G N-terminus [220]. A stretch of 29 amino acids in the N-terminus of human eIF4G interacts with RRM1 and RRM2 of human PABP [220], as is the case for yeast PABP. Despite its high homology with yeast PABP, human PABP does not interact with yeast eIF4G [287], most probably because the PABP-binding sites in the human and yeast eIF4G proteins are quite divergent. However, the fact that this interaction has been conserved through evolution (or arose twice), despite the divergence of the protein sequences, underscores its paramount functional significance.

There are several mechanisms by which mRNA circularization could enhance translation initiation. First, circularization should increase the concentration of

terminating ribosomes in the vicinity of the mRNA 5′-cap structure and thereby facilitate ribosome recycling. This notion is bolstered by the finding that PABP also interacts with the termination factor eRF3. Thus, PABP may bridge eRF3 and eIF4G [288] (see below), looping out the 3′-UTR, and thus facilitating the direct shunting of ribosomes to the 5′-end of the mRNA. Secondly, PABP may participate in 60S subunit joining [289]. Thirdly, interaction of PABP with eIF4G may cause an allosteric effect that increases the affinity of eIF4E for the cap structure. It was also reported that in plants PABP enhances the helicase activity of eIF4F [290].

7.2.4
Translational Control by mRNA Circularization

mRNA circularization plays important roles in translational control through proteins unrelated to PABP, and many of these mechanisms are important during metazoan development. Whereas PABP circularizes the mRNA by interacting with eIF4G, other proteins cause circularization by interacting with eIF4E and thereby inhibiting eIF4E–eIF4G interaction and translation in a manner similar to the inhibitory mechanism for 4E-BPs. Certain mRNAs (such as cyclin B) contain cytoplasmic polyadenylation elements (CPEs) in their 3′-UTR, which are required for polyad-enylation and subsequent translation during *Xenopus* egg development. Polyadenylation is mediated by CPEB (cytoplasmic-polyadenylation binding protein). Maskin is a CPEB-interacting protein that inhibits polyadenylation and subsequent translation by interacting with eIF4E and displacing it from eIF4G [291]. Thus, by interacting with both eIF4E at the 5′-end and CPEB at the 3′-UTR, Maskin circularizes the mRNA and prevents complex formation with eIF4G (Fig. 7.2-10C). It is noteworthy that the motif in Maskin responsible for its binding to eIF4E is similar to that in eIF4G, but with the important difference that the tyrosine in the YXXXXLΦ motif is substituted by a threonine. This might explain why the interaction between maskin and eIF4E is rather weak [292].

Another recent example of 5′-cap-dependent translational control, which is mediated by the 3′-UTR and mRNA circularization, involves *caudal* mRNA translation in *Drosophila* [293]. *Caudal* is a transcription factor in the *Drosophila* embryo whose translation is specifically repressed in the anterior compartment by Bicoid, another transcription factor. Bicoid binds simultaneously to the Bicoid response element (BRE) in *caudal* mRNA and to eIF4E bound to the cap structure, consequently interfering with eIF4G binding (Fig. 7.2-10D). Thus, by competing with eIF4G binding to eIF4E through the common binding motif YXXXXLΦ, Bicoid inhibits specifically the translation of *caudal* mRNA.

Stimulation of translation via circularization occurs with other partners, which substitute for PABP, in mRNAs where a poly(A) tail is absent. For example, mammalian histone mRNAs are not polyadenylated and possess at their 3′-end a short stem-loop structure, which is required for optimal translation. This structure is bound by a protein, stem-loop binding protein (SLBP), which also binds to eIF4G, thus circularizing the mRNA. Consistent with this, SLBP stimulates translation. Curiously, SLBP does not bind to the PABP-overlapping binding site on eIF4G, but

rather at a site overlapping the eIF3-binding site [294]. Some viral mRNAs also do not contain a poly(A) tail. Rotavirus mRNAs are capped but not polyadenylated, and contain a sequence (UGACC) in their 3′-UTRs that is recognized by the viral NSP3 protein [295]. NSP3 interacts with the N-terminus of eIF4G to stimulate viral mRNA translation [296, 297]. In addition, NSP3 displaces PABP from its complex with eIF4G, and thus inhibits host protein synthesis [296]. In summary, these examples ascribe an important role for PABP as a translation factor that stimulates ribosome recruitement, and stress the importance of circularization for translational activation.

7.2.5 Regulation of eIF4 Function by Phosphorylation

7.2.5.1 eIF4E Phosphorylation

As discussed above, Ser^{209} is the only phosphorylation site on eIF4E that is conserved in metazoans. This residue is phosphorylated under many conditions including addition of growth factors, mitogens, hormones, and also in response to stress, such as arsenite or anisomycin treatment. The Mnk kinases which phosphorylate eIF4E in response to these conditions, are phosphorylated and activated by two different MAP kinase signaling cascades (Fig. 7.2-15) [298, 299]. The biological significance of eIF4E phosphorylation was clearly demonstrated in *Drosophila* where it was shown that alanine substitution of Ser^{251} (equivalent to mammalian Ser^{209}) caused slow development and resulted in smaller flies [300]. Significantly, the Asp^{251} mutation, which should mimic the phosphorylation state, rescued the small fly phenotype. It should be noted, however, that phosphorylation of eIF4E is not essential for general translation *in vivtro* and *in vitro* [301, 302]. Thus, the phosphorylation of eIF4E is probably critical for high-level translation of a subset of mRNAs, which encode proteins that function in cell growth and development.

7.2.5.2 eIF4E-4E-BPs

As discussed above, a major mechanism for the regulation of cap-dependent translation involves the family of proteins that inhibit translation initiation by binding to eIF4E, termed the 4E-BPs (see Ref. [204] for review. The family consists of three members (4E-BP1, 4E-BP2, and 4E-BP3 in mammals), which share 56–59% sequence identity. The conservation is especially prominent in the middle regions of the 4E-BPs, which contain the binding sites for eIF4E (including the YXXXXLΦ motif described above), and also in the flanking sequences that contain the phosphorylation sites, which regulate binding of 4E-BPs to eIF4E.

The phosphorylation state of several serine and threonine residues in the 4E-BPs regulates their affinity for eIF4E. Hypophosphorylated 4E-BPs bind strongly to eIF4E, but hyperphosphorylation reduces binding. Seven Ser/Thr phosphorylation sites were reported in the mammalian 4E-BP1 protein. Several of these sites were mapped by mass spectrometry, whereas others were inferred from mutagenesis studies. Two phosphorylated residues, Thr^{-37} and Thr^{-46}, lie on the N-terminal side

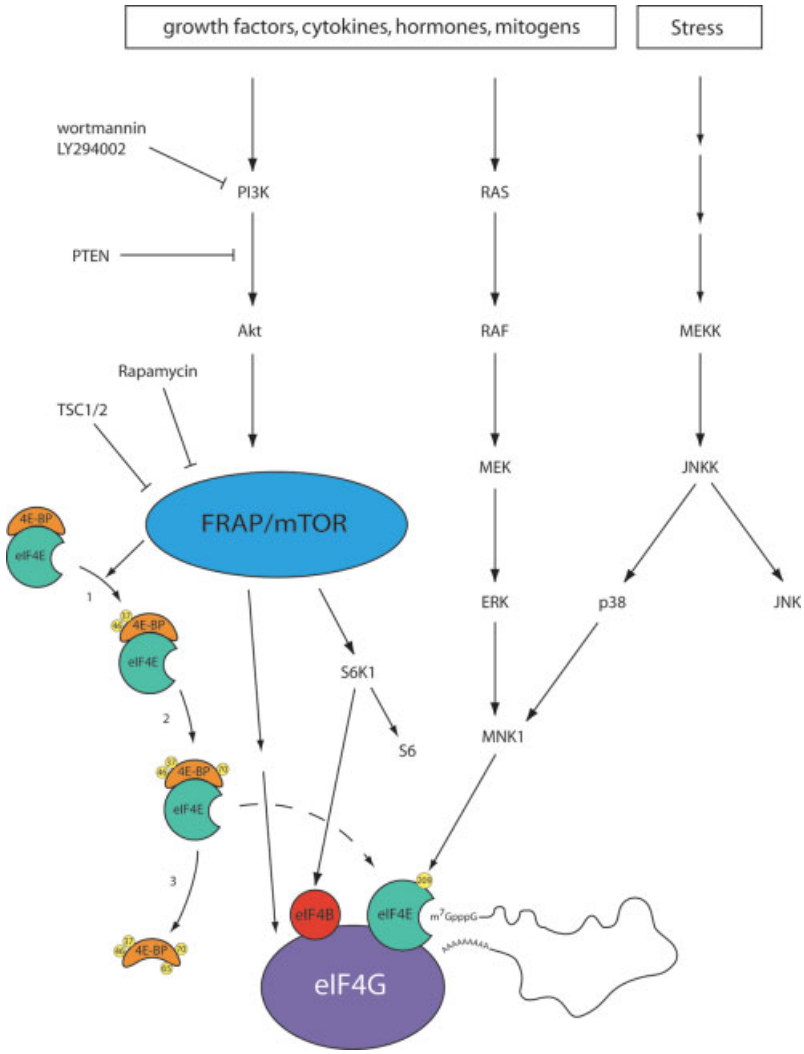

Figure 7.2-15 Signaling pathways leading to phosphorylation of translation-initiation components. Extracellular stimuli activate the PI3 kinase and Ras pathways. PI3 kinase signals through Akt and FRAP/mTOR to several translation components: 4E-BP, eIF4B, eIF4G and S6. Phosphorylation of 4E-BPs occurs in an ordered, hierarchical manner. Two tumor suppressor genes products: PTEN (phosphatase and tensin homolog deleted on chromosome ten), and TSC1/2 (tuberous sclerosis complex consisting of two proteins tuberin and hamartin), inhibit signaling through this pathway. Ras pathway activation leads to the phosphorylation and activation of Mnk, which directly phosphorylates eIF4E. Mnk is also phosphorylated by the stress-activated p38 MAP kinase.

of the eIF4E-binding motif, and five phosphorylated residues map on the C-terminal side: Ser-65, Thr-70, Ser-83, Ser-102, and Ser-112 (Ser-102 and Ser-112 exist only in 4E-BP1). Mutational studies combined with extensive 2D tryptic mapping analyses and the use of phospho-specific antibodies have demonstrated that 4E-BP1 phosphorylation is a highly ordered, hierarchical process [303]. Thus, dissociation of 4E-BP1 from eIF4E is a multistep process, in which phosphorylation of Thr-37 and Thr-46 acts as a "priming" event for Thr-780 and then Ser-65 phosphorylation. The role of Ser-83 phosphorylation remains to be elucidated. Ser-112 was reported to be phosphorylated by ATM (ataxia-telagengecia mutated) [304].

Crystallographic studies have suggested a mechanism to explain how 4E-BP phosphorylation may prevent binding to eIF4E. The presence of acidic patches on eIF4E flanking the bound 4E-BP peptide suggests that phosphorylation of the 4E-BPs on residues proximal to the eIF4E-binding site could induce electrostatic repulsion between the two proteins. The ordered phosphorylation of 4E-BP1 culminates in the phosphorylation of Ser-65 which is only 4 Å from Glu 70 in eIF4E. However, phosphorylation of this residue alone is not sufficient to disrupt eIF4E binding, suggesting that phosphorylation of other residues is also required [303]. The pathway that mediates 4E-BP phosphorylation relays signals from PI3K to Akt/PKB and FRAP/mTOR. The signaling pathway is illustrated in Fig. 7.2-15.

FRAP-mTOR (FKBP12-rapamycin-associated protein/mammalian target of rapamycin) is a member of the PIK family, whose members include cell-proliferation checkpoint proteins, such as ATM, ATR and DNA-PK, which function as protein kinases [305]. FRAP/mTOR is the mammalian homolog of yeast TOR proteins, which inhibit translation initiation and arrest yeast cells in the G1 phase in response to nutrient deprivation [306]. TOR genes were initially isolated by using a genetic screen for yeast mutants conferring resistance to rapamycin, an immunosuppressant drug that severely blocks T-cell growth at G1 [307]. Rapamycin acts intracellularly by binding to the immunophilin FK506-binding protein 12 (FKBP12). The FKBP12–rapamycin complex then specifically interacts with FRAP/mTOR and inhibits its activity. In mammalian cells, rapamycin blocks cap-dependent, but not IRES-mediated translation, through inhibition of 4E-BP phosphorylation [308]. In addition, expression of a rapamycin-resistant FRAP/mTOR mutant protein confers rapamycin resistance to 4E-BP1 phosphorylation. Whereas FRAP/mTOR directly phosphorylates only the "priming" sites, Thr-37 and Thr-46 in 4E-BP1 and 4E-BP2, the kinase probably plays an indirect, but critical, regulatory role in the phosphorylation of the downstream sites, Ser-65 and Thr-70 [309]. The kinases(s) responsive to FRAP/mTOR activation, and responsible for Ser-65 and Thr-70 phosphorylation remain(s) to be identified.

7.2.5.3 eIF4G Phosphorylation

Both eIF4GI and eIF4GII are phosphoproteins [310, 311], but their phosphorylation is differentially regulated in the cell [311]. Two clusters of phosphorylation sites were demonstrated in eIF4GI (Fig. 7.2-11A). One cluster maps to the N-terminus and

contains Ser^{314} (numbering is according to the full-length eIF4GI cDNA clone [312]), but it is unclear what conditions promote this phosphorylation [311]. Another cluster of serum-stimulated phosphorylation sites was mapped to the hinge region between the middle and C-terminal domains. These consist of Ser^{1148}, Ser^{1188}, and Ser^{1232} and are sensitive to PI3K and FRAP/mTOR inhibitors [311]. The effect of eIF4GI phosphorylation on its activity is unclear as no evidence for changes in activity or association with other initiation factors has been reported following phosphorylation. However, it is expected that eIF4GI phosphorylation would engender a conformational change in the protein that affects its activity. Clearly, the generation of "knock-in" mice with substitutions in the phosphorylation sites will be essential for assessing the biological significance of eIF4G phosphorylation. It is interesting that total phosphorylation of eIF4GII and p97 is lower than eIF4GI, and is not modulated by serum or mitogens. This is consistent with the fact that the phosphorylated C-terminal region in eIF4GI is not conserved in eIF4GII and p97, and this region is not phosphorylated in the latter proteins [311].

7.2.5.4 eIF4B Phosphorylation

eIF4B is phosphorylated in response to a variety of extracellular stimuli that induce cell growth and proliferation, such as serum, insulin and phorbol esters [313, 314]. One of the sites, Ser^{422} (Fig. 7.2-110B), is phosphorylated by S6K1 (S6 kinase 1), both *in vivo* and *in vitro*. S6K1 is a direct phosphorylation target for FRAP/mTOR (Fig. 7.2-15). This is consistent with the sensitivity of Ser^{422} phosphorylation to wortmannin and LY92900, which inhibit PI3K activity [315]. Thus, the PI3K/Akt-PKB/FRAP-mTOR signaling pathway regulates the phosphorylation state of eIF4B, eIF4G and 4E-BPs, underscoring its importance in controlling translation rates.

7.2.6 Translational Control by Paips – PABP Interacting Proteins

Two proteins that strongly interact with PABP and affect translation were identified by Far-Western interaction screening [316, 317]. Paip1 is a ~56 kDa protein, which activates translation *in vivo*. It is homologous to the central region of eIF4G and interacts with eIF4A [316] (Fig. 7.2-11A). Paip1 is also involved in mRNA turnover, as it is found in a protein complex with PABP that recognizes the major protein-coding region determinant of instability (mCRD) of the c-*fos* proto-oncogene mRNA [318]. Paip2, a much smaller protein (MW = 14 kDa), preferentially inhibits the translation of mRNAs containing a poly(A) tail, and also IRES-containing mRNAs that are eIF4G-dependent [317]. Paip2 inhibits the formation of 80S initiation complexes [317]. Although it is possible that Paip2 inhibits the conversion of 48S preinitiation complexes to 80S initiation complexes [289], Paip 2 also partially inhibits the formation of 48S preinitiaition complexes (Kahvejian and Sonenberg, unpublished). In an RNA-binding assay, Paip2 strongly hinders the interaction of PABP with poly(A) and disrupts the poly(A)-organizing activity of PABP [283, 317]. These last

findings suggest that Paip2 impedes initiation by disrupting the circular conformation of the mRNA. Thus, Paip2 may inhibit translation at several levels, including the recycling of ribosomes on the same mRNA, 48S preinitiation complex formation, and 40S-60S subunit joining. Paip1 binds to PABP with a 1:1 stoichiometry [319], whereas Paip2 binds with a 2:1 stoichiometry [317]. Paip1 interacts with RRM1+RRM2, and the C-terminus of PABP [319], whereas Paip2 interacts with RRM2+RRM3, and the C-terminus of PABP (Fig. 7.2-11C) [317].

The C-terminus of PABP interacts with Paip1 and Paip2, and with other proteins (see below) that contain the PABP C-terminus-binding motif, a 15-amino-acid stretch with the consensus sequence vxxsxLnpNAkeFvp [284, 285]. The translation-termination factor eRF3 contains this 15-amino-acid motif in its N-terminus and interacts with the C-terminus of PABP, as discussed above [288, 320]. An interesting protein that contains the PABP C-terminal binding motif, Ataxin-2, is implicated in spinocerebellar ataxia [321], and interacts with another RRM containing protein A2BP1 [322]. The function of Ataxin-2 is unknown, but its interaction with PABP may shed new light on spinocerebellar ataxia. Paip2 may therefore compete with C-terminus-binding partners of PABP, and modulate aspects of PABP function, which are unrelated to translation. Paip1 and Paip2 also interact with the C-terminus of the HYD ubiquitin ligase via the same 15-amino-acid stretch [285], potentially targeting these proteins for degradation. Perhaps ubiquitination serves as a regulator of mRNA circularization and translation. It is interesting to note that Paip1 and Paip2 exist only in metazoa. They may thus represent a higher-order mechanism for translational control in multicellular eukaryotes.

7.2.7 AUG Recognition during Scanning

7.2.7.1 AUG is the Predominant Signal for Initiation and is Selected by Proximity to the 5′-end by the Scanning Mechanism

Evidence for the Scanning Mechanism

Most mRNAs in eukaryotes are translated by the scanning mechanism, and genetic analysis in yeast played an important role in uncovering this process. Sherman and co-workers [323–325] isolated revertants of mutations in the start codon of *CYC1*, encoding cytochrome *c*, and found that translation could be restored by creation of an AUG at any of six locations in a span of 25 nucleotides near the 5′-end of the gene. This finding implied that AUG is the only sequence critically required for initiation. They also showed that an AUG could function efficiently as a start codon only if it occurred as the 5′-proximal AUG triplet in the mRNA. The null allele *cyc1-341*, containing AUGs at positions 1 and 5 plus the UAA terminator at position 3, could revert to a functional allele by elimination of the AUG at codon 1. Thus, the AUG at codon 5 could function efficiently as a start site so long as it was not preceded by another AUG [325]. Similarly, the nonfunctional *cyc1-362* allele was found to contain a single base pair change that introduced a new AUG 20 nt upstream of

the normal start codon, initiating a short upstream ORF (uORF). The fact that the uORF in *cyc1-362* blocked initiation at the normal start codon also implied that ribosomes were incapable of re-initiating downstream following termination of translation at the uORF [326]. This behavior is in sharp contrast with the ability of bacterial ribosomes to re-initiate translation efficiently on polycistronic mRNAs. A genetic analysis of initiation codon mutations at *HIS4* showed that for this gene also, 5′-proximal location is much more important than surrounding sequence context in determining whether an AUG triplet can function as a start codon [327].

These genetic findings were in accordance with previous observations by Kozak that most eukaryotic mRNAs are monocistronic and lack AUG codons upstream of their initiation sites. Combining these facts with observations that the m^7G cap stimulates translation and experiments showing that mammalian ribosomes cannot bind circular mRNAs [328], but will migrate on mRNA after binding at the 5′-end [329], Kozak proposed the scanning model. According to this hypothesis, the 40S subunit binds to the mRNA at the 5′-end and threads along the mRNA until reaching an AUG, whereupon an 80S initiation complex is assembled [330]. The scanning hypothesis is consistent with observations that insertions of secondary structure into the mRNA leader inhibit translation initiation [255, 331]. In addition, extensive mutational analysis of preproinsulin mRNA demonstrated that 5′-proximal AUG triplets are utilized preferentially as start sites and that insertion of an uORF inhibits initiation at the downstream cistron [332, 333], just as observed for yeast *CYC1*.

The scanning hypothesis was modified after the discovery that sequences immediately surrounding the start codon, particularly at the –3 and +4 positions (where A is designated the +1 base), can have a strong effect on initiation frequency, to the point where a 5′-proximal AUG can be by-passed if it occurs in an unsuitable sequence context. This exception to the first AUG rule was called "leaky scanning" [334]. The "first AUG rule" also can be violated in mammalian cells when an uORF is located a considerable distance upstream from the protein coding sequences, and Kozak hypothesized that ribosomes can resume scanning after translating the uORF and re-initiate downstream if they have sufficient time to reassemble a 48S preinitiation complex before reaching the next start codon. A separation of ~80 nt was sufficient for a high rate of re-initiation on preproinsulin mRNA [335].

Initiation Factor Requirements for Scanning

Although there is considerable evidence, both genetic and biochemical, that ribosomes move along the mRNA by a scanning process, the mechanism of scanning is neither understood at the molecular level, nor have scanning ribosomes been observed by any imaging technique. Nonetheless, as discussed below, important contributions to scanning of eIF4F, eIF1, and eIF1A, have begun to emerge. It is clear that energy derived from ATP hydrolysis is required for scanning; however, a critical issue is whether the 48S preinitiation complex actively uses the energy to traverse the mRNA or whether ATP-dependent unwinding of the mRNA by eIF4F is necessary solely to facilitate ribosome diffusion [336].

Recent support for the idea that ribosomes can diffuse on the 5′-UTR of an mRNA was obtained by Pestova and Kolupaeva [171]. The authors used an artificial mRNA with an unstructured 5′-UTR and demonstrated that significant ribosome binding to the initiation codon occurred in the absence of ATP and the eIF4 factors, provided that eIF1 was present along with eIF3 and the TC. These results are consistent with earlier data indicating that the requirement for ATP, eIF4A, and eIF4B is significantly reduced for mRNAs with diminished secondary structure in their 5′-UTR (such as alfalfa mosaic virus RNA4) [337]. The eIF1 was not required for 48S preinitiation complex formation at the start codon on the unstructured mRNA provided that eIF4F was present. From these findings, it was concluded that the 43S complex (40S/eIF3/TC) can bind to mRNA but requires either eIF1 or eIF4F to locate the AUG start codon. In this view, eIF1 and eIF4F have overlapping functions in ribosomal scanning. The results suggested that eIF1A also increases the processivity of scanning [171]. However, it seems possible that binding to mRNA, rather than scanning, was the critical step stimulated by eIF1 in these studies. A requirement for eIF1 in mRNA binding was discounted because the 40S–eIF3–TC complex could bind to mRNA and form a stable complex on an AUG triplet located only 1–2 nt from the 5′-end in the absence of both eIF1 and eIF4F factors. However, mRNA binding in this latter case could be facilitated by direct base-pairing of Met-tRNA$_i^{Met}$ with the 5′-proximal AUG codon.

The study of Pestova and Kolupaeva [171] provided clear evidence that eIF4F is involved in scanning, since it was not required for ribosome binding at the start codon in the unstructured mRNA leader, but was essential for this reaction when stable secondary structure was introduced into the leader, or in the case of native β-globin mRNA. The requirement of eIF4A for scanning must be mediated through its binding to eIF4G, as the former functions only as a subunit of eIF4F, whereby it cycles through the complex during the initiation process [258]. Thus, the function of eIF4G in scanning (see below) must be dependent on its ability to bind eIF4A.

Translational Control by Leaky Scanning

The phenomenon of leaky scanning has several important consequences for gene expression. First, translation of an mRNA can be down-regulated by a naturally occurring upstream AUG codon in the mRNA leader, in inverse proportion to the probability of leaky scanning past the first AUG. Secondly, Kozak showed that a 5′-proximal uORF can reduce the inhibitory effect of a second uORF located further downstream that is too close to the first uORF for efficient re-initiation following translation of the latter. In this way, translation of the first uORF promotes leaky scanning past the second uORF and enables subsequent reinitiation at the coding sequences downstream [335]. This is the mechanism employed in *GCN4* translational control, where translation of uORF1 allows ribosomes to by-pass uORFs 2–4 and reinitiate at *GCN4* when TC levels are reduced by eIF2α phosphorylation [338].

Leaky scanning can also allow the production of multiple proteins from the same mRNA. Interesting examples of this last phenomenon involve proteins that function

in mitochondria and cytoplasm and require a leader peptide for import into mitochondria. Ribosomes initiating at the first AUG produce the longer protein containing the leader peptide, whereas the shorter protein is translated by ribosomes that leaky-scan past the first AUG and initiate at the second start site [339]. Finally, there are numerous instances of translational repression by uORFs in which the uORF-encoded peptide blocks translation termination at the uORF stop codon and produces a barrier to the progression of scanning 40S subunits attempting to leaky scan past the uORF start site and reach the coding sequences downstream. In some cases, the inhibitory effect of the uORF-encoded peptide on termination can be modulated by nutrients, providing a mechanism for translational control of the downstream coding sequences (see Refs. [340, 341] for recent reviews).

7.2.7.2 The Anticodon of $tRNA_i^{Met}$, eIF2 Subunits, eIF1, and eIF5 are Determinants of AUG Selection during Scanning

Genetic experiments by Donahue and co-workers showed that the anticodon of $tRNA_i^{Met}$ plays a key role in the recognition of an AUG start codon by the scanning 40S ribosome [28]. They showed that overproducing a mutant form of $tRNA_i^{Met}$ containing an anticodon of 3′-UCC-5′ versus 3′-UAC-5′ restored expression of a *his4* allele with AGG in place of the AUG start codon. Other *his4* alleles with different start codons were not suppressed by $tRNA_i^{Met}$ (UCC), showing that codon–anticodon base pairing was required for suppression. Moreover, introduction of an extra AGG codon upstream of the AGG start site abolished suppression, indicating that the upstream AGG was recognized preferentially by the mutant $tRNA_i^{Met}$ (UCC) – a hallmark of the scanning process. This work established that perfect base-pairing between the anticodon of the initiator and the start codon, regardless of their exact sequences, is a fundamental requirement for efficient initiation in yeast. As discussed earlier, Donahue *et al.* also isolated mutations in eIF1, the three subunits of eIF2, and eIF5 that increased expression of a defective *his*4 allele containing AUU in place of AUG at the start codon. These Sui⁻ mutations allow a UUG present at the third codon of *his4* to be recognized as a start site by Met-$tRNA_i^{Met}$, despite the predicted U-U mismatch at the first position of the codon–anticodon duplex [59, 78, 170, 342]. Biochemical analysis of Sui⁻ mutants led to the proposal that the intrinsic rate of GTP hydrolysis by eIF2, and its modulation by the GAP eIF5, are important determinants of AUG recognition during scanning (see Ref. [343] and references therein).

7.2.7.3 eIF1 plays a role in TC binding, scanning, and AUG selection

The eIF1 is a ~12.5 kDa polypeptide (Table 7.2-1), essential in yeast [170], which plays an important role in assembly of preinitiation complexes and selection of AUG start codons. Early biochemical studies indicated that mammalian eIF1 has a weak stimulatory effect on binding of TC and mRNA to 40S or 80S initiation complexes in the presence of other factors [37, 133, 344]. As noted above, more recent studies showed that yeast eIF1 is critically required along with eIF1A for 48S complex formation in a

reconstituted system using a model mRNA [135]. In addition, mammalian eIF1 was found to augment the functions of eIF3 and eIF1A in promoting TC binding in the absence of mRNA [33]. The finding that mammalian eIF1 stimulated Met-puromycin synthesis by 80S initiation complexes only in the absence of AUG suggested that eIF1 can partially substitute for the start codon in positioning TC in the P-site [344]. Mammalian eIF1 also prevented 60S subunit joining in the absence of mRNA [133], and it enhanced the activities of eIF3 and eIF1A in this regard [33], consistent with a ribosome anti-association activity for eIF1.

The results of the yeast Sui$^-$ mutant selection first revealed that eIF1/SUI1 is required for stringent selection of AUG as the start codon [170]. As described above, mammalian eIF1 participates with eIF1A in promoting stable 48S complex formation at the start codon on globin mRNA [196]. When using a synthetic mRNA with a leader devoid of secondary structure, eIF1 was not required for scanning in the presence of eIF4F. However, in the absence of eIF1, there was an increase in the selection of (i) near-cognate start codons (e.g., AUU), (ii) AUG triplets surrounded by a suboptimal sequence context, and (iii) AUG triplets located within 4 nt of the 5′-end. Pestova et al proposed that eIF1 binds to the 40S ribosome near the P-site, similar to bacterial IF3, and influences the positions of mRNA, Met-tRNA$_i^{Met}$, or both, such that the initiator interacts strongly only with cognate AUG triplets in the proper context. Thus, in the absence of eIF1, the 43S complex can scan an unstructured leader (when eIF4F, 4A, 4B, and 1A are present), but the decoding site improperly accepts noncognate start codons or AUGs in a poor sequence context [171].

The solution structure of eIF1 has been solved by NMR (Fig. 7.2-8C) and the fold resembles that of certain ribosomal proteins and RNA-binding proteins; however, there is no evidence for direct interaction of eIF1 with RNA. The Sui$^-$ alleles of yeast *SUI1* (*D83Y, D83G*, *Q84P*, and *G107R*) [170, 345] alter residues predicted to be clustered together on the surface of eIF1 (Fig. 7.2-8C) and thus may comprise an important domain for eIF1 function in AUG selection [4]. Interestingly, the *SUI1* allele known as *mof2-1* (*G107R*) increases programmed –1 ribosomal frame-shifting on yeast L-A virus mRNA (maintenance of frame, or Mof phenotype) in addition to its Sui$^-$ phenotype, and the *sui1-1* allele (*D83G*), but not Sui$^-$ alleles of *SUI2* or *SUI3* affecting eIF2α or eIF2β, respectively, has a weak Mof$^-$ phenotype. The Mof$^-$ phenotype was recapitulated in *mof2-1* translation extracts and rescued with recombinant eIF1/SUI1. Thus, it was proposed that eIF1 plays a role in accurate decoding during the elongation phase. This unexpected activity seems to be conserved in humans, as human eIF1 cDNA complemented the Mof$^-$ phenotype of the *mof2-1* mutant [345]. Ostensibly at odds with this model, it was found that eIF1 cannot destabilize 80S initiation complexes, but only 48S complexes, formed on AUG triplets located at the extreme 5′-end of the mRNA [171].

7.2.7.4 eIF5 Functions as a GTPase Activating Protein for eIF2 in AUG Selection and Subunit Joining

The eIF5 is a 45–49 kDa polypeptide that stimulates hydrolysis of the GTP bound to TC in a 48S preinitiation complex positioned at the AUG start codon (Table 7.2-1).

This leads to release of eIF2-GDP, leaving Met-tRNA$_i^{Met}$ base-paired to AUG in the P-site of a 40S initiation complex that is competent to join with a 60S subunit in a manner stimulated by eIF5B (see below). The eIF5 functions catalytically and cannot stimulate GTP hydrolysis by TC that is free of ribosomes [38, 346, 347]. Thus, eIF5 may be regarded as a 40S-ribosome-dependent-GAP for eIF2 whose function is contingent upon a perfect codon–anticodon match between Met-tRNA$_i^{Met}$ and the AUG. The gene encoding the factor in yeast, *TIF5*, is essential [348] and depletion of eIF5 from yeast cells impairs translation initiation *in vivo*, leading to accumulation of vacant 80S couples [349].

As discussed above, the *TIF5* allele *SUI5-G31R* increases the rate of eIF5-stimulated GTP hydrolysis by the TC in a model assay for eIF5 GAP function, providing a plausible explanation for its defect in AUG selection (Sui$^-$ phenotype) [53]. By contrast, the *ssu2-1* mutation in the N-terminus of eIF5 (G62S) (Fig. 7.2-1D) led to a substantial reduction in eIF5 GAP activity *in vitro*, in accordance with its Ts$^-$ phenotype [72]. The catalytic domains of the GAPs for Ras and Rho have been shown to contain a critical arginine residue flanked by conserved hydrophobic residues that plays a catalytic role in stablilizing the transition state of the GTP hydrolysis reaction, known as an "arginine finger" [350]. It was shown that mutating such an invariant arginine residue in mammalian eIF5 (Arg-^{15}) destroys its GAP function in model 48S complexes and its ability to support both eIF5-dependent translation in a yeast extract and growth of a *tif5Δ* yeast strain. Mutations of this residue did not diminish interaction of eIF5 with recombinant eIF2β, with eIF2 holoprotein in the presence of GTPγS, or with model 43S complexes; hence, the mutation impairs eIF5 catalytic function and not substrate binding [351, 352]. Furthermore, the eIF2-GDP/eIF5 complex is stabilized by aluminum fluoride (AlF_4^-), a compound that combined with GDP acts as a structural mimic of the transition state of the GTPase reaction by G proteins [350]. These findings are consistent with the idea (but do not prove) that eIF5 functions as a GAP by inserting Arg^{15} into the GTP-binding pocket of eIF2γ to stabilize the transition state for GTP hydrolysis. Mutation of a second conserved arginine residue in eIF5 (Arg-^{48}) to methionine had only a modest effect on GAP function, but it did destabilize the eIF2–GDP–AlF_4^-–eIF5 complex [352]. Conserved Lys-^{33} and Lys-^{55} residues also contribute to catalytic function [351]. Because GTP hydrolysis requires pairing of Met-tRNA$_i^{Met}$ with AUG in the P-site, some component of the 48S complex besides eIF5, possibly a segment of the ribosome itself, most probably interacts with the switch-I or switch-II segments in eIF2γ to trigger GTP hydrolysis. This prediction is also supported by the fact that eIF5 is not present in archaea, suggesting that it evolved to enhance or regulate the GAP activity of the ribosome.

It was mentioned earlier that the AA-boxes in the CTD of eIF5 are required for stable binding of eIF5 to the β-subunit of eIF2 and to eIF2 holoprotein, both *in vitro* and *in vivo*, and also to the NIP1/c subunit of eIF3. Mutations in the AA-boxes of mammalian eIF5 that impair its interaction with the NTD of eIF2β (without reducing eIF5–eIF3c association), reduced the GAP activity of eIF5 *in vitro* [71] and its ability to support both eIF5-dependent translation in a yeast extract and growth of a

tif5Δ yeast strain. These findings suggest that the eIF5-CTD–eIF2*β* interaction is important for anchoring eIF2 to eIF5 in a manner that facilitates productive interaction of the catalytic domain of eIF5 (in the NTD) with the GTP-binding pocket of eIF2*γ*. Surprisingly, even more extensive mutations in the AA-boxes of yeast eIF5, encoded by *tif5-7A* and *tif5-12A*, did not impair eIF5 GAP activity in model 48S complexes [72] even though they eliminated stable binding between eIF5 and eIF2. The *tif5-7A* mutations weaken eIF5–NIP1/eIF3c interaction and destabilize the MFC *in vivo* [34, 69], and they impair binding of Met-tRNA$_i^{Met}$ and mRNA to 40S ribosomes in a yeast extract [72]. The latter is consistent with the idea that stabilization of the MFC by the eIF5-CTD promotes 48S complex assembly. The mRNA-binding defect in the *tif5-7A* extract could result indirectly from reduced TC binding, but there is also evidence that the AA-boxes in the eIF5-CTD promote interaction between eIF3 and eIF4G *in vivo* [72]. In the same study, it was shown that the C-terminal half of recombinant yeast eIF4G can bind directly to the eIF5-CTD, dependent on the AA-boxes, and this interaction can occur simultaneously with the eIF5-CTD–NIP1 interaction *in vitro*. Thus, the eIF5-CTD may bridge an interaction between eIF3 and eIF4G and thereby enhance mRNA binding to 40S ribosomes in yeast cells.

In spite of the impaired 48S assembly observed in *tif5-7A* cell-free extracts, the rate-limiting defect produced by this mutation *in vivo* lies downstream of 48S formation. Thus, 48S complexes containing eIF1, eIF2 and eIF3, but lacking eIF5, accumulated in the polysome fraction of *tif5-7A* cells. It is possible that dissociation of eIF5 from 48S complexes simply impairs the ability of eIF5 to perform its GAP function effectively on recognition of the start codon, even though this defect was not observed *in vitro* with model 48S complexes. Ostensibly at odds with this idea, 48S complexes accumulated in the *tif5-7A* mutant but not in *ssu2-1* (*tif5-G62S*) cells. Considering that the mutant eIF5 encoded by *ssu2-1* is defective for GAP activity *in vitro*, it appears that 48S complexes positioned at the AUG decay to free 40S subunits if GTP hydrolysis does not occur immediately following AUG recognition [72]. If so, then accumulation of stable 48S complexes in *tif5-7A* cells may signify a delay in reaching the start codon during the scanning process. Given that both eIF1 and eIF4G interact with the eIF5-CTD [34], and both are implicated in scanning and AUG recognition [171, 196, 343], a reduced rate of scanning may be the rate-limiting defect in *tif5-7A* cells.

7.2.8
Joining of 60S Subunits to 40S Ribosomal Complexes

Following scanning of the 40S subunit and selection of the AUG start codon, the next step in translation initiation is the joining of a 60S subunit containing the peptidyl-transferase active site, to form an 80S ribosome that is competent for elongation. Whereas the TC and factors eIF1, eIF1A, eIF3 and eIF5 are thought to be associated with the scanning 40S subunit, none of these factors are present on the 80S ribosome [36, 37]. Hydrolysis of the GTP in the TC leads to release of eIF2•GDP, and presumably the other factors, from the 48S preinitiation complex. However, the precise timing and requirements for factor release from the 48S complex has not

been determined, and interpretation of results from previous work is complicated by the recent realization that two factors, eIF5 and eIF5B, are necessary for the conversion of the 48S complex to an 80S ribosome. As described earlier, eIF5 promotes GTP hydrolysis by the TC leading to release of eIF2•GDP. The Met-tRNA$_i^{Met}$ remains bound in the ribosomal P-site with its anticodon base-paired to the start codon on the mRNA. Previously, it was thought that the 60S ribosomal subunit binds passively to this 48S complex following release of eIF2 and the other factors. However, reconstitution of the subunit joining step of protein synthesis using an authentic mRNA and the full complement of known mammalian initiation factors revealed the requirement for an additional factor termed eIF5B.

7.2.8.1 eIF5B Catalyzes a Second GTP-dependent Step in Translation Initiation

The eIF5B is a 112 kDa (yeast) to 139 kDa (mammals) polypeptide, with an electrophoretic mobility in SDS/PAGE closer to 150 kDa, probably owing to a highly charged N-terminus containing several runs of polylysine, polyaspartate and polyglutamate. The *FUN12* gene encoding yeast eIF5B is nonessential for viability; however, *Δfun12* strains exhibit a severe slow-growth phenotype with a doubling time 3-fold greater than wild-type [201]. The eIF5B is an ortholog of prokaryotic IF2, and contains at its center a consensus GTP-binding domain [5] (Fig. 7.2-16A). Similar to IF2, eIF5B binds GTP and GDP with similar affinities [353, 354], consistent with the lack of requirement for a guanine-nucleotide exchange factor for these factors. Early biochemical studies indicated that eIF5B (previously referred to as eIF-5 or IF-M2A, 355) stimulated the GTPase activity of eIF2, the role now ascribed to eIF5. However, with the realization that eIF5B is a GTPase and that eIF5 promotes GTP hydrolysis by eIF2, the proposed GAP-like function of eIF5B should be viewed cautiously.

The determination that both eIF2 and eIF5B are GTPases suggests that there are two GTP-dependent steps in eukaryotic translation initiation as opposed to the single GTP requirement in bacteria. The requirement for eIF5B to promote subunit joining was revealed when 48S complexes were assembled on β-globin mRNA using the full complement of known mammalian translation-initiation factors, including eIF1, eIF1A, eIF2, eIF3, eIF4A, eIF4B, eIF4F and radioactively labeled Met-tRNA$_i^{Met}$. Addition of recombinant eIF5 was insufficient to convert the 48S complexes in to 80S complexes, and the factor eIF5B was isolated from the ribosomal salt wash and shown to promote 80S complex formation [353]. Consistent with the latter, eIF5B was necessary to convert 48S complexes to 80S ribosomes competent for methionyl-puromycin (MP) synthesis [353]. This assay mimics the formation of the first peptide bond and monitors the transfer of labeled Met from Met-tRNA$_i^{Met}$ to puromycin, an aminoacyl-tRNA analog. In assays containing eIF1, eIF1A, eIF2 and eIF3, both eIF5 and eIF5B were necessary for MP synthesis. Interestingly, if 48S complexes were formed in the presence of only eIF1A and eIF2, then eIF5 was sufficient for MP synthesis [353]. Thus, eIF5 may promote GTP hydrolysis by eIF2 leading to release of eIF2•GDP from the 48S complex, and eIF5B may be required for the subsequent removal of eIF1, eIF3, and eIF5, which is probably necessary for 60S subunit joining.

When 48S complexes are mixed with 60S subunits and eIF5B in the presence of nonhydrolyzable GDPNP in place of GTP, 80S complex formation is unaffected; however, the 80S complexes are not able to synthesize MP [353]. Thus, GTP hydrolysis by eIF5B is not required for 80S complex formation, but rather for conversion of the 80S complex to a translation competent state. Consistent with this idea, kinetic analysis of translation initiation in RRL revealed a requirement for GTP hydrolysis late in the pathway to prepare the 80S complex for elongation [356].

Both yeast and mammalian eIF5B possess potent ribosome-dependent GTPase activities. The 60S subunit was reported to stimulate weakly the GTPase activity of human eIF5B [353] with the 40S and 60S subunits required for maximal GTPase activity. In contrast, the GTPase assays of yeast eIF5B [354] and rabbit eIF5B (called IF-M2A at the time) [355] revealed an absolute requirement for both ribosomal subunits. The G4 sequence motif (NKxD) in G domains interacts with the guanine base of the nucleotide establishing guanine specificity. Thus, the side chain of Asp-759 in human eIF5B (Asp-533 in yeast eIF5B) is predicted to interact via a hydrogen bond with the 2-amino group of GTP. Substitution of Asn for Asp-759 in human eIF5B severely impaired the ribosome-dependent GTPase and the subunit joining activities of the factor. These results indicate that GTP binding by eIF5B is necessary for subunit joining. The D759N mutation in human eIF5B endowed the factor with XTPase activity [357] (Fig. 7.2-16A). This nucleotide-specificity switch can be explained by the side chain of Asn-759 interacting via a hydrogen bond with the 2-keto group on XTP. Consistent with this explanation, human eIF5B-D759N stimulated subunit joining and MP synthesis when the assays were supplemented with XTP in addition to the GTP required by eIF2 to form a TC and bind Met-tRNA$_i^{Met}$ to the ribosome [357]. Thus, the requirement for both GTP and XTP in assays employing the human eIF5B-D759N mutant demonstrates that there are two nucleotide (GTP)-dependent steps in eukaryotic translation initiation.

7.2.8.2 GTPase Switch Regulates Ribosome Affinity of eIF5B and Governs Translational Efficiency

The eIF5B has a homolog in archaea, aIF5B, which functionally substitutes for yeast eIF5B both *in vivo* and *in vitro* [5, 198]. The crystal structure of eIF5B from the archaea *Methanobacterium thermoautotrophicum* (*M. therm.*) revealed a four-domain protein resembling a chalice [198] (Fig. 7.2-16B). All archaea lack the nonconserved NTD found in eukaryotic eIF5B and some bacterial IF2 proteins. As deletion of the NTD has no obvious effect on eIF5B function in yeast [6], the crystal structure represents the functionally important regions of the factor. Domain I of aIF5B is the GTP-binding domain and it resembles the G domains found in other G proteins like Ras, EF-Tu, and the heterotrimeric G proteins. Domain II of aIF5B is a β-barrel fold that, together with domain I, can be nearly superimposed on domains I and II of eIF2γ and the translation-elongation GTPases EF-Tu and EF-G. Domains I–III form the cup of the chalice-shaped factor and they are connected via a 40 Å long α-helical stem to domain IV, a second β-barrel fold, which represents the base of the chalice-

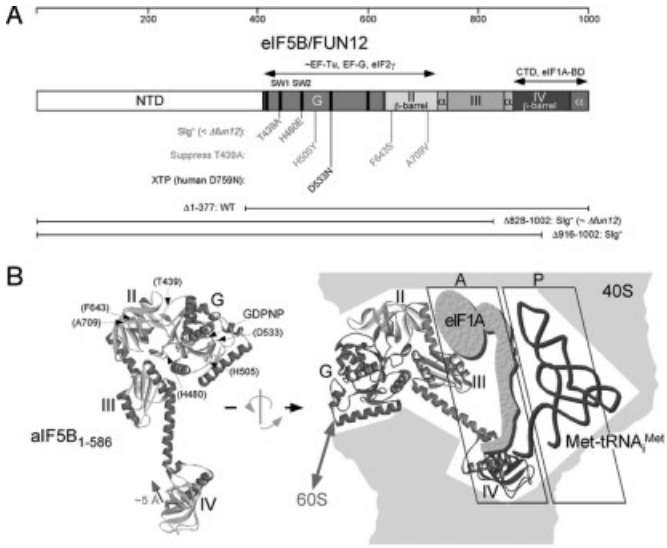

Figure 7.2-16 Structural and functional properties of eIF5B. **(A)** The 1002-amino-acid yeast eIF5B, encoded by the *FUN12* gene, is depicted schematically and divided into the following structural domains: nonconserved NTD, GTP-binding domain (G, red), β-barrel domain II (yellow), domain III (green), and β-barrel domain IV (blue). Domain IV plus the C-terminal α-helices (purple) comprise the C-terminal domain (CTD) containing the binding domain (BD) for eIF1A [6]. Recent NMR studies mapped the binding interface to the C-terminal α-helices in eIF5B (purple) and the CTD of eIF1A [197]. The G domain and domain II of eIF5B and aIF5B are conserved in both sequence and structure with the corresponding domains in eIF2γ (Fig. 7.2-5A), and the translational GTPases EF-Tu and EF-G [198]. Locations of key point and deletion mutations are indicated below the schematic. Depicted in red are dominant-negative mutations in the conserved Switch 1 (SW1) and Switch 2 (SW2) regions of the G domain that confer a growth defect in *fun12Δ* cells greater than that of the *fun12Δ* allele itself [354, 357]. Three mutations that suppress the toxic effects of the SW1 T439A mutation are indicated in green [354], and the G4 sequence motif mutation that alters the nucleotide specificity of eIF5B from GTP to XTP is labeled in black [357]. eIF5B alleles lacking the NTD retain full activity *in vivo*, whereas, partial or full removal of the CTD abolishes eIF5B function [6]. (B) Structure of *M. therm.* aIF5B. (Left) Ribbons representation of the ventral, GTP-binding face of aIF5B in complex with GDPNP (PDB ID code: 1G7T, 198). α-helices are depicted in red, and β-sheets are colored blue. Locations of the four domains of the protein and the key point mutations described in (A) are indicated. The arrow adjacent to domain IV reflects the ~5 Å movement of this domain away from the reader when the factor is bound to GDP [198]. (Right) Model of eIF5B binding and interactions on the 40S subunit. The dorsal face of aIF5B is presented in ribbons representation with the domains colored as in (A): red, G domain; yellow, domain II; green, domain III; blue, domain IV; purple, C-terminal α-helices. The structure has been rotated 180 about a vertical axis and then tilted relative to the structure in the left panel to reflect the predicted mode of eIF5B binding to the 40S ribosome (tan). Domain IV contacts the CTD of eIF1A (blue) in the A-site and is positioned near the aminoacyl end of the Met-tRNA$_i^{Met}$ (brown) in the P-site, domain II contacts the small ribosomal subunit, and the G domain contacts the GTPase center on the large subunit [197, 360, 361]. The aIF5B images in both panels were generated using the program WebLab Viewer Lite (v. 3.2, Accelrys, Inc.).

shaped molecule (Figs. 7.2-16A and B). As mentioned above, the eIF1A-binding site maps to domain IV of eIF5B [6] and an eIF5B allele lacking domain IV is functionally impaired *in vivo* (Fig. 7.2-16A), suggesting that the eIF5B–eIF1A interaction is important. Moreover, NMR structural analysis and chemical-shift experiments suggest that the C-terminal 14 residues of eIF1A bind to a narrow hydrophobic groove on the surface of domain IV formed by the two α-helices at the extreme C-terminus of eIF5B [197] (Fig. 7.2-16B). The eIF5B homolog in *Drosophila melanogaster* has been reported to bind to the DEAD-box RNA helicase VASA, encoded by the gene *vas* [358]; however, the VASA-binding site on eIF5B has not been mapped. Interestingly, mutations in *Drosophila* eIF5B enhance the embryonic patterning and germ cell specification defects of *vas* mutants, suggesting that the physical interaction between eIF5B and VASA is important for the translation of at least a subset of mRNAs encoding proteins that play important roles in early development [358].

Comparison of the structures of aIF5B in its active GTP-bound state and inactive GDP-bound state revealed that modest conformational changes in the active site of the G domain resulted in rotations of domains II and III that trigger lever-type motions of the long helical stem and domain IV [198] (see Fig. 7.2-16B, left panel). This lever-type motion amplifies over a distance of 90 Å, the intricate molecular rearrangements distinguishing GTP from GDP in the G domain active site, and results in an ~5 Å swing of domain IV. Interestingly, these domain rearrangements share some resemblance to the stroke-like motions observed in the ATPase motors like myosin. This similarity raised the possibility that eIF5B functions as a molecular motor, as proposed for the translation elongation-factor GTPase EF-G [359]; however, this possibility now seems very unlikely (see below).

Several studies have addressed the role of GTP hydrolysis by eIF5B. Pestova et al. [353] showed that GTP hydrolysis was not required for subunit joining *per se*, but for formation of a functional 80S competent for translation (MP synthesis). In addition, GTP hydrolysis was essential for the catalytic activity of eIF5B to promote subunit joining. The eIF5B functioned equally well in the presence of GTP versus nonhydrolyzable GDPNP to generate stoichiometric amounts of 80S complexes; however, GDPNP blocked the catalytic reutilization of eIF5B. In addition, the 80S complexes formed in the presence of GDPNP were defective for MP synthesis. Examination of the 80S complexes formed in these assays revealed the stable binding of eIF5B to 80S complexes formed using GDPNP, but not GTP [353]. Further evidence that GTP hydrolysis by eIF5B is not required for subunit joining, but is necessary for a later step in the translation pathway was obtained from studies of eIF5B mutants. Mutation of the conserved Thr-439 in Switch 1 of yeast eIF5B to Ala, or substitution of Glu for the conserved Switch 2 His480 in yeast eIF5B and the corresponding His706 in human eIF5B lowered the ribosome-dependent GTPase activity of the factor to below background levels [354, 357]. The mutant factors retained subunit-joining activity; however, they were defective for stimulating protein synthesis both *in vivo* and *in vitro*. In addition, the mutant factors exhibited a dominant-negative phenotype in yeast causing a slow-growth phenotype in strains co-expressing wild-type eIF5B, and severely impairing the growth of strains lacking eIF5B [354] (Fig. 7.2-16A).

Finally, the human eIF5B-H706E mutant mimicked wild-type eIF5B in the presence of GDPNP and was stably bound to the 80S product of the subunit joining reaction [357].

The results of the above studies suggest that GTP hydrolysis by eIF5B is required for dissociation of the factor from the ribosome following subunit joining. However, the experiments did not distinguish whether GTP hydrolysis by eIF5B was necessary for mechanical work on the ribosome required for protein synthesis, or if GTP hydrolysis and the domain rearrangements in eIF5B simply functioned as a switch lowering the ribosome-binding affinity of eIF5B. Three mutations in yeast eIF5B, one in the G domain (H505Y) and two in domain II (F643S and A709V), were isolated as suppressors of the eIF5B-T439A mutation [354] (Figs. 7.2-16A and B, left panel). The H505Y suppressor mutation lowered the ribosome-binding activity of eIF5B yet restored nearly wild-type translation *in vivo* without restoring eIF5B GTPase activity [354]. The uncoupling of eIF5B GTPase and translational activities by the suppressor mutations revealed that eIF5B GTPase activity is not essential for mechanical work in translation initiation. Instead, the eIF5B GTPase switch regulates the ribosome-binding affinity of the factor. These results suggest that similar to eIF2, eIF5B is performing both regulatory and catalytic roles in translation initiation.

Yeast lacking eIF5B or expressing eIF5B alleles that lack GTPase activity exhibit a Gcn$^-$ phenotype [354]. This Gcn$^-$ phenotype was attributed, at least in part, to a defect in translating uORF1 on the *GCN4* mRNA. Translation of uORF1 on the *GCN4* mRNA is necessary to restrict ribosomes to the reinitiation mode where the levels of TC determine whether ribosomes translate or scan past the inhibitory uORF3 and uORF4. Removal of uORF1 prevents ribosomes from bypassing uORF2, uORF3, or uORF4, and blocks *GCN4* expression. A 2–5-fold increase in the number of ribosomes leaky scanning past uORF1 without initiating translation was observed in strains lacking eIF5B or expressing GTPase-deficient forms of the factor [354]. The increased leaky scanning is consistent with the subunit joining function of eIF5B. Ribosomes scanning from the 5′-cap will stop at the uORF1 start codon, release eIF2, and await eIF5B-catalyzed subunit joining. In the absence of eIF5B or in cells expressing GTPase-deficient mutants of eIF5B, subunit joining may be inefficient or the 80S complexes formed may be aberrant, and ribosomes will either resume scanning or disengage from the mRNA.

Bacterial IF2 binds fMet-tRNA^{Met} to the 30S subunit and, similar to eIF5B, is released from the ribosome following subunit joining. The binding site for fMet-tRNA$_i^{Met}$ has been mapped to domain IV of IF2, and the tRNA recognition involves primarily fMet and perhaps a few residues of the acceptor stem (reviewed in Refs. [1, 7] and Chap. 7.1). Formylation of the amino acid is a critical determinant for binding to IF2; and neither aIF5B nor eIF5B has been shown to bind Met-tRNA$_i^{Met}$, consistent with the lack of formylation of Met-tRNA$_i^{Met}$ in archaea and eukaryotes. However, eIF5B may stabilize the binding of Met-tRNA$_i^{Met}$ to the 80S complex. Substantially greater amounts of Met-tRNA$_i^{Met}$ were bound to 80S complexes formed by wild-type eIF5B in the presence of GDPNP versus GTP [354]. As eIF5B would

remain bound to the 80S complexes formed using GDPNP, the factor may stabilize Met-tRNA$_i^{Met}$ binding. In a similar manner, eIF5B may stabilize 48S complexes following the release of eIF2•GDP. Polysomes with halfmers containing a 48S complex bound at the start codon of an mRNA accumulate in yeast with reduced amounts of 60S subunits. These halfmers fail to form in strains lacking eIF5B [357], suggesting that eIF5B stabilizes this intermediate in the translation-initiation pathway. Consistent with the proposed role of eIF5B to stabilize Met-tRNA$_i^{Met}$ binding to 48S and 80S complexes, the slow-growth phenotype of yeast strains lacking eIF5B can be partially suppressed by overexpressing tRNA$_i^{Met}$ [201].

Synthesizing the results of the various *in vivo* and *in vitro* studies on eIF5B, the following model can be proposed for eIF5B function. Following scanning, GTP hydrolysis by eIF2, and release of eIF2•GDP, eIF5B•GTP binds to the 48S complex. The binding of eIF5B may stimulate release of eIF1, eIF1A, or eIF3, or alter the 40S structure to permit 60S subunit joining. In the 80S complex, eIF5B is positioned such that domain IV is near the top of the A-site in close proximity to the Met of the P-site-bound Met-tRNA$_i^{Met}$ (Fig. 7.2-16B, right panel). Based on the cryo-EM images of EF-Tu and EF-G bound to the ribosome, the GTP-binding domain of eIF5B is likely to contact the GTPase-activating center on the large subunit, whereas domain II contacts the small subunit (see Refs. [360, 361]). Joining of the 60S subunit triggers the GTPase activity of eIF5B, the factor changes conformation, and dissociates from the ribosome. Finally, the 80S ribosome is prepared to enter the elongation phase of protein synthesis with Met-tRNA$_i^{Met}$ in the P-site and a vacant A-site ready to accept the first elongator tRNA in complex with eEF1A and GTP.

7.2.9
IRES-mediated Translation Initiation

Although it is clear that canonical cap-dependent initiation plays a central role in the recruitment of ribosomes to a large number of mRNAs, translation can initiate by a cap-independent mechanism on some mRNAs, and under specific conditions. This mode of initiation entails the binding of 40S ribosomes to an internal ribosome entry site, or IRES, which is mostly (but not always) part of the 5′-UTR of the mRNA. IRES-mediated translation was first discovered in picornavirus mRNAs (poliovirus [362] and encephalomyocarditis virus [363]). Unlike all nuclear-transcribed cellular mRNAs, these viral mRNAs do not possess a cap structure and, therefore, must be translated by a cap-independent mechanism. All picornavirus RNAs (including enteroviruses, rhinoviruses, aphthoviruses and others) contain an IRES. Other viruses that do not contain a cap structure, such as HCV [364] and cricket paralysis virus (CrPV) [365], also translate by an IRES-mediated mechanism. However, there are striking differences among the mechanisms of IRES-mediated translation initiation on picornaviruses, HCV, and CrPV mRNAs. Picornaviruses require the same canonical set of translation-initiation factors as required for cellular mRNAs, with the exception of eIF4E. (The picornavirus, hepatitis A virus is the sole exception in this regard because its translation is dependent on eIF4E) [366–

368]. The function of the cap structure and eIF4E in translation of picornavirus mRNA is supplanted by a direct interaction of eIF4G with the IRES, as shown for EMCV RNA. This interaction is enhanced by eIF4A [223]. Efficient translation of picornavirus mRNAs *in vitro* and possibly *in vivo* requires the participation of non-canonical initiation factors, which are termed ITAFs (IRES *trans*-acting factors) (see Ref. [244] for review).

Another class of viruses, exemplified by HCV, uses a much simpler mechanism of internal ribosome binding. This involves the direct binding of the 40S subunit, assisted by eIF2 and eIF3, to the IRES, which includes the initiator AUG [185]. This relatively simple, prokaryotic-like, mode of ribosome binding was a key factor for the successful solution of the structure of the HCV–IRES–40S ribosome complex by cryo-electron microscopy [183]. Yet, even a more basic and extraordinary mechanism of translation initiation that does not involve any initiation factors or initiator tRNA was described for some insect viruses such as cricket paralysis virus (CrPV) [365] and Plautia stali intestine virus [369]. In this case, 40S ribosomes bind directly to a non-AUG initiation codon. The large 60S subunit joins the complex without any requirement for eIF5 or eIF5B. Most remarkably, the P-site CCU triplet is not decoded, as it base-pairs with a pseudoknot sequence in the 18S rRNA. Thus, the first decoded triplet is in the A-site.

Internal ribosome binding is not restricted to viruses, which do not contain a cap structure, but also occurs on both viral and cellular mRNAs that contain a cap structure. Among the capped viral mRNAs that contain an IRES are those of retroviruses, including HIV-1 [370]. There are approximately 50 cellular mRNAs, which have been reported to contain an IRES (a database that lists these mRNAs is accessible at http://ifr31w3.toulouse.inserm.fr/IRESdatabase/). However, this list is certain to grow, as the estimated number of IRES-containing mRNAs is ~10% of the total mRNA population. This estimate is based on the number of mRNAs that are resistant to inhibition of translation following poliovirus infection, which causes a dramatic shut-off of cap-dependent host protein synthesis [371]. An important common feature of IRES-containing cellular mRNAs is that they encode for proteins which play key roles in cell growth, proliferation, and differentiation, e.g., fibroblast growth factor-2 (FGF-2), Myc, vascular endothelial growth factor (VEGF) and inhibition of apoptosis factor (XIAP).

A very interesting and evolving aspect of cellular IRESs is their function in translational control. IRES-containing cellular mRNAs can be translated to differing extents by the cap-dependent mechanism, but the IRES allows for translation under conditions where cap-dependent translation is inhibited. Inhibition of cap-dependent translation occurs under diverse conditions of stress, such as apoptosis, serum starvation, hypoxia and γ-irradiation [372]. Thus, proteins, which are important for cell function under these conditions are often encoded by IRES-containing mRNAs. For example, VEGF and the transcription factor known as hypoxia-inducible factor-1 (HIF-1) are required for cell growth under hypoxic conditions, where cap-dependent translation is inhibited. Similarly, Myc and Apaf-1 are required during apoptosis. IRES-mediated translation also can be regulated during the cell cycle. Cap-dependent

translation is repressed during mitosis as a result of 4E-BP dephosphorylation [373]. Short-lived proteins that are essential for cell survival must be synthesized during mitosis. Two such proteins whose mRNAs contain a mitosis-restricted IRES were identified: ornithine decarboxylase [370, 374] and PITSLRE protein kinase [375]. Retroviruses stimulate cells to become arrested in mitosis. Consistent with this, translation of retrovirus and HCV mRNAs, which is IRES-dependent, is enhanced in mitotically arrested cells [376].

Finally, there are additional mechanisms of translation initiation that seem to be hybrids of cap- and IRES-dependent mechanisms, known collectively as ribosomal shunting. Ribosome binding to these mRNAs is cap-dependent and entails a period of scanning; however, the scanning ribosomes then physically by-pass relatively large stretches of the 5′-UTR and rebind to the mRNA in the vicinity of the start codon. Examples of initiation by shunting include the 35S mRNA of the cauliflower mosaic virus, major late mRNAs of adenovirus and Sendai virus mRNA [377]. Just as in the case of IRES function, there appears to be a diversity of *cis*-acting sequences and structures in the mRNA that stimulate shunting on these viral mRNAs. It is probable that shunting will also be found to operate in cellular mRNAs.

7.2.10 Future Prospects

There is now a firm fundamental understanding of the mechanism of translation initiation in eukaryotes. Much of this knowledge has been traditionally obtained through the use of genetic analysis in yeast and biochemical assays in mammalian systems. More recently, a great deal of progress has been made by solving the 3D structures of individual translation factors, collecting vast new information on the interactions among initiation factors, and the analysis of functional multi-subunit complexes. Indeed, it is possible that recruitment of ribosomes to mRNAs occurs in just a two-step process, whereby ribosomes first interact with eIF1A and a multi-factor initiation factor complex that includes eIF1, eIF2, eIF3, eIF5, and Met-tRNA$_i^{Met}$, which is then recruited to the mRNA, via bridging with eIF4F. The new data provide a strong basis for studying structure–function relationships in the translation-initiation machinery. The next important advance in structural studies of translation will be solving the 3D structures of stable multi-subunit initiation factors (such as eIF3 and eIF2). Cryoelectron microscopy studies are already underway to determine the structures of these factors. It would certainly be more challenging to obtain structures of transient complexes including eIF3 in a complex with eIF5, eIF1, and eIF2 or the eIF4F complex. The ultimate goal of the structural studies is undoubtedly to obtain the 3D structure of the ribosomes complexed with initiation factors and mRNA.

An important, but difficult, issue to address in translational control mechanisms is how are the phosphorylation states of different initiation factors integrated to effect the translation of a specific set(s) of mRNAs. For example, serum simultaneously stimulates the phosphorylation of eIF4E, eIF4B, eIF4G, the eIF4E-repressor proteins 4E-BPs and ribosomal protein S6. However, it is unclear, except for 4E-BPs,

how (and if) phosphorylation of other translation components affects translation in serum-stimulated cells. The ultimate manner to assess the importance of phosphorylation of these factors is to generate 'knock-in' mutant mice and cells expressing nonphosphorylatable forms of the relevant factors. It is probable that general translation rates would not be affected by the abolition of eIF4B, and eIF4G phosphorylation, as was documented for eIF4E: as described above, eIF4E phosphorylation can be abrogated in mammalian cells without any effect on global translation rates [302]. However, mutation of the single phosphorylation site on eIF4E in flies causes a reduction in size and development of the flies [300]. The identification of mRNAs, whose translation is affected by the phosphorylation of initiation factors, would necessitate polysome profiling in combination with microarray analysis [378].

Another important area of future research involves uncovering the full range of biological processes, which are affected by eIF2α phosphorylation. It is now abundantly clear that the paradigm established in yeast for the mechanism of stimulation of *GCN4* translation upon eIF2α phosphorylation [15] applies to all organisms. One of the intriguing examples is the selective increase in the translation of activating transcription factor 4 (ATF4) following the phosphorylation of eIF2α by PERK under ER stress conditions. ATF4 in turn regulates the unfolded protein response (UPR) to stress [379]. The stress response is implicated in the etiology of many diseases, including diabetes. Knockout mice for PERK develop diabetes before reaching 1 month of age. Indeed, a familial diabetes mellitus disease known as Wolcott–Rallison syndrome (WRS), an autosomal recessive disorder, is caused by a mutation in PERK [380]. A fascinating connection between stress, eIF2α phosphorylation and disease was recently proposed to explain the pathophysiology of two linked inherited diseases: leukoencephalopathy with VWM, which is a brain disease, and premature ovarian failure (OF). These diseases can be caused by mutations in each of the five different subunits of eIF2B [122, 123, 381]. It stands to reason that the mutations in eIF2B increase the susceptibility of particular organs such as brain and ovaries to cellular stress. Other eIF2α kinases also are involved in disease development. In addition to functioning as a major player in the host antiviral defense arsenal, PKR also appears to function as a tumor suppressor [382]. Importantly, investigators are taking advantage of these attributes to target preferentially cancer cells, which have lost PKR or its upstream effectors due to mutations, for killing by oncolytic viruses [383].

With regard to human disease, phosphorylation of 4E-BPs has been extensively studied in relation to cell growth and its possible relevance to cancer development. Rapamycin, which inhibits 4E-BP phosphorylation is an anticancer drug candidate, whose antitumorigenic activity could be mediated by its activity on 4E-BP. Consistent with this idea, eIF4E and eIF4G are overexpressed in a large number of tumors, and they can oncogenically transform rodent cells in culture [384, 385].

A very promising and nascent research area in translational control concerns synaptic plasticity. This term refers to the ability of individual synapses in a neuron to undergo enduring changes in strength in response to experience. These changes play key roles in learning and memory. Synaptic plasticity is affected by local translation

(see Refs. [386, 387] for reviews). It has been known for two decades that ribosomes and translation factors are localized in dendrites beneath the post-synaptic sites. Local protein synthesis is required for the development of long-term potentiation (LTP) and long-term depression (LTD), which are associated with memory. The exact mechanism of translational up-regulation in synapses is not known, but several signaling pathways that are responsible for the phosphorylation of translation-initiation factors are involved. In particular, the PI3K/Akt-PKB/FRAP-mTOR pathway has been implicated, as rapamycin inhibits both this signaling pathway and LTP and conversely both are stimulated by brain-derived growth factor (BDNF) [388, 389]. An alternative mechanism to activate local translation in synapses is via increased polyadenylation of αCaMKII in response to different stimuli, such as light (for dark-reared rats) [390] or NMDA [391].

One of the most revolutionary, but controversial, concepts in translation is the possibility of nuclear translation in eukaryotes. The current dogma is that the mRNA can be translated only after it is exported from the nucleus to the cytoplasm. However, a recent report concluded that translation occurs in the nucleus [392]. This idea is attractive because it provides the simplest explanation for the mechanism of nonsense-mediated decay (NMD) in mammalian cells and its association with nuclear events. NMD of a subset of mRNAs in mammalian cells is physically associated with the nucleus and is affected by splicing. Thus, the first round of nuclear translation could provide a surveillance or proofreading mechanism prior to mRNA export [235]. However, there is a raging debate as to whether nuclear translation does indeed occur [393, 394]. One of the arguments consistent with nuclear translation is the existence of a pool of initiation and elongation factors in the nucleus. However, not all of the known initiation factors are found in the nucleus [393]. Thus, if translation takes place in the nucleus it is imperative to identify the factors that are involved. If translation happens not to occur in the nucleus then it would be important to understand the nuclear functions of initiation factors, such as eIF4E and eIF4G.

Based on the immense assembled knowledge on the architecture of the translation-initiation apparatus and the mechanistic insights into translation, it is anticipated that the next decade will reveal further progress in understanding the important contributions of this machinery to complex biological processes ranging from cell growth and development to memory and metabolism. Such progress will undoubtedly impinge on the efforts to cure major diseases such as cancer, diabetes, obesity and Alzheimer.

Acknowledgements

We thank Leos Valasek, Klaus Nielsen and Christie Hamilton for helpful comments on the paper and assistance in preparation of figures. We also thank Felecia Johnson for help in preparing the paper.

References

1 C. Gualerzi, L. Brandi, E. Caserta et al.: in *The Ribosome. Structure, Function, Antibiotics, and Cellular Interactions,* eds R. A. Garrett, S. R. Douthwaite, A. Liljas et al., ASM Press, Washington, DC 2000, 477–494.

2 N. C. Kyrpides, C. R. Woese, *Proc. Natl. Acad. Sci. USA* **1998**, *95,* 224–228.

3 M. Sette, P. van Tilborg, R. Spurio, et al., *EMBO J.* **1997**, *16,* 1436–1443.

4 C. M. Fletcher, T. V. Pestova, C. U. T. Hellen et al., *EMBO J.* **1999**, *18,* 2631–2639.

5 J. H. Lee, S. K. Choi, A. Roll-Mecak et al., *Proc. Natl. Acad. Sci. USA* **1999**, *96,* 4342–4347.

6 S. K. Choi, D. S. Olsen, A. Roll-Mecak et al., *Mol. Cell. Biol.* **2000**, *20,* 7183–7191.

7 R. Boelens, C. O. Gualerzi, *Curr. Protein Pept. Sci.* **2002**, *3,* 107–119.

8 N. Sonenberg, T. E. Dever, *Curr. Opin. Struct. Biol.* **2003**, *13,* 56–63.

9 M. C. Ganoza, M. C. Kiel, H. Aoki, *Microbiol. Mol. Biol. Rev.* **2002**, *66,* 460–485.

10 H. A. Kang, J. W. Hershey, *J. Biol. Chem.* **1994**, *269,* 3934–3940.

11 N. Tolstrup, C. W. Sensen, R. A. Garrett et al., *Extremophiles* **2000**, *4,* 175–179.

12 R. J. Jackson: in *Translation in Eukaryotes,* ed. Trachsel, CRC Press, Boca Raton, FL 1991, 193–230.

13 C. G. Proud, *Curr. Toic Cell. Regul.* **1992**, *32,* 243–369.

14 J.-J. Chen: in *Translational Control of Gene Expression,* eds N. Sonenberg, J. W. B. Hershey and M. B. Mathews, Cold Spring Harbor Laboratory Press, Cold Spring Harbor, NY 2000, 529–546.

15 A. G. Hinnebusch: in *Translational Control of Gene Expression,* eds N. Sonenberg, J.W.B. Hershey and M. B. Mathews, Cold Spring Harbor Laboratory Press, Cold Spring Harbor, NY 2000, 185–243.

16 R. Kaufman: in *Translational Control of Gene Expression*, eds N. Sonenberg, J. W. B. Hershey and M. B. Mathews, Cold Spring Harbor Laboratory Press, Cold Spring Harbor, NY 2000, 503–527.

17 D. Ron, H. P. Harding: in *Translational Control of Gene Expression,* eds N. Sonenberg, J. W. B. Hershey and M. B. Mathews, Cold Spring Harbor Laboratory Press, Cold Spring Harbor, NY 2000, 547–560.

18 J. Deng, H. P. Harding, B. Raught et al., *Curr. Biol.* **2002**, *12,* 1279–1286.

19 A. G. Hinnebusch: in *Translational Control,* eds J. W. B. Hershey, M. B. Mathews and N. Sonenberg, Cold Spring Harbor Laboratory Press, Cold Spring Harbor, NY 1996, 199–244.

20 E. M. Hannig, A. M. Cigan, B. A. Freeman et al., *Mol. Cell. Biol.* **1992**, *13,* 506–520.

21 D. Tzamarias, I. Roussou, G. Thireos, *Cell* **1989**, *57,* 947–954.

22 A. M. Cigan, M. Foiani, E. M. Hannig et al., *Mol. Cell. Biol.* **1991**, *11,* 3217–3228.

23 M. Foiani, A. M. Cigan, C. J. Paddon et al., *Mol. Cell. Biol.* **1991**, *11,* 3203–3216.

24 D. R. Dorris, F. L. Erickson, E. M. Hannig, *EMBO J.* **1995**, *14,* 2239–2249.

25 N. P. Williams, A. G. Hinnebusch, T. F. Donahue, *Proc. Natl. Acad. Sci. USA* **1989**, *86,* 7515–7519.

26 T. E. Dever, W. Yang, S. str•m et al., *Mol. Cell. Biol.* **1995**, *15,* 6351–6363.

27 S. Harashima, A. G. Hinnebusch, *Mol. Cell. Biol.* **1986**, *6,* 3990–3998.

28 A. M. Cigan, L. Feng, T. F. Donahue, *Science* **1988**, *242,* 93–97.

29 R. Benne, J. W. B. Hershey, *Proc. Natl. Acad. Sci. USA* **1976**, *73,* 3005–3009.

30 U. A. Bommer, G. Lutsch, J. Stahl et al., *Biochimie* **1991**, *73,* 1007–1019.

31 S. Srivastava, A. Verschoor, J. Frank, *J. Mol. Biol.* **1992**, *220,* 301–304.

32 J. Chaudhuri, D. Chowdhury, U. Maitra, *J. Biol. Chem.* **1999**, *274,* 17975–17980.

33 R. Majumdar, A. Bandyopadhyay, U. Maitra, *J. Biol. Chem.* **2003**, *278,* 6580–6587.

34 K. Asano, J. Clayton, A. Shalev et al., *Genes Dev.* **2000**, *14*, 2534–2546.
35 H. Trachsel, T. Staehelin, *Biochim. Biophys. Acta* **1979**, *565*, 305–314.
36 D. T. Peterson, W. C. Merrick, B. Safer, *J. Biol. Chem.* **1979**, *254*, 2509–2519.
37 R. Benne, J. W. B. Hershey, *J. Biol. Chem.* **1978**, *253*, 3078–3087.
38 J. Chaudhuri, A. Chakrabarti, U. Maitra, *J. Biol. Chem.* **1997**, *272*, 30975–30983.
39 U. von Pawel-Rammingen, S. Aström, A. S. Byström, *Mol. Cell. Biol.* **1992**, *12*, 1432–1442.
40 S. U. Astrom, U. von Pawel-Rammingen, A. S. Bystrom, *J. Mol. Biol.* **1993**, *233*, 43–58.
41 H. J. Drabkin, B. Helk, U. L. RajBhandary, *J. Biol. Chem.* **1993**, *268*, 25221–25228.
42 D. Farruggio, J. Chaudhuri, U. Maitra et al., *Mol. Cell. Biol.* **1996**, *16*, 4248–4256.
43 H. J. Drabkin, M. Estrella, U. L. Rajbhandary, *Mol. Cell. Biol.* **1998**, *18*, 1459–1466.
44 S. Kiesewetter, G. Ott, M. Sprinzl, *Nucleic Acids Res.* **1990**, *18*, 4677–4682.
45 S. U. Astrom, A. S. Bystrom, *Cell* **1994**, *79*, 535–546.
46 C. Forster, K. Chakraburtty, M. Sprinzl, *Nucleic Acids Res.* **1993**, *21*, 5679–5683.
47 S. U. Astrom, M. E. Nordlund, F. L. Erickson et al., *Mol. Gen. Genet.* **1999**, *261*, 967–976.
48 T. Wagner, M. Gross, P. B. Sigler, *J. Biol. Chem.* **1984**, *259*, 4706–4709.
49 H. J. Drabkin, U. L. RajBhandary, *Mol. Cell. Biol.* **1998**, *18*, 5140–5147.
50 N. J. Gaspar, T. G. Kinzy, B. J. Scherer et al., *J. Biol. Chem.* **1994**, *269*, 3415–3422.
51 E. Schmitt, S. Blanquet, Y. Mechulam, *EMBO J.* **2002**, *21*, 1821–1832.
52 F. L. Erickson, E. M. Hannig, *EMBO J.* **1996**, *15*, 6311–6320.
53 H. Huang, H. Yoon, E. M. Hannig et al., *Genes Dev.* **1997**, *11*, 2396–2413.
54 F. L. Erickson, L. D. Harding, D. R. Dorris et al., *Mol. Gen. Genet.* **1997**, *253*, 711–719.
55 H. Trachsel: in *Translational Control*, eds J. W. B. Hershey, M. B. Mathews and N. Sonenberg, Cold Spring Harbor Laboratory Press, Plainview, NY 1996, 113–138.
56 A. Flynn, S. Oldfield, C. G. Proud, *Biochim. Biophys. Acta* **1993**, *1174*, 117–121.
57 G. M. Thompson, E. Pacheco, E. O. Melo et al., *Biochem. J.* **2000**, *347*, 703–709.
58 S. Cho, D. W. Hoffman, *Biochemistry* **2002**, *41*, 5730–5742.
59 T. F. Donahue, A. M. Cigan, E. K. Pabich et al., *Cell* **1988**, *54*, 621–632.
60 V. K. Pathak, P. J. Nielsen, H. Trachsel et al., *Cell* **1988**, *54*, 633–639.
61 X. Ye, D. R. Cavener, *Gene* **1994**, *142*, 271–274.
62 B. Castilho-Valavicius, G. M. Thompson, T. F. Donahue, *Gene Expr.* **1992**, *2*, 297–309.
63 N. N. Hashimoto, L. S. Carnevalli, B. A. Castilho, *Biochem. J.* **2002**, *367*, 359–368.
64 S. Das, T. Maiti, K. Das et al., *J. Biol. Chem.* **1997**, *272*, 31712–31718.
65 H. Rosen, G. Di Segni, R. Kaempfer, *J. Biol. Chem.* **1982**, *257*, 946–952.
66 R. Gonsky, D. Itamar, R. Harary et al., *Biochimie*, **1992**, *74*, 427–434.
67 A. Flynn, I. N. Shatsky, C. G. Proud et al., *Biochim. Biophys. Acta* **1994**, *1219*, 293–301.
68 J. P. Laurino, G. M. Thompson, E. Pacheco et al., *Mol. Cell. Biol.* **1999**, *19*, 173–181.
69 K. Asano, T. Krishnamoorthy, L. Phan et al., *EMBO J.* **1999**, *18*, 1673–1688.
70 J. Chaudhuri, K. Das, U. Maitra, *Biochemistry* **1994**, *33*, 4794–4799.
71 S. Das, U. Maitra, *Mol. Cell. Biol.* **2000**, *20*, 3942–3950.
72 K. Asano, A. Shalev, L. Phan et al., *EMBO J.* **2001**, *20*, 2326–2337.
73 C. J. Bult, O. White, E. J. Olsen et al., *Science* **1996**, *273*, 1058–1073.
74 H.-P. Klenk, R. A. Clayton, J.-F. Tomb et al., *Nature* **1997**, *390*, 364–370.
75 D. R. Smith, L. A. Doucette-Stamm, C. Deloughery et al., *J. Bacteriol.* **1997**, *179*, 7135–7155.
76 J. W. B. Hershey, *Annu. Rev. Biochem.* **1991**, *60*, 717–755.

77 T. E. Dever, L. Feng, R. C. Wek et al., *Cell* **1992**, *68*, 585–596.
78 A. M. Cigan, E. K. Pabich, L. Feng et al., *Proc. Natl. Acad. Sci. USA* **1989**, *86*, 2784–2788.
79 S. Qu, D. R. Cavener, *Gene* **1994**, *140*, 239–242.
80 H. Ernst, R. F. Duncan, J. W. B. Hershey, *J. Biol. Chem.* **1987**, *262*, 1206–1212.
81 M. Bycroft, T. J. P. Hubbard, M. Proctor et al., *Cell* **1997**, *88*, 235–242.
82 M. C. Nonato, J. Widom, J. Clardy, *J. Biol. Chem.* **2002**, *277*, 17057–17061.
83 C. R. Vazquez de Aldana, T. E. Dever, A. G. Hinnebusch, *Proc. Natl. Acad. Sci. USA* **1993**, *90*, 7215–7219.
84 T. Krishnamoorthy, G. D. Pavitt, F. Zhang et al., *Mol. Cell. Biol.* **2001**, *21*, 5018–5030.
85 F. L. Erickson, J. Nika, S. Rippel et al., *Genetics* **2001**, *158*, 123–132.
86 J. Nika, S. Rippel, E. M. Hannig, *J. Biol. Chem.*, **2000**, *276*, 1051–1056.
87 G. D. Pavitt, K. V. A. Ramaiah, S. R. Kimball et al., *Genes Dev.* **1998**, *12*, 514–526.
88 L. Feng, H. Yoon, T. F. Donahue, *Mol. Cell. Biol.* **1994**, *14*, 5139–5153.
89 A. G. Rowlands, R. Panniers, E. C. Henshaw, *J. Biol. Chem.* **1988**, *263*, 5526–5533.
90 K. L. Manchester, *Biochem. Biophys. Res. Commun.* **1997**, *239*, 223–227.
91 J. N. Dholakia, A. J. Wahba, *J. Biol. Chem.* **1989**, *264*, 546–550.
92 J. Nika, W. Yang, G. D. Pavitt et al., *J. Biol. Chem.* **2000**, *275*, 26011–26017.
93 D. J. Goss, L. J. Parkhurst, *J. Biol. Chem.* **1984**, *259*, 7374–7377.
94 D. D. Williams, N. T. Price, A. J. Loughlin et al., *J. Biol. Chem.* **2001**, *276*, 24697–24703.
95 J. R. Fabian, S. R. Kimball, N. K. Heinzinger et al., *J. Biol. Chem.* **1997**, *272*, 12359–12365.
96 K. L. Manchester, *Biochem. Biophys. Res. Commun.* **2001**, *289*, 643–646.
97 E. M. Hannig, A. G. Hinnebusch, *Mol. Cell. Biol.* **1988**, *8*, 4808–4820.
98 S. R. Kimball, J. R. Fabian, G. D. Pavitt et al., *J. Biol. Chem.* **1998**, *273*, 12841–12845.
99 B. L. Craddock, C. G. Proud, *Biochem. Biophys. Res. Commun.* **1996**, *220*, 843–847.
100 D. D. Williams, G. D. Pavitt, C. G. Proud, *J. Biol. Chem.* **2001**, *276*, 3733–3742.
101 E. Gomez, G. D. Pavitt, *Mol. Cell. Biol.* **2000**, *20*, 3965–3976.
102 E. Gomez, S. S. Mohammad, G. D. Pavitt, *EMBO J.* **2002**, *21*, 5292–5301.
103 X. Wang, F. E. Paulin, L. E. Campbell et al., *EMBO J.* **2001**, *20*, 4349–4359.
104 S. R. Kimball, N. K. Heinzinger, R. L. Horetsky et al., *J. Biol. Chem.* **1998**, *273*, 3039–3044.
105 E. V. Koonin, *Protein Sci.* **1995**, *4*, 1608–1617.
106 T. G. Anthony, J. R. Fabian, S. R. Kimball et al., *Biochim. Biophys. Acta* **2000**, *1492*, 56–62.
107 N. S. B. Thomas, R. L. Matts, R. Petryshyn et al., *Proc. Natl. Acad. Sci. USA* **1984**, *81*, 6998–7002.
108 G. D. Pavitt, W. Yang, A. G. Hinnebusch, *Mol. Cell. Biol.* **1997**, *17*, 1298–1313.
109 A. G. Rowlands, K. S. Montine, E. C. Henshaw et al., *Eur. J. Biochem.* **1988**, *175*, 93–99.
110 A. M. Cigan, J. L. Bushman, T. R. Boal et al., *Proc. Natl. Acad. Sci. USA* **1993**, *90*, 5350–5354.
111 C. J. Paddon, E. M. Hannig, A. G. Hinnebusch, *Genetics* **1989**, *122*, 551–559.
112 J. L. Bushman, A. I. Asuru, R. L. Matts et al., *Mol. Cell. Biol.* **1993**, *13*, 1920–1932.
113 W. Yang, A. G. Hinnebusch, *Mol. Cell. Biol.* **1996**, *16*, 6603–6616.
114 C. R. Vazquez de Aldana, A. G. Hinnebusch, *Mol. Cell. Biol.* **1994**, *14*, 3208-3222
115 M. V. Davies, M. Furtado, J. W. B. Hershey et al., *Proc. Natl. Acad. Sci. USA* **1989**, *86*, 9163–9167.

116 R. J. Kaufman, M. V. Davies, V. K. Pathak et al., *Mol. Cell. Biol.* **1989,** *9,* 946–958.
117 S. Y. Choi, B. J. Scherer, J. Schnier et al., *J. Biol. Chem.* **1992,** *267,* 286–293.
118 P. Murtha-Riel, M. V. Davies, B. J. Scherer et al., *J. Biol. Chem.* **1993,** *268,* 12946–12951.
119 K. V. Ramaiah, M. V. Davies, J. J. Chen et al., *Mol. Cell. Biol.* **1994,** *14,* 4546–4553.
120 A. Sudhakar, T. Krishnamoorthy, A. Jain et al., *Biochemistry* **1999,** *38,* 15398–15405.
121 N. S. B. Thomas, R. L. Matts, D. H. Levin et al., *J. Biol. Chem.* **1985,** *260,* 9860–9866.
122 P. A. J. Leegwater, G. Vermeulen, A. A. M. Konst et al., *Nat. Genet.* **2001,** *29,* 383–388.
123 M. S. van der Knaap, P. A. Leegwater, A. A. Konst et al., *Ann. Neurol.* **2002,** *51,* 264–270.
124 A. De Benedetti, C. Baglioni, *J. Biol. Chem.* **1983,** *258,* 14556–14562.
125 M. Gross, R. Redman, D. A. Kaplansky, *J. Biol. Chem.* **1985,** *260,* 9491-9500.
126 M. Gross, M. Wing, C. Rundquist et al., *J. Biol. Chem.* **1987,** *262,* 6899–6907.
127 K. V. A. Ramaiah, R. S. Dhindsa, J. J. Chen et al., *Proc. Natl. Acad. Sci. USA,* **1992,** *89,* 12063–12067.
128 A. Chakrabarti, U. Maitra, *J. Biol. Chem.* **1992,** *267,* 12964–12972.
129 P. Raychaudhuri, U. Maitra, *J. Biol. Chem.* **1986,** *261,* 7723–7728.
130 P. P. Mueller, P. Grueter, A. G. Hinnebusch et al., *J. Biol. Chem.* **1998,** *273,* 32870–32877.
131 N. K. Gupta, A. L. Roy, M. K. Nag et al.: in *Post-transcriptional Control of Gene Expression,* eds J. E. G. McCarthy and M. F. Tuite, Springer,- Berlin, Heidelberg 1990, 521–526, *Vol. H49*
132 M. Salimans, H. Goumans, H. Amesz et al., *Eur. J. Biochem.* **1984,** *145,* 91–98.
133 H. Trachsel, B. Erni, M. H. Schreier et al., *J. Mol. Biol.* **1977,** *116,* 755–767.
134 J. Chaudhuri, K. Si, U. Maitra, *J. Biol. Chem.* **1997,** *272,* 7883–7891.
135 M. A. Algire, D. Maag, P. Savio et al., *RNA* **2002,** *8,* 382–397.
136 H. A. Thompson, I. Sadnik, J. Scheinbuks et al., *Biochemistry* **1977,** *16,* 2221–2230.
137 L. H. Hartwell, C. S. McLaughlin, *Proc. Natl. Acad. Sci. USA* **1969,** *62,* 468–474.
138 P. Danaie, B. Wittmer, M. Altmann et al., *J. Biol. Chem.* **1995,** *270,* 4288–4292.
139 L. Phan, X. Zhang, K. Asano et al., *Mol. Cell. Biol.* **1998,** *18,* 4935–4946.
140 E. A. Burks, P. P. Bezerra, H. Le et al., *J. Biol. Chem.* **2001,** *276,* 2122–2131.
141 J. R. Greenberg, L. Phan, Z. Gu et al., *J. Biol. Chem.* **1998,** *273,* 23485–23494.
142 L. Valásek, H. Trachsel, J. Haek et al., *J. Biol. Chem.* **1998,** *273,* 21253–21260.
143 T. Naranda, M. Kainuma, S. E. McMillan et al., *Mol. Cell. Biol.* **1997,** *17,* 145–153.
144 P. Hanachi, J. W. B. Hershey, H. P. Vornlocher, *J. Biol. Chem.* **1999,** *274,* 8546–8553.
145 M.-H. Verlhac, R.-H. Chen, P. Hanachi et al., *EMBO J.* **1997,** *16,* 6812–6822.
146 K. Asano, L. Phan, J. Anderson et al., *J. Biol. Chem.* **1998,** *273,* 18573–18585.
147 H. P. Vornlocher, P. Hanachi, S. Ribeiro et al., *J. Biol. Chem.* **1999,** *274,* 16802–16812.
148 L. Valásek, J. Haek, H. Trachsel et al., *J. Biol. Chem.* **1999,** *274,* 27567–27572.
149 L. Valásek, L. Phan, L. W. Schoenfeld et al., *EMBO J.* **2001,** *20,* 891–904.
150 L. Valásek, J. Haek, K. H. Nielsen et al., *J. Biol. Chem.* **2001,** *276,* 43351–43360.
151 A. Shalev, L. Valásek, C. A. Pise-Masison et al., *J. Biol. Chem.* **2001,** *276,* 34948–34957.
152 Y. Akiyoshi, J. Clayton, L. Phan et al., *J. Biol. Chem.* **2000,** *276,* 10056–10062.
153 A. Bandyopadhyay, T. Matsumoto, U. Maitra, *Mol. Biol. Cell* **2000,** *11,* 4005–4018.
154 C. R. Chen, Y. C. Li, J. Chen et al., *Proc. Natl. Acad. Sci. USA* **1999,** *96,* 517–522.

155 R. Crane, R. Craig, R. Murray et al., *Mol. Biol. Cell* **2000**, *11*, 3993–4003.
156 A. Bandyopadhyay, V. Lakshmanan, T. Matsumoto et al., *J. Biol. Chem.* **2002**, *277*, 2360–2377.
157 T. Naranda, S. E. MacMillan, J. W. B. Hershey, *J. Biol. Chem.* **1994**, *269*, 32286–32292.
158 M. T. Garcia-Barrio, T. Naranda, R. Cuesta et al., *Genes Dev.* **1995**, *9*, 1781–1796.
159 J. Anderson, L. Phan, R. Cuesta et al., *Genes Dev.* **1998**, *12*, 3650–3662.
160 O. Calvo, R. Cuesta, J. Anderson et al., *Mol. Cell. Biol.* **1999**, *19*, 4167–4181.
161 J. Anderson, L. Phan *Proc. Natl. Acad. Sci. USA* **2000**, *97*, 5173–5178.
162 L. Valásek, K. H. Nielsen, A. G. Hinnebusch, *EMBO J.* **2002**, *21*, 5886–5898.
163 L. Phan, L. W. Schoenfeld, L. Valásek et al., *EMBO J.* **2001**, *20*, 2954–2965.
164 D. R. H. Evans, C. Rasmussen, P. J. Hanic-Joyce et al., *Mol. Cell. Biol.* **1995**, *15*, 4525–4535.
165 C. Morris-Desbois, V. Bochard, C. Reynaud et al., *J. Cell Sci.* **1999**, *112*, 3331–3342.
166 A. Yahalom, T. H. Kim, E. Winter et al., *J. Biol. Chem.* **2000**, *276*, 334–340.
167 H. C. Yen, E. C. Chang, *Proc. Natl. Acad. Sci. USA* **2000**, *97*, 14370–14375.
168 T. Naranda, S. E. MacMillan, T. F. Donahue et al., *Mol. Cell. Biol.* **1996**, *16*, 2307–2313.
169 A. Bandyopadhyay, U. Maitra, *Nucleic Acids Res.* **1999**, *27*, 1331–1337.
170 H. J. Yoon, T. F. Donahue, *Mol. Cell. Biol.* **1992**, *12*, 248–260.
171 T. V. Pestova, V. G. Kolupaeva, *Genes Dev.* **2002**, *16*, 2906–2922.
172 B. J. Lamphear, R. Kirchweger, T. Skern et al., *J. Biol. Chem.* **1995**, *270*, 21975–21983.
173 N. Methot, M. S. Song, N. Sonenberg, *Mol. Cell. Biol.* **1996**, *16*, 5328–5334.
174 J. W. B. Hershey, W. C. Merrick: in *Translational Control of Gene Expression*, eds N. Sonenberg, J. W. B. Hershey and M. B. Mathews, Cold Spring Harbor Laboratory Press, Cold Spring Harbor, NY 2000, 33–88.
175 P. Westermann, O. Nygard, *Nucleic Acids Res.* **1984**, *12*, 8887–8897.
176 K. L. Block, H. P. Vornlocher, J. W. B. Hershey, *J. Biol. Chem.* **1998**, *273*, 31901–31908.
177 K. Asano, H.-P. Vornlocher, N. J. Richter-Cook et al., *J. Biol. Chem.* **1997**, *272*, 27042–27052.
178 K. Asano, T. G. Kinzy, W. C. Merrick et al., *J. Biol. Chem.* **1997**, *272*, 1101–1109.
179 O. Nygard, P. Westermann, *Nucleic Acids Res.* **1982**, *10*, 1327–1334.
180 D. V. Sizova, V. G. Kolupaeva, T. V. Pestova et al., *J. Virol.* **1998**, *72*, 4775–4782.
181 E. Buratti, S. Tisminetzky, M. Zotti et al., *Nucleic Acids Res.* **1998**, *26*, 3179–3187.
182 J. S. Kieft, K. Zhou, R. Jubin et al., *RNA*, **2001**, *7*, 194–206.
183 C. M. Spahn, J. S. Kieft, R. A. Grassucci et al., *Science*, **2001**, *291*, 1959–1962.
184 G. Lutsch, R. Benndorf, P. Westermann et al., *Eur. J. Cell Biol.* **1986**, *40*, 257–265.
185 T. V. Pestova, I. N. Shatsky, S. P. Fletcher et al., *Genes Dev.* **1998**, *12*, 67–83.
186 L. Valásek, A. Mathew, B. S. Shin et al., *Genes Dev*, **2003**, *17*, 786–799.
187 C. M. Spahn, R. Beckmann, N. Eswar et al., *Cell*, **2001**, *107*, 373–386.
188 C. L. Wei, M. Kainuma, J. W. Hershey, *J. Biol. Chem.* **1995**, *270*, 22788–22794.
189 M. Kainuma, J. W. B. Hershey, *Biochimie*, **2001**, *83*, 505–514.
190 A. Thomas, H. Goumans, H. O. Voorma et al., *Eur. J. Biochem.* **1980**, *107*, 39–45.
191 J. B. Battiste, T. V. Pestova, C. U. T. Hellen et al., *Mol. Cell*, **2000**, *5*, 109–119.
192 D. Moazed, R. R. Samaha, C. Gualerzi et al., *J. Mol. Biol.* **1995**, *248*, 207–210.
193 A. P. Carter, W. M. Clemons, Jr. D. E. Brodersen et al., *Science*, **2001**, *291*, 498–501.
194 C. L. Wei, S. E. MacMillan, J. W. B. Hershey, *J. Biol. Chem.* **1995**, *270*, 5764–5771.

195 D. S. Olsen, E.M. S. et al., *EMBO J.* **2003,** *22,* 193–204.
196 T. V. Pestova, S. I. Borukhov, C. U. T. Hellen, *Nature,* **1998,** *394,* 854–859.
197 A. Marintchev, V. G. Kolupaeva, T. V. Pestova et al., *Proc. Natl. Acad. Sci. USA,* **2003,** *100,* 1535–1540.
198 A. Roll-Mecak, C. Cao, T. E. Dever et al., *Cell,* **2000,** *103,* 781–792.
199 C. O. Gualerzi, C. L. Pon, *Biochemistry,* **1990,** *29,* 5881–5889.
200 J. M. Palacios Moreno, L. Drskjotersen, J. E. Kristensen et al., *FEBS Lett.* **1999,** *455,* 130–134.
201 S. K. Choi, J. H. Lee, W. L. Zoll et al., *Science,* **1998,** *280,* 1757–1760.
202 A. J. Shatkin, *Cell,* **1976,** *9,* 645–653.
203 Y. Furuichi, A. J. Shatkin, *Adv. Virus Res.* **2000,** *55,* 135–184.
204 A. C. Gingras, B. Raught, N. Sonenberg, *Ann. Rev. Biochem.* **1999,** *68,* 913–963.
205 N. Sonenberg, M. A. Morgan, W. C. Merrick et al., *Proc. Natl. Acad. Sci. USA,* **1978,** *75,* 4843–4847.
206 N. Sonenberg, M. A. Morgan, D. Testa et al., *Nucleic Acids Res.* **1979,** *7,* 15–29.
207 M. Altmann, P. P. Mueller, J. Pelletier et al., *J. Biol. Chem.* **1989,** *264,* 12145–12147.
208 J. Marcotrigiano, A. C. Gingras, N. Sonenberg et al., *Cell,* **1997,** *89,* 951–961.
209 H. Matsuo, H. Li, A. M. McGuire et al., *Nat. Struct. Biol.* **1997,** *4,* 717–724.
210 J. Marcotrigiano, A.-C. Gingras, N. Sonenberg et al., *Nucleic Acids Symp. Ser.* ed. **1997,** 8–11.
211 G. C. Scheper, B. van Kollenburg, J. Hu et al., *J. Biol. Chem.* **2002,** *277,* 3303–3309.
212 J. Zuberek, A. Wyslouch-Cieszynska, A. Niedzwiecka et al., *RNA,* **2003,** *9,* 52–61.
213 K. Tomoo, X. Shen, K. Okabe et al., *Biochem. J.* **2002,** *362,* 539–544.
214 A. Niedzwiecka, J. Marcotrigiano, J. Stepinski et al., *J. Mol. Biol.* **2002,** *319,* 615–635.
215 C. Goyer, M. Altmann, H. S. Lee et al., *Mol. Cell. Biol.* **1993,** *13,* 4860–4874.
216 T. Ohlmann, D. Prevot, D. Decimo et al., *J. Mol. Biol.* **2002,** *318,* 9–20.
217 M. Bushell, D. Poncet, W. E. Marissen et al., *Cell Death Differ.* **2000,** *7,* 628–636.
218 S. Morino, H. Imataka, Y. V. Svitkin et al., *Mol. Cell. Biol.* **2000,** *20,* 468–477.
219 S. Z. Tarun, A. B. Sachs, *EMBO J.* **1996,** *15,* 7168–7177.
220 H. Imataka, A. Gradi, N. Sonenberg, *EMBO J.* **1998,** *17,* 7480–7489.
221 H. Le, R. L. Tanguay, M. L. Balasta et al., *J. Biol. Chem.* **1997,** *272,* 16247–16255.
222 J. Marcotrigiano, I. B. Lomakin, N. Sonenberg et al., *Mol. Cell,* **2001,** *7,* 193–203.
223 I. B. Lomakin, C. U. Hellen, T. V. Pestova, *Mol. Cell. Biol.* **2000,** *20,* 6019–6029.
224 H. Imataka, N. Sonenberg, *Mol. Cell. Biol.* **1997,** *17,* 6940–6947.
225 S. Pyronnet, H. Imataka, A. C. Gingras et al., *EMBO J.* **1999,** *18,* 270–279.
226 A. J. Waskiewicz, J. C. Johnson, B. Penn et al., *Mol. Cell. Biol.* **1999,** *19,* 1871–1880.
227 E. De Gregorio, T. Preiss, M. W. Hentze, *EMBO J.* **1999,** *18,* 4865–4874.
228 T. V. Pestova, I. N. Shatsky, C. U. T. Hellen, *Mol. Cell. Biol.* **1996,** *16,* 6870–6878.
229 W. Li, G. J. Belsham, C. G. Proud, *J. Biol. Chem.* **2001,** *276,* 29111–29115.
230 N. L. Korneeva, B. J. Lamphear, F. L. Hennigan et al., *J. Biol. Chem.* **2001,** *276,* 2872–2879.
231 H. S. Yang, A. P. Jansen, A. A. Komar et al., *Mol. Cell. Biol.* **2003,** *23,* 26–37.
232 J. D. Lewis, E. Izaurralde, *Eur. J. Biochem.* **1997,** *247,* 461–469.
233 P. Fortes, T. Inada, T. Preiss et al., *Mol. Cell,* **2000,** *6,* 191–196.
234 L. McKendrick, E. Thompson, J. Ferreira et al., *Mol. Cell. Biol.* **2001,** *21,* 3632–3641.
235 Y. Ishigaki, X. Li, G. Serin et al., *Cell,* **2001,** *106,* 607–617.
236 C. Vilela, C. Velasco, M. Ptushkina et al., *EMBO J.* **2000,** *19,* 4372–4382.

237 P. E. C. Hershey, S. M. McWhirter, J. Gross et al., *J. Biol. Chem.* **1999,** *274,* 21297–21304.

238 J. Marcotrigiano, A. C. Gingras, N. Sonenberg et al., *Mol. Cell,* **1999,** *3,* 707–716.

239 S. Mader, H. Lee, A. Pause et al., *Mol. Cell. Biol.* **1995,** *15,* 4990–4997.

240 A. Haghighat, S. Mader, A. Pause et al., *EMBO J.* **1995,** *14,* 5701–5709.

241 N. Levy-Stumpf, L. P. Deiss, H. Berissi et al., *Mol. Cell. Biol.* **1997,** *17,* 1615–1625.

242 H. Imataka, S. Olsen, N. Sonenberg, *EMBO J.* **1997,** *16,* 817–825.

243 S. Yamanaka, K. S. Poksay, K. S. Arnold et al., *Genes Dev.* **1997,** *11,* 321–333.

244 C. U. Hellen, P. Sarnow, *Genes Dev.* **2001,** *15,* 1593–1612.

245 S. Henis-Korenblit, N. L. Strumpf, D. Goldstaub et al., *Mol. Cell. Biol.* **2000,** *20,* 496–506.

246 S. Henis-Korenblit, G. Shani, T. Sines et al., *Proc. Natl. Acad. Sci. USA* **2002,** *99,* 5400–5405.

247 P. Linder, P. P. Slonimski, *Nucleic Acids Res.* **1988,** *16,* 10359.

248 R. Duncan, J. W. Hershey, *J. Biol. Chem.* **1983,** *258,* 7228–7235.

249 T. von der Haar, J. E. McCarthy, *Mol. Microbiol.* **2002,** *46,* 531–544.

250 N. K. Tanner, P. Linder, *Mol. Cell,* **2001,** *8,* 251–262.

251 G. W. Rogers, Jr. N. J. Richter, W. C. Merrick et al., *J. Biol. Chem.* **1999,** *274,* 12236–12244.

252 G. W. Rogers, Jr. A. A. Komar, W. C. Merrick et al., *Prog. Nucleic Acid Res. Mol. Biol.* **2002,** *72,* 307–331.

253 F. Rozen, I. Edery, K. Meerovitch et al., *Mol. Cell. Biol.* **1990,** *10,* 1134–1144.

254 G. W. Rogers, Jr. N. J. Richter, W. F. Lima et al., *J. Biol. Chem.* **2001,** *276,* 30914–30922.

255 J. Pelletier, N. Sonenberg, *Cell,* **1985,** *40,* 515–526.

256 S. B. Baim, D. F. Pietras, D. C. Eustice et al., *Mol. Cell. Biol.* **1985,** *5,* 1839–1846.

257 Y. Svitkin, A. Pause, A. Haghighat et al., *RNA,* **2001,** *7,* 382–394.

258 J. Yoder-Hill, A. Pause, N. Sonenberg et al., *J. Biol. Chem.* **1993,** *268,* 5566–5573.

259 Q. Li, H. Imataka, S. Morino et al., *Mol. Cell. Biol.* **1999,** *19,* 7336–7346.

260 J. de la Cruz, I. Iost, D. Kressler et al., *Proc. Natl. Acad. Sci. USA* **1997,** *94,* 5201–5206.

261 R. Y. Chuang, P. L. Weaver, Z. Liu et al., *Science* **1997,** *275,* 1468–1471.

262 I. Iost, M. Dreyfus, P. Linder, *J. Biol. Chem.* **1999,** *274,* 17677–17683.

263 P. Leroy, P. Alzari, D. Sassoon et al., *Cell* **1989,** *57,* 549–559.

264 A. O. Noueiry, J. Chen, P. Ahlquist, *Proc. Natl. Acad. Sci. USA* **2000,** *97,* 12985–12990.

265 J. Benz, H. Trachsel, U. Baumann, *Struct. Fold Des.* **1999,** *7,* 671–679.

266 E. R. Johnson, D. B. McKay, *RNA* **1999,** *5,* 1526–1534.

267 J. M. Caruthers, E. R. Johnson, D. B. McKay, *Proc. Natl. Acad. Sci. USA* **2000,** *97,* 13080–13085.

268 R. M. Story, H. Li, J. N. Abelson, *Proc. Natl. Acad. Sci. USA* **2001,** *98,* 1465–1470.

269 R. Coppolecchia, P. Buser, A. Stotz et al., *EMBO J.* **1993,** *12,* 4005–4011.

270 N. Methot, E. Rom, H. Olsen et al., *J. Biol. Chem.* **1997,** *272,* 1110–1116.

271 N. Methot, A. Pause, J. Hershey et al., *Mol. Cell. Biol.* **1994,** *14,* 2307–2316.

272 T. Naranda, W. B. Strong, J. Menaya et al., *J. Biol. Chem.* **1994,** *269,* 14465–14472.

273 N. Methot, G. Pickett, J. Keene et al., *RNA* **1996,** *2,* 38–50.

274 E. Martinez-Salas, S. L. Quinto, R. Ramos et al., *Biochimie,* **2002,** *84,* 755–763.

275 K. Ochs, L. Saleh, G. Bassili et al., *J. Virol.* **2002,** *76,* 2113–2122.

276 M. Altmann, B. Wittmer, N. Methot et al., *EMBO J.* **1995,** *14,* 3820–3827.

277 N. J. Richter-Cook, T. E. Dever, J. O. Hensold et al., *J. Biol. Chem.* **1998,** *273,* 7579–7587.

278 A. B. Sachs, R. W. Davis, R. D. Kornberg, *Mol. Cell. Biol.* **1987,** *7,* 3268–3276.

279 M. Gorlach, C. G. Burd, G. Dreyfuss, *Exp. Cell Res.* **1994,** *211,* 400–407.
280 N. K. Gray, J. M. Coller, K. S. Dickson et al., *EMBO J.* **2000,** *19,* 4723–4733.
281 A. Sachs: in *Translational Control of Gene Expression,* eds N. Sonenberg, J. W. B. Hershey and M. B. Mathews, Cold Spring Harbor Laboratory Press, Cold Spring Harbor, NY 2000, 447–465.
282 R. C. Deo, J. B. Bonanno, N. Sonenberg et al., *Cell* **1999,** *98,* 835–845.
283 K. Khaleghpour, A. Kahvejian, G. De Crescenzo et al., *Mol. Cell. Biol.* **2001,** *21,* 5200–5213.
284 G. Kozlov, J. F. Trempe, K. Khaleghpour et al., *Proc. Natl. Acad. Sci. USA* **2001,** *98,* 4409–4413.
285 R. C. Deo, N. Sonenberg, S. K. Burley, *Proc. Natl. Acad. Sci. USA* **2001,** *98,* 4414–4419.
286 D. R. Gallie, *Genes Dev.* **1991,** *5,* 2108–2116.
287 L. J. Otero, M. P. Ashe, A. B. Sachs, *EMBO J.* **1999,** *18,* 3153–3163.
288 N. Uchida, S. Hoshino, H. Imataka et al., *J. Biol. Chem.* **2002,** *277,* 50286–50292.
289 A. Searfoss, T. E. Dever, R. Wickner, *Mol. Cell. Biol.* **2001,** *21,* 4900–4908.
290 C. C. Wei, M. L. Balasta, J. Ren et al., *Biochemistry* **1998,** *37,* 1910–1916.
291 B. Stebbins-Boaz, Q. Cao, C. H. de Moor et al., *Mol. Cell* **1999,** *4,* 1017–1027.
292 Q. Cao, J. D. Richter, *EMBO J.* **2002,** *21,* 3852–3862.
293 D. Niessing, S. Blanke, H. Jackle, *Genes Dev.* **2002,** *16,* 2576–2582.
294 J. Ling, S. J. Morley, V. M. Pain et al., *Mol. Cell. Biol.* **2002,** *22,* 7853–7867.
295 D. Poncet, C. Aponte, J. Cohen, *J. Virol.* **1993,** *67,* 3159–3165.
296 M. Piron, P. Vende, J. Cohen et al., *EMBO J.* **1998,** *17,* 5811–5821.
297 P. Vende, M. Piron, N. Castagne et al., *J. Virol.* **2000,** *74,* 7064–7071.
298 B. Raught, A.-C. Gingras, N. Sonenberg: in *Translational Control of Gene Expression,* eds N. Sonenberg, J. W. B. Hershey and M. B. Mathews, Cold Spring Harbor Laboratory Press, Plainview, NY 2000, 245–294.
299 C. G. Proud, *Essays Biochem.* **2001,** *37,* 97–108.
300 P. E. Lachance, M. Miron, B. Raught et al., *Mol. Cell. Biol.* **2002,** *22,* 1656–1663.
301 L. McKendrick, S. J. Morley, V. M. Pain et al., *Eur. J. Biochem.* **2001,** *268,* 5375–5385.
302 S. J. Morley, S. Naegele, *J. Biol. Chem.* **2002,** *277,* 32855–32859.
303 A.-C. Gingras, B. Raught, S. P. Gygi et al., *Genes Dev.* **2001,** *15,* 2852–2864.
304 D. Q. Yang, M. B. Kastan, *Nat. Cell Biol.* **2000,** *2,* 893–898.
305 C. T. Keith, S. L. Schreiber, *Science* **1995,** *270,* 50–51.
306 J. L. Crespo, M. N. Hall, *Microbiol. Mol. Biol. Rev.* **2002,** *66,* 579–591.
307 R. T. Abraham, G. J. Wiederrecht, *Annu. Rev. Immunol.* **1996,** *14,* 483–510.
308 L. Beretta, A.-C. Gingras, Y. V. Svitkin et al., *EMBO J.* **1996,** *15,* 658–664.
309 A. C. Gingras, S. P. Gygi, B. Raught et al., *Genes Dev.* **1999,** *13,* 1422–1437.
310 P. T. Tuazon, W. C. Merrick, J. A. Traugh *J. Biol. Chem.* **1989,** *264,* 2773–2777.
311 B. Raught, A.-C. Gingras, S. P. Gygi et al., *EMBO J.* **2000,** *19,* 434–444.
312 M. P. Byrd, M. Zamora, R. E. Lloyd, *Mol. Cell. Biol.* **2002,** *22,* 4499–4511.
313 R. Duncan, J. W. Hershey, *J. Biol. Chem.* **1985,** *260,* 5493–5497.
314 S. J. Morley, J. A. Traugh, *J. Biol. Chem.* **1990,** *265,* 10611–10616.
315 B. Raught, F. Peiretti, A.-C. Gingras et al., **2003** HEMBO J. in press.
316 A. W. B. Craig, A. Haghighat, A. T. K. Yu et al., *Nature* **1998,** *392,* 520–523.
317 K. Khaleghpour, Y. V. Svitkin, A. W. Craig et al., *Mol. Cell* **2001,** *7,* 205–216.
318 C. Grosset, C. Y. Chen, N. Xu et al., *Cell* **2000,** *103,* 29–40.
319 G. Roy, G. De Crescenzo, K. Khaleghpour et al., *Mol. Cell. Biol.* **2002,** *22,* 3769–3782.
320 S. Hoshino, M. Imai, T. Kobayashi et al., *J. Biol. Chem.* **1999,** *274,* 16677–16680.
321 D. Lorenzetti, S. Bohlega, H. Y. Zoghbi, *Neurology* **1997,** *49,* 1009–1013.

322 H. Shibata, D. P. Huynh, S. M. Pulst, *Hum. Mol. Genet.* **2000**, *9*, 1303–1313.
323 F. Sherman, J. W. Stewart, A. M. Schweingruber, *Cell* **1980**, *20*, 215–222.
324 J. W. Stewart, F. Sherman, N. A. Shipman et al., *J. Biol. Chem.* **1971**, *246*, 7429–7445.
325 F. Sherman, J. W. Stewart: in *The Molecular Biology of the Yeast Saccharomyces Metabolism and Gene Expression*, eds J. N. Strathern, E. W. Jones and J. R. Broach, Cold Spring Harbor Laboratory Press, Cold Spring Harbor, NY 1982, 301–334.
326 J. I. Stiles, J. W. Szostak, A. T. Young et al., *Cell* **1981**, *25*, 277–284.
327 T. F. Donahue, A. M. Cigan, *Mol. Cell. Biol.* **1988**, *8*, 2955–2963.
328 M. Kozak, *Nature* **1979**, *280*, 82–85.
329 M. Kozak, A. J. Shatkin, *J. Biol. Chem.* **1978**, *253*, 6568–6577.
330 M. Kozak, *Cell* **1978**, *15*, 1109–1123.
331 M. Kozak, *Proc. Natl. Acad. Sci. USA* **1986**, *83*, 2850–2854.
332 M. Kozak, *Cell* **1983**, *34*, 971–978.
333 M. Kozak, *Nucleic Acids Res.* **1984**, *12*, 3873–3893.
334 M. Kozak, *Cell* **1986**, *44*, 283–292.
335 M. Kozak, *Mol. Cell. Biol.* **1987**, *7*, 3438–3445.
336 N. Sonenberg, *Gene Expr.* **1993**, *3*, 317–323.
337 L. Gehrke, P. E. Auron, G. J. Quigley et al., *Biochemistry* **1983**, *22*, 5157–5164.
338 J. P. Abastado, P. F. Miller, B. M. Jackson et al., *Mol. Cell. Biol.* **1991**, *11*, 486–496.
339 C. L. Wolfe, Y. C. Lou, A. K. Hopper et al., *J. Biol. Chem.* **1994**, *269*, 13361–13366.
340 D. R. Morris, A. P. Geballe, *Mol. Cell. Biol.* **2000**, *20*, 8635–8642.
341 A. P. Geballe, M. S. Sachs: in *Translational Control of Gene Expression*, eds N. Sonenberg, J. W. B. Hershey and M. B. Mathews, Cold Spring Harbor Laboratory Press, Cold Spring Harbor, NY 2000, 595–614.
342 B. Castilho-Valavicius, H. Yoon, T. F. Donahue, *Genetics*, **1990**, *124*, 483–495.
343 T. Donahue, in *Translational Control of Gene Expression*, eds N. Sonenberg, J. W. B. Hershey and M. B. Mathews, Cold Spring Harbor Laboratory Press, Cold Spring Harbor, NY 2000, 487–502.
344 A. Thomas, W. Spaan, H. van Steeg et al., *FEBS Lett.* **1980**, *116*, 67–71.
345 Y. Cui, J. D. Dinman, T. G. Kinzy et al., *Mol. Cell. Biol.* **1998**, *18*, 1506–1516.
346 P. Raychaudhuri, A. Chaudhuri, U. Maitra, *J. Biol. Chem.* **1985**, *260*, 2132–2139.
347 A. Chakrabarti, U. Maitra, *J. Biol. Chem.* **1991**, *21*, 14039–14045.
348 D. Chakravarti, U. Maitra, *J. Biol. Chem.* **1993**, *268*, 10524–10533.
349 T. Maiti, U. Maitra, *J. Biol. Chem.* **1997**, *272*, 1833–18340.
350 K. Scheffzek, M. R. Ahmadian, A. Wittinghofer, *Trends Biochem. Sci.* **1998**, *23*, 257–262.
351 S. Das, R. Ghosh, U. Maitra, *J. Biol. Chem.* **2001**, *276*, 6720–6726.
352 F. E. Paulin, L. E. Campbell, K. O'Brien et al., *Curr. Biol.* **2001**, *11*, 55–59.
353 T. V. Pestova, I. B. Lomakin, J. H. Lee et al., *Nature* **2000**, *403*, 332–335.
354 B. S. Shin, D. Maag, A. Roll-Mecak, et al., *Cell* **2002**, *111*, 1015–1025.
355 W. C. Merrick, W. M. Kemper, W. F. Anderson, *J. Biol. Chem.* **1975**, *250*, 5556–5562.
356 J. R. Lorsch, D. Herschlag, *EMBO J.* **1999**, *18*, 6705–6717.
357 J. H. Lee, T. V. Pestova, B. S. Shin, et al., *Proc. Natl. Acad. Sci. USA* **2002**, *99*, 16689–16694.
358 P. Carrera, O. Johnstone, A. Nakamura et al., *Mol. Cell* **2000**, *5*, 181–187.
359 M. V. Rodnina, A. Savelsbergh, V. I. Katunin et al., *Nature* **1997**, *385*, 37–41.
360 A. Roll-Mecak, B. S. Shin, T. E. Dever et al., *Trends Biochem. Sci.* **2001**, *26*, 705–709.
361 V. Ramakrishnan, *Cell* **2002**, *108*, 557–572.
362 J. Pelletier, G. Kaplan, V. R. Racaniello et al., *Mol. Cell. Biol.* **1988**, *8*, 1103–1112.
363 S. K. Jang, H.-G. Kr•usslich, M. J. H. Nicklin et al., *J. Virol.* **1988**, *62*, 2636–2643.

364 K. Tsukiyama-Kohara, N. Iizuka, M. Kohara et al., *J. Virol.* **1992,** *66,* 1476–1483.

365 J. E. Wilson, T. V. Pestova, C. U. Hellen et al., *Cell* **2000,** *102,* 511–520.

366 A. M. Borman, K. M. Kean, *Virology* **1997,** *237,* 129–136.

367 I. K. Ali, L. McKendrick, S. J. Morley et al., *J. Virol.* **2001,** *75,* 7854–7863.

368 T. V. Pestova, C. U. T. Hellen, I. V. Shatsky, *Mol. Cell. Biol.* **1996,** *16,* 6859–6869.

369 J. Sasaki, N. Nakashima, *Proc. Natl. Acad. Sci. USA* **2000,** *97,* 1512–1515.

370 A. Brasey, M. Lopez-Lastra, T. Ohlmann et al., *J. Virol.* **2003,** *77,* 3939–3949.

371 G. Johannes, M. S. Carter, M. B. Eisen et al., *Proc. Natl. Acad. Sci. USA* **1999,** *96,* 13118–13123.

372 M. Holcik, N. Sonenberg, R. G. Korneluk, *Trends Genet.* **2000,** *16,* 469–473.

373 S. Pyronnet, J. Dostie, N. Sonenberg, *Genes Dev.* **2001,** *15,* 2083–2093.

374 S. Pyronnet, L. Pradayrol, N. Sonenberg, *Mol. Cell* **2000,** *5,* 607–616.

375 S. Cornelis, Y. Bruynooghe, G. Denecker et al., *Mol. Cell* **2000,** *5,* 597–605.

376 M. Honda, S. Kaneko, E. Matsushita et al., *Gastroenterology* **2000,** *118,* 152–162.

377 R. J. Schneider: in *Translational Control of Gene Expression,* eds N. Sonenberg, J. W. B. Hershey and M. B. Mathews, Cold Spring Harbor Laboratory Press, Plainview, NY 2000, 581–593.

378 M. S. Carter, K. M. Kuhn, P. Sarnow, in *Translational Control of Gene Expression,* eds N. Sonenberg, J. W. B. Hershey and M. B. Mathews Cold Spring Harbor Laboratory Press, NY 2000, 615–636.

379 H. P. Harding, I. Novoa, Y. Zhang et al., *Mol. Cell* **2000,** *6,* 1099–1108.

380 M. Delepine, M. Nicolino, T. Barrett et al., *Nat. Genet.* **2000,** *25,* 406–409.

381 A. Fogli, D. Rodriguez, E. Eymard-Pierre et al., *Am. J. Hum. Genet.* **2003,** *72,* 6.

382 A. E. Koromilas, S. Roy, G. N. Barber, et al., *Science* **1992,** *257,* 1685–1689.

383 J. C. Bell, K. A. Garson, B. D. Lichty et al., *Curr. Gene. Ther.* **2002,** *2,* 243–254.

384 A. Lazaris-Karatzas, K. S. Montine, N. Sonenberg, *Nature* **1990,** *345,* 544–547.

385 J. W. B. Hershey, S. Miyamoto: in *Translational Control of Gene Expression,* eds N. Sonenberg, J. W. B. Hershey and M. B. Mathews, Cold Spring Harbor Laboratory Press, Cold Spring Harbor, NY 2000, 637–654.

386 C. Job, J. Eberwine, *Nat. Rev. Neurosci.* **2001,** *2,* 889–898.

387 O. Steward, E. M. Schuman, *Annu. Rev. Neurosci.* **2001,** *24,* 299–325.

388 N. Takei, M. Kawamura, K. Hara et al., *J. Biol. Chem.* **2001,** *276,* 42818–42825.

389 H. Tang, G. Reis, H. Kang et al., *Proc. Natl. Acad. Sci. USA* **2002,** *99,* 461–472.

390 S. Wu, D. Wells, J. Tay et al., *Neuron* **1998,** *21,* 1129–1139.

391 Y. S. Huang, M. Y. Jung, M. Sarkissian et al., *EMBO J.* **2002,** *21,* 2139–2148.

392 F. J. Iborra, D. A. Jackson, P. R. Cook, *Science* **2001,** *293,* 1139–1142.

393 M. T. Bohnsack, K. Regener, B. Schwappach et al., *EMBO J.* **2002,** *21,* 6205–6215.

394 J. E. Dahlberg, E. Lund, E. B. Goodwin, *RNA,* **2003,** *9,* 1–8.

395 M. Sprinzl, C. Horn, M. Brown et al., *Nucleic Acids Res.* **1998,** *26,* 148–153.

396 U. L. RajBhandary, C. M. Chow: in *tRNA Structure, Biosynthesis, and Function,* eds D. Soll and U. L. Raj Bhandary, American Society for Microbiology Press, Washington, DC 1995, 511–528.

397 G. Kozlov, N. Siddiqui, S. Coillet-Matillon et al., *J. Biol. Chem.* **2002,** *277,* 22822–22828.

398 L. Aravind, C. P. Pontings, *Protein Sci.* **1998,** *7,* 1250–1254

399 K. Hofmann, P. Bucher, *Trends Biochem. Sci.* **1998,** *23,* 204–205